

# TRABAJO ESPECIAL DE GRADO

## MODELAJE DE GENERACIÓN DE GAS BIOGÉNICO EN UNA ZONA SITUADA AL SUR DE LA CUENCA DEL MAR DEL NORTE, HOLANDA

### (MODELLING BIOGENIC GAS GENERATION IN THE NORTHERN DUTCH OFFSHORE)

TUTOR ACADÉMICO: Prof. Ricardo Alezones

Prof. Stefano Lo Russo

TUTOR INDUSTRIAL: Dr. Hanneke Verweij

Dr. Susanne Nelskamp

Presentado ante la Ilustre  
Universidad Central de Venezuela

Por el Br Guaipo S., María A.

Para optar al Título de  
Ingeniero Geólogo

Caracas, 2013



Guaipo S., María A.

## MODELAJE DE GENERACIÓN DE GAS BIOGÉNICO EN UNA ZONA SITUADA AL SUR DE LA CUENCA DEL MAR DEL NORTE, HOLANDA

**Tutor Académico:** Prof Stefano Lo Russo, Prof Ricardo Alezones.

**Tutor Industrial:** Dr Hanneke Verweij, Dr Susanne Nelskamp.

**Tesis.** Caracas, U.C.V. Facultad de Ingeniería. Escuela de Ingeniería Geológica. Año 2013, 106p.

**Palabras Claves:** Generación biogas, Modelaje- gas biogénico, Metano, Delta Eridanos,  
Biogenix®(Programa).

**Resumen.** Se han encontrado acumulaciones someras de gas metano en la zona holandesa de la cuenca del Mar del Norte (bloques A, B y F), específicamente en los sedimentos no consolidados del Plioceno-Pleistoceno. Actualmente se debate sobre el origen de dicho gas, si es biogénico, termogénico o una mezcla de ambos. El presente trabajo tiene por objeto modelar la generación de gas biogénico en los depósitos del Delta Eridanos y estimar los volúmenes de biogás producidos por unidad sismo-estratigráfica. Para este propósito, se seleccionaron diversos pozos pertenecientes a los bloques previamente mencionados y se crearon modelos 1D de soterramiento y temperatura usando los programas PetroMod ® y Biogenix ®. Los resultados obtenidos sugieren que la temperatura requerida para la iniciación del gas se ha alcanzado en las capas más profundas de la secuencia sismo-estratigráfica del Delta Eridanos, donde el horizonte S5 es el que mejor representa las condiciones para la generación de biogás, ya que se encuentra dentro de la ventana de temperatura óptima (30-50 °C), presenta altas tasas de sedimentación y al considerar la evaluación de los distintos escenarios de Carbono orgánico total (COT), en este horizonte, se genera una cantidad significativa de gas biogénico.

# MODELAJE DE GENERACIÓN DE GAS BIOGÉNICO EN UNA ZONA SITUADA AL SUR DE LA CUENCA DEL MAR DEL NORTE, HOLANDA

María Alexandra Guaipo Sarmiento<sup>1</sup>

[1mariaguaipo@yahoo.com](mailto:mariaguaipo@yahoo.com)

## INTRODUCCIÓN

Este estudio forma parte del proyecto “*Shallow Gas*” que está siendo desarrollado por el departamento de Petróleo y Gas del TNO (Organización de los Países Bajos para la Investigación Científica Aplicada) con el apoyo de otras cinco operadoras y cuya finalidad es mejorar la determinación de áreas prospectivas en la costa afuera holandesa. La gran demanda de gas en el mercado, en estas últimas décadas, ha despertado un renovado interés por explorar su potencial en el mar del Norte, teniendo en cuenta la presencia del gas a profundidades por debajo de 1.000 metros en el sector holandés de la cuenca de Mar del Norte y la disponibilidad de una tecnología de producción avanzada.

De hecho, recientes interpretaciones de datos sísmicos 2D y 3D al norte de la costa holandesa revelaron información sobre indicadores de hidrocarburos en sedimentos no consolidados del Plioceno - Pleistoceno. Se han identificado diversas expresiones subsuperficiales en los bloques A, B y F; entre estas anomalías se encuentran turbidez acústica, apantallamientos acústicos, y puntos brillantes. Sin duda, las últimas características sugieren sistemas altamente dinámicos de acumulación/ migración de gas.

En tal sentido, con el fin de establecer una relación entre estas características y el origen del gas, el “*Shallow Gas Project*” creó un modelo de la cuenca del Delta Eridanos, centrado en la caracterización de los sistemas de gases a profundidades someras, que permite evaluar si la zona ofrece las condiciones favorables necesarias para la generación de gas biogénico.

La importancia de la presencia de estas acumulaciones de gas en los depósitos del Delta Eridanos radica en que éstas pueden ser un indicador de las reservas de hidrocarburos localizados a mayor profundidad (Schroot y Schuttenhelm, 2003) y además, pueden representar una valiosa fuente adicional de gas.

Por otro lado, el gas biogénico es importante debido a su relevancia para el calentamiento global (Clayton, 2009) y además, se produce en un marco geológico predecible y puede ser lo suficientemente grande como para ser considerado yacimiento de gas comercial (Rice & Claypool, 1981).

El objetivo principal del presente trabajo fue modelar la generación de gas biogénico en el sector holandés de la cuenca del Mar del Norte, específicamente en los bloques A, B y F (Figura 1) y

estimar los volúmenes de gas producidos por unidad sismoestratigráfica que se definieron para los depósitos del Delta Eridanos.

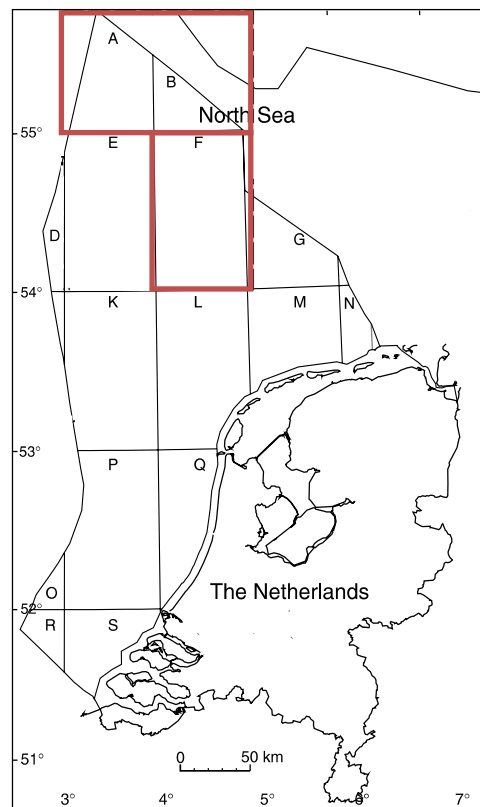


Figura 1. Area de estudio en el sector holandés del Mar del Norte (Modificado Schroot, Klaver&Schuttenhelm,2005)

Entre los objetivos específicos de este trabajo se encuentran

- Explicar el origen del gas metanogénico y mencionar algunos ejemplos análogos.
- Describir las condiciones necesarias para la generación de metano y relacionarlos con el Delta Eridanos.
- Establecer dónde y cuándo se produjo la generación de gas, y correlacionar los resultados con las unidades sismoestratigráficas de los depósitos Delta Eridanos.
- Examinar los efectos de oscilación de la temperatura de la superficie del mar en el Cenozoico y su impacto en la generación de gas biogénico.
- Revisar los aspectos que son favorables para la acumulación de gas biogénico en los depósitos terciarios de Graben Central y Step Graben.
- Seleccionar como caso de estudio un pozo representativo de cada bloque y evaluar tres posibles COT escenarios para estimar el volumen de generación de gas utilizando el programa Biogenix ®.
- Ilustrar la distribución de la generación de gas entre los 25 pozos en bloques A, B y F.

## METODOLOGÍA

La metodología aplicada en este proyecto incluyó las siguientes fases:

- Extracción de un modelo 1D del proyecto 3D desarrollado en el “*Shallow Gas Project*” con el modelo Petrel ®, el cual ofreció información referente a la historia de sedimentación al sur de la cuenca del Mar del Norte y la profundidad de los horizontes sismoestratigráficos definidos en los depósitos del Delta Eridanos.
- Selección de pozos en la zona de estudio: tener una mejor perspectiva de la distribución de la ocurrencia del gas, se consideró la ubicación de los pozos en la zona de estudio con respecto a la progradación del Delta Eridanos. Se seleccionaron 25 pozos: A11-01, A12-03, A14-01, A15-02, A15-03, A18-01, A18-02, B10-02, B13-02, B14-01, B16-01, B17-05, B17-06, B18-03, F01-01, F04-01, F05-02, F09-02, F12-02, F17-03 y F17-07. El principal criterio considerado para la selección de los pozos fue la disponibilidad de información, que incluyó las mediciones de carbono orgánico total (COT) y temperatura para la calibración.
- Modelaje de la generación de hidrocarburos en los pozos seleccionados de los bloques A, B y F. Para ello se utilizó PetroMod 1D ® Software<sup>i</sup> versión v12 (Schlumberger), el cual combina la información geológica y geofísica para modelar la evolución de una cuenca sedimentaria. Los datos de entrada del modelo son: la estratigrafía actual, la asignación de las edades, la descripción litológica y las propiedades de las rocas madre (datos geoquímicos).
- Estimación volumétrica de generación de gas biogénico en la zona interesada utilizando el Programa Biogenix ®, el cual es un algoritmo, que se puede utilizar para predecir la presencia y cantidades de metano libre generado en los sedimentos. El programa utiliza como datos de entrada, la productividad de la materia orgánica primaria en las aguas superficiales o valores definidos de COT y calcula en base volumen total de gas presente la cantidad adsorbida, disuelta, el volumen de gas libre y la saturación de gas en los espacios porosos (Clayton C. , 2009 ).

La información utilizada en el presente estudio se obtuvo a partir de varias fuentes publicadas: la nomenclatura estratigráfica de los Países Bajos (Van Adrichem Boogaert y Kouwe, 1997) y la base de datos NLOG.

## RESULTADOS Y DISCUSIÓN

La literatura sugiere que el 20 % de los reservorios de metano es de origen biogénico (Rice & Claypool, 1981), un porcentaje considerable que podría estar disponible para la explotación. Por ello, es de particular interés realizar un exhaustivo estudio en esta área para adquirir un mejor entendimiento de los procesos involucrados en la generación del biogás.

Para iniciar el proceso metanogénico es necesario que se cumplan determinadas condiciones como: ambiente anóxico, bajas temperaturas, sustrato rico en materia orgánica, altas tasas de sedimentación, ambiente con bajo contenido de sulfato y suficiente espacio poroso. En cambio, para la acumulación del gas biogénico, es imperativo los siguientes requerimientos: estructuras y trampas estratigráficas tempranas, estado físico, altas tasas de sedimentación y baja presión de reservorio.

Los Deltas del Cenozoico constituyen áreas favorables para la generación del biogás. Los principales ejemplos análogos a la zona de estudio son Deltas Níger, Nilo, Baram, Mahakam, Mekong, Ganges, Orinoco y Po.

### **Resultados obtenidos con el software PetroMod:**

#### **-Temperatura**

Con el fin de estudiar cuales pozos satisfacen las condiciones para la creación potencial de gas biogénico, se ha evaluado las unidades sísmicos estratigráficas que están limitadas dentro del rango óptimo de temperatura.

Se ha introducido un conjunto de datos detallados para representar las variaciones de temperatura de superficie, teniendo en cuenta las fluctuaciones de temperatura debido a los efectos de calentamiento y enfriamiento durante el Cenozoico tardío. En la figura 2, Se presenta una historia de la temperatura reconstruida de la cuenca del pozo A15-03, proporcionado por PetroMod. La temperatura (en grados Celsius) está representada por el eje de ordenadas y el tiempo (expresado en millones de años) en el eje de abscisas. La línea discontinua indica el dominio en la que aparece la ventana de temperatura óptima para la generación de gas biogénico. La incorporación de una serie de datos de temperatura glacial-interglaciales no tiene un efecto relevante sobre el comportamiento global debido a las oscilaciones de temperaturas para cada horizonte disminuye al aumentar la profundidad.

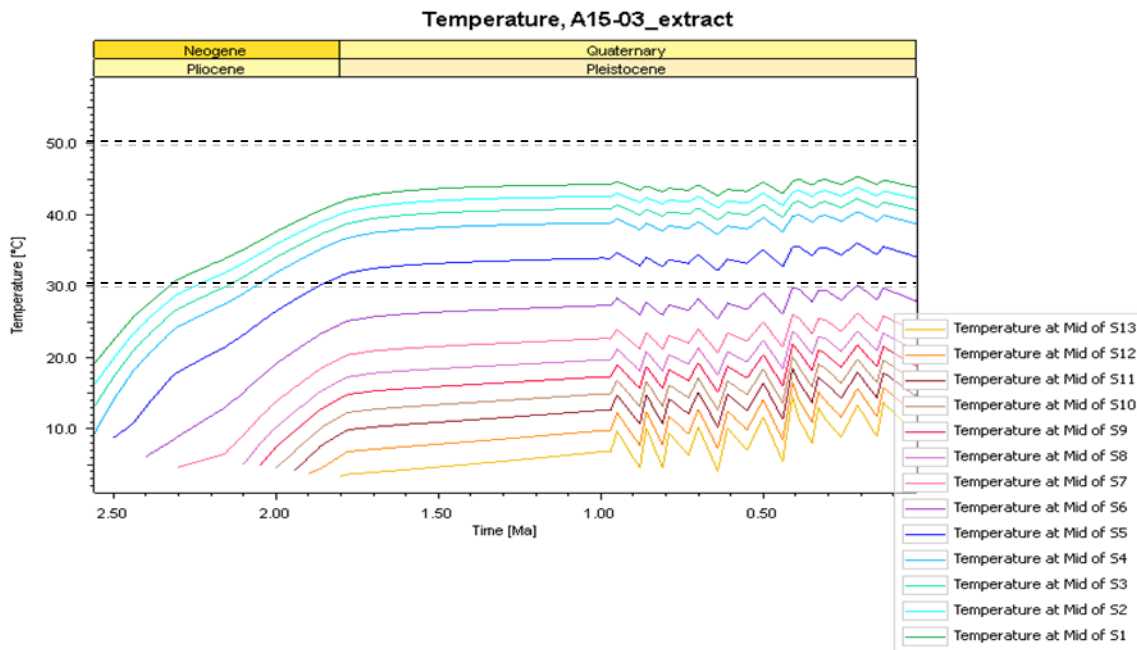


Figura 2 Historia de temperatura para el pozo A15-03

Las unidades sísmicas que se reúnen el primer requisito para la metanogénesis (temperatura 30-50 C) en el bloque F son de S1 a S5 y en los bloques A y B corresponden a S1 - S6 y S1 - S7, respectivamente.

En la figura 3 se muestra la ubicación de los pozos y distribución del dominio de temperatura óptima en los bloques A, B y F. Se ha sugerido un aumento de la temperatura con la progradación del delta. La ventana de temperatura favorable abarca un amplio rango de unidades sísmicas para los bloques A y B, que corresponden a la secuencia de mayor deposición.

Se pueden observar algunas excepciones, en el pozo B13 - 02 el rango se extiende hasta que la unidad S9 , mientras que para algunos pozos situados en la parte sureste del área de estudio, bloque F ( F03 - 07 , F03 - 08 ) y bloque B ( B14- 01 , B18- 03 ), la temperatura óptima se encuentra en los intervalos S1 hasta S3 .

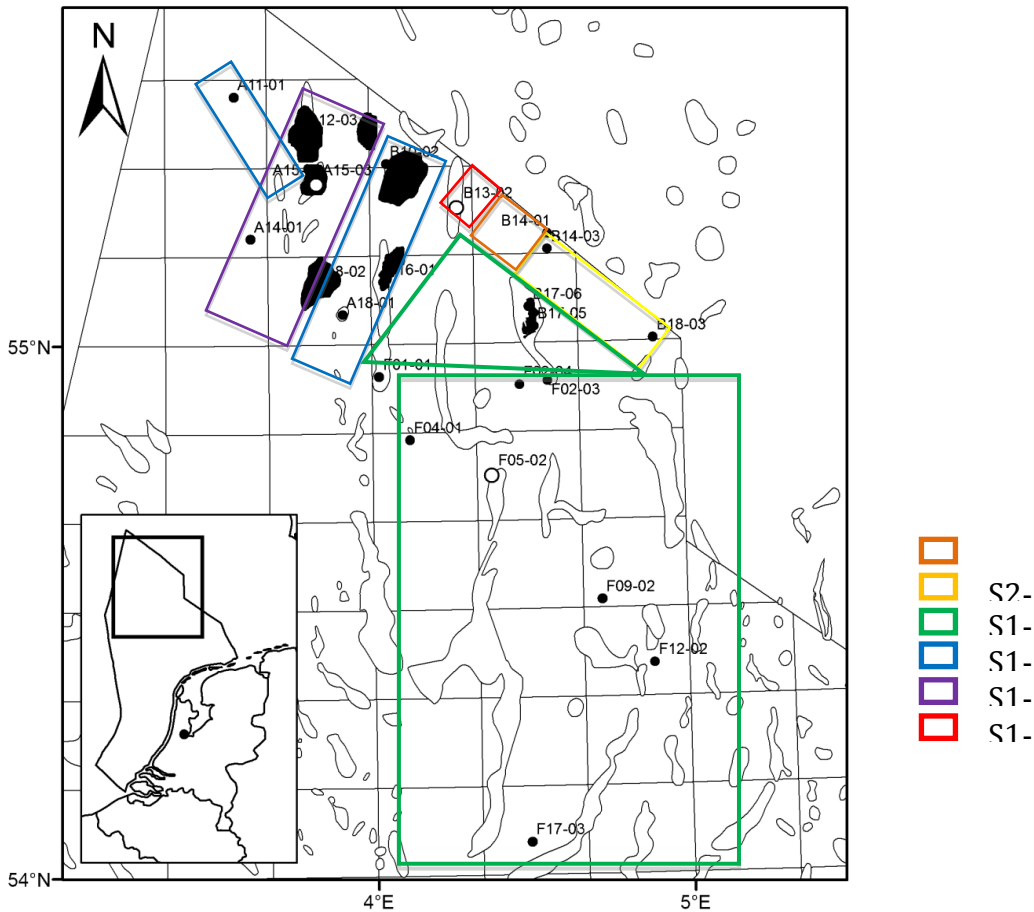


Figura 3 Distribución de los pozos en el area de estudio. Los recuadros representan las unidades sísmicas que se encuentran en el rango de temperatura.

- Tasas de sedimentación

Los resultados del modelo en los tres bloques sugieren que las unidades mas jóvenes (S13 hasta S5) presentan altas tasas de sedimentación.

Se debe tener en cuenta que las litologías mixtas creadas para cada formación, grupo y unidad sismoestratigráfica en el área de estudio, podría crear cierto nivel de incertidumbre en los resultados de los modelos, ya que un cambio en el contenido litológico, modificaría sus propiedades asociadas por defecto.

-Contenido de Materia orgánica

El potencial de gas disponible depende de la cantidad de materia orgánica presente en el area. El modelo incluye COT de las capas mas someras (Plioceno y Pleistoceno).El rango de valores de COT comprende 0,55-3,5%.

Los resultados del modelado corroboraron que los depósitos Delta Eridanos constituyen una zona perfecta para la generación de gas microbiana atribuible a la presencia de los factores mencionados que fomentan la metanogénesis.

## Resultados obtenidos con el programa Biogenix

Como caso de estudio, se ha realizado la simulación con Biogenix de tres pozos representativos en la zona (A15-03, B13-02 y F05-02) para la evaluación del potencial de generación de gas en los sedimentos no consolidados de la cuenca sur del Mar del Norte.

En la figura se muestra el gas volumétrico obtenido con el modelo Híbrido en el pozo A15-03 considerando los tres escenarios de COT. Se concluye que:

- La expulsión de gas (con 6% de saturación ) es alcanzada en las unidades mas antiguas( S1-S4 ).
- GGI, corresponde a la fracción del potencial de sustrato total que se ha convertido en metano, es obtenida a profundidades 1073m- 1193m.
- La máxima tasa de generación es obtenida en la unidad S5 ( 893m) en los tres casos.
- Gas adsorbido es el gas acumulado en la superficie de un material sólido. Este incrementa
- El gas total incluye gas libre adsorbido y disuelto. En la figura 4, se puede apreciar un incremento del gas generado con un aumento del porcentaje COT.
- El gas libre total se refiere a la fase gaseosa presente en un reservorio y se localiza en las unidades mas antiguas.

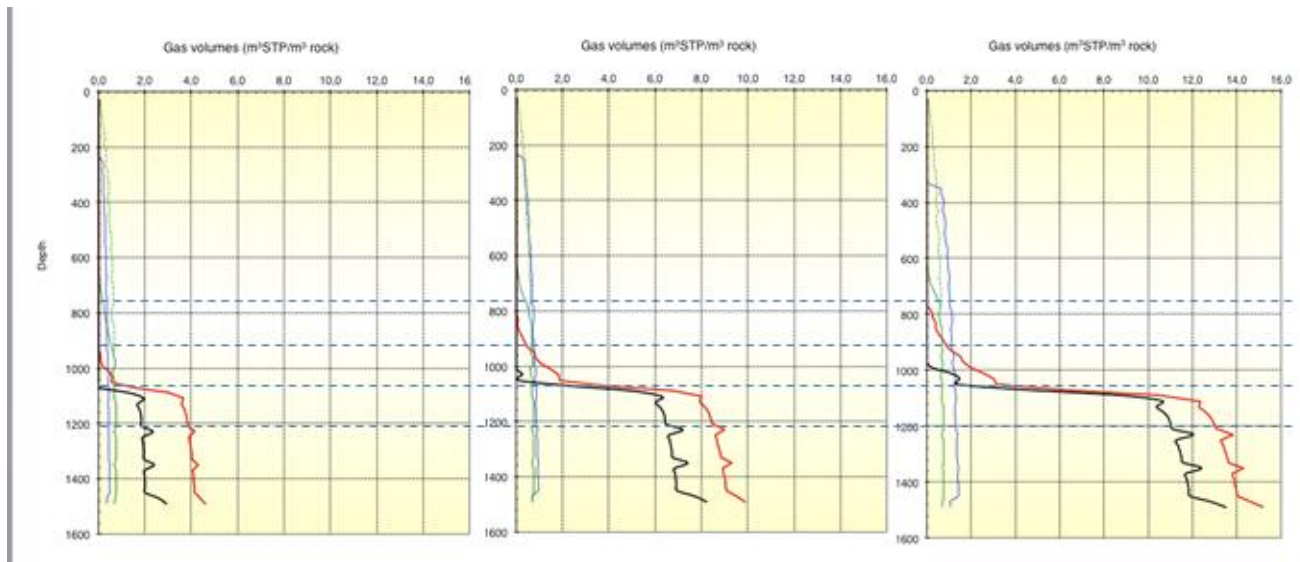


Figura 4 Volumen de gas ( $m^3$  STP/ $m^3$  roca) en el pozo A15-03 evaluado con 1, 2 y 3% de COT

## CONCLUSIONES

PetroMod ® 1D ha demostrado ser una herramienta útil para identificar cuales unidades sísmicas en los depósitos del intradelta cumplen con el rango óptimo de temperatura y altas tasas de sedimentación. Asimismo, los resultados ofrecen los datos necesarios para la aplicación del programa Biogenix®. Modelado de los 25 pozos seleccionados indican que la probabilidad de encontrar esta fuente no convencional podría aumentar en la zona norte del área de estudio (Bloques A y B) .

El Programa Biogenix ® proporciona una mejor comprensión de la materia orgánica mínima metabolizable necesaria para que los procesos de metanogénesis pueda ocurrir en la zona de estudio. También resultó adecuada para la evaluación de los tres escenarios de COT ( 1 % , 2 % , 3 % ) en los diversos pozos de los tres bloques seleccionados (A, B , F) y para estimar el rango de profundidad en la secuencia deltaica para generación de biogas. A pesar de que los volúmenes de gas calculados puede variar significativamente dependiendo de los diversos métodos de evaluación que ofrece el programa (modelos Termal- Híbrido), el modelo permitió establecer una indicación general de las posibles unidades sísmicas donde se puede encontrar el gas metanogénico.

Además, los resultados del modelo Biogenix ® sugieren que el potencial de gas biogénico iniciaría en las capas más antiguas de la deposición del intradelta, siendo el horizonte sísmo-estratigráfico S5 el que mejor representa las condiciones para la generación de gas microbiana en los depósitos deltaicos, donde se encontró abundante materia orgánica, el rango de temperatura óptima definida ( 30-50 ° C) y se alcanzaron altas tasas de sedimentación. Asimismo, la mayor parte de volumen de gas se genera en esta unidad al realizar escenarios con diferentes valores de carbono orgánico total(COT).

Al comparar los resultados de Biogenix con respecto a la profundidad en la que se podrían encontrar acumulaciones de gas, el pozo B13 - 02 concuerda con los dos niveles mientras que en los pozos A15 - 03 y F05 - 02 coincidió con solo una zona de acumulación de gas.

Los resultados del modelo indican que la metanogénesis iniciaría en un nivel de profundidad de 800-1200 m , lo que contradice la expectativa general de que el biogas se podría presentar a poca profundidad ( 400 - 600m ). Es importante señalar que este resultado requeriría más estudios ser considerados como definitivos, como el análisis de muestras de núcleo a diferentes profundidades.



## ABSTRACT

---

Shallow gas accumulations have been found in the northern Dutch offshore in Pliocene-Pleistocene unconsolidated sediments. However, there is still an on-going debate about the origin of the gas, whether it is biogenic, thermogenic or a mixture of both sources.

The purpose of this study is to model the generation of biogenic gas in the Late Cenozoic Eridanos Delta Deposits of the southern North Sea Basin and estimate the generated amount of gas. For this purpose, several wells from the A, B and F blocks were selected. For these wells 1D temperature models were created using PetroMod® which were then used as input for Biogenix®.

Biogenix® is a tool that evaluates the microbial gas generation in shallow sediments up to 80 °C. Several scenarios were modelled using different temperatures and TOC values as input to get a possible range of the amount of biogenic gas in the study area.

The results of applying PetroMod® and Biogenix® for the 25 wells considered in the study allowed to reconstruct depths of burial and suggest that the temperature required for the initiation of gas have been achieved in the lowest layers of the seismostratigraphic sequence and that, generally, occurs at depths greater than 800 m. The temperature fluctuation due to glacial-interglacial changes does not influence significantly the results for the biogenic gas generation in the area of study.

The horizon S5 is the one that better depicts the conditions for biogenic gas generation in the Eridanos Delta deposits because it is found within the optimal temperature window of 30-50 °C defined, presents high sedimentation rates and when considering the performing TOC scenarios, significant gas volume is generated at this horizon.

## ACKNOWLEDGEMENTS

---

I want to thank Central University of Venezuela. I would like to express my sincerest gratitude to Hanneke Verweij and Stefano Lo Russo for providing me the opportunity to develop this interesting research topic and for their supervision and guidance during my thesis. Special thanks to Dr Susanne Nelskamp, her constructive and valuable recommendations were gratefully acknowledged. Also, to the Petroleum Geosciences group at TNO for the disposition to help at any time.

This work has been carried out at Polytechnic of Turin and it would not be possible without the support of the Dutch Organization for Applied Scientific Research (TNO), *Geological Survey of the Netherlands*.

I also want to extend my appreciation to my friends and professors of the Geological, Geophysical and Mines engineering school at Central University of Venezuela that encouraged me to initiate the double degree program in Italy. I owe sincere and earnest thankfulness to Alexis Berthi, Betssymar Maza, Virginia Rojas, Rossi Mendez, Corina Rojas and Rosa Espinoza.

In addition, I would like to thank to my friends of Petroleum Engineering at Polytechnic of Turin and the Mediterranean team in Utrecht, who made my stay in a foreign country more bearable and enjoyable.

I am particularly grateful for the assistance given by Maria Nuria De Cesaris and her constant moral support throughout my thesis writing.

Last but not least, to my family for being supportive towards the completion of this project. To my mother for her endless love, unconditional trust and for giving me strength to reach my goals and foremost, to my father who always encouraged me to pursue my dreams.

# INDEX

---

<b>CHAPTER 1 INTRODUCTION</b> .....	<b>1</b>
1.1 Objectives.....	2
1.1.1 Specific Objectives.....	2
1.2 Case Study Area .....	3
1.2.1 Geological Setting: Eridanos Delta.....	3
1.2.2 Seismic Stratigraphic Units.....	6
1.3 Pleistocene Glaciation in the Dutch area of the North Sea .....	8
<b>CHAPTER 2: THEORETICAL FRAMEWORK</b> .....	<b>10</b>
2.1 Thermogenic Gas.....	10
2.2 Biogenic Gas.....	10
2.2.1 How is formed Biogenic gas in Marine Sediments?.....	12
2.2.2 Conditions for Methane Gas Generation .....	14
2.2.3. Conditions for Biogenic Gas Accumulation.....	17
2.2.4. Biogenic Gas Characterization and Properties.....	18
2.2.5.Discriminating between Thermogenic and Biogenic gas.....	19
2.2.6. Biogenic gas occurrences.....	20
<b>CHAPTER 3 METHODOLOGY</b> .....	<b>22</b>
3.1 Workflow Used.....	22
3.2 Database .....	23
3.3 Selection of the Wells.....	24
<b>CHAPTER 4 PETROMOD BASIN MODELLING</b> .....	<b>25</b>
4.1 Input data for Basin Modelling .....	25
4.1.1 Present- day Stratigraphy and Age Assignment .....	26
Age Assignment for the Seismic Units.....	27
4.1.2 Lithological Description.....	28
Lithological description of the Seismic Units.....	29
4.1.3. Boundary conditions.....	30
Sediment-water interface temperature.....	30
Water depth .....	32
Basal Heat flow.....	32
4.1.4 Geochemical Data (Source Rock Properties).....	33
4.2 Calibration of the Model.....	33
4.2.1. Temperature .....	34
4.2.2 Heat Flow .....	35
4.3 PetroMod Modelling Results and Discussions.....	36
4.3.1 Porosity .....	36
4.3.2 Thermal conductivity .....	37
4.3.3 Temperature .....	39
4.3.4. Does the subsurface temperature fluctuation affect the biogenic gas generation?.....	44
4.3.5.Relation between the Seismic Stratigraphy Units and biogenic gas generation .....	44

<b>CHAPTER 5 MODELLING BIOGENIC GAS GENERATION .....</b>	<b>52</b>
<b>5.1. Input Biogenix Modelling.....</b>	<b>52</b>
5.1.1. Depth Profile Options .....	52
5.1.2 Custom Input.....	53
5.1.3. Biogenic Model Used.....	53
5.1.4 Expulsion Model .....	55
5.1.5 Calculation of Gas Volumes.....	55
<b>5.2 Output Biogenix Modelling .....</b>	<b>56</b>
5.2.1 Model Comparison .....	57
5.2.2 TOC Scenarios Assessment .....	58
<b>CONCLUSIONS.....</b>	<b>71</b>
<b>RECOMMENDATIONS.....</b>	<b>73</b>
<b>REFERENCES.....</b>	<b>74</b>
<b>APPENDIX 1 International Geologic Time Scale of Gradstein et al.....</b>	<b>81</b>
<b>APPENDIX 2 Paleo-water depth (PWD) input .....</b>	<b>82</b>
<b>APPENDIX 3 Surface water interface temperature (SWIT) input.....</b>	<b>83</b>

---

## LIST OF TABLES

---

<b>Table 1.</b> Five paleoenvironments defined by Kuhlmann & Wong (2008). .....	7
<b>Table 2.</b> Carbon Isotopic compositions of the primary biogenic gas. ....	19
<b>Table 3.</b> Carbon and Hydrogen signatures of Biogenic Gas and Thermogenic Gas.....	20
<b>Table 4.</b> Synthesis of published gas occurrences in Tertiary delta deposits. ....	21
<b>Table 5.</b> Age assignment for each layer of the North Sea Basin from Carboniferous until Quaternary, expressed in Millions of years. ....	26
<b>Table 6.</b> Age assignment per each seismic unit of the southern North Sea Basin, expressed in Millions of years. The highlighted numbers (in red) indicate absolute ages obtained by previous chronology studies. ....	28
<b>Table 7.</b> Lithology of the stratigraphic horizons from Carboniferous Limestone Group to North Sea Supergroup. ....	29
<b>Table 8.</b> Mixed Lithologies of the seabed and the 13 seismic stratigraphic units. ....	30
<b>Table 9.</b> Porosity percentage per seismic stratigraphic layer for the 25 selected wells. ....	37
<b>Table 10.</b> Temperature per each seismic unit at well A15-03. The values in red represent the units that belong to the optimal temperature window.....	41
<b>Table 11.</b> Temperature per each seismic unit at well B12-03.The values in red represent the units that belong to the optimal temperature window.....	41
<b>Table 12.</b> Temperature per each seismic unit at well F05-02. The values in red represent the units that belong to the optimal temperature window. ....	42
<b>Table 13.</b> Seismic Units within the optimal range of temperature (30-50°C) for all blocks considered. ....	45
<b>Table 14.</b> Sedimentation rate (m/Ma) per seismic stratigraphic layer for the selected wells located in Block A. ....	48
<b>Table 15.</b> Sedimentation rate (m/Ma) per seismic stratigraphic layer for the selected wells located in Block B. ....	49
<b>Table 16.</b> Sedimentation rate (m/Ma) per seismic stratigraphic layer for the selected wells located in Block F.....	50
<b>Table 17.</b> Biogenix results at well A15-03 considering 1 % total organic content. ....	61
<b>Table 18.</b> Biogenix results at well A15-03 considering 2% total organic content. ....	62

<b>Table 19.</b> Biogenix results at well A15-03 considering 3% total organic content.....	62
<b>Table 20.</b> Biogenix results at well B2-03 considering 1 % total organic content.....	65
<b>Table 21.</b> Biogenix results at well B2-03 considering 2% total organic content.....	65
<b>Table 22.</b> Biogenix results at well B2-03 considering 3% total organic content.....	66
<b>Table 23.</b> Biogenix results at well F05-02 considering 1% of total organic content.....	68
<b>Table 24.</b> Biogenix results at well F05-02 considering 2% of total organic content.....	69
<b>Table 25.</b> Biogenix results at well F05-02 considering 3% of total organic content.....	69

## LIST OF FIGURES

---

<b>Figure 1.</b> Dutch North Sea Sector showing the location of study area, Blocks A, B and F (Modified after Schroot, Klaver & Schüttenhelm, 2005).....	3
<b>Figure 2.</b> Eridanos fluvio-deltaic System. The inset shows the Southern North Sea Basin. Legend: LBH: London-Brabant High, CG: Central Graben and VG: Viking Graben (Modified after Overeem, Weltje, Bishop-kay, & Kroonenberg, 2001).....	4
<b>Figure 3.</b> Paleogeographical maps showing the development of the Eridanos fluvio-deltaic systems and Rhine Meuse River during the Early Pleistocene. The inset shows the study area, corresponding to blocks A, B and F. (Modified after Westerhoff, Geluk, & De Mulder, 2003)..	5
<b>Figure 4.</b> East west trending seismic section showing the prograding character of Upper Cenozoic Delta deposits and the main seismic stratigraphic units (Modified after Kuhlmann & Wong, 2008).....	7
<b>Figure 5.</b> Tree r-RNA showing the main domains; Bacteria, Archaea and Eukarya. The Korarchaeota and Nanoarchaeota phyla are indicated with dashed branches (Allers & Mevarech, 2005). .....	11
<b>Figure 6.</b> Cross section of open marine environment showing succession of ecosystem that leads to methane generation (Modified after Rice & Claypool, 1981). .....	13
<b>Figure 7.</b> Methanogen activity level as a function of temperature (Katz, 2011).....	15
<b>Figure 8.</b> Global Mean Surface Temperature based on Wygrala study; history of surface temperature for a certain location on earth (indicated with the black line).....	31
<b>Figure 9.</b> Sediment-water interface temperature boundary condition used in the model (Nelskamp & Verweij, 2012). .....	31
<b>Figure 10.</b> Water depth through time used in the model (Nelskamp & Verweij, 2012). .....	32
<b>Figure 11.</b> Temperature reconstruction plot validated by calibration against diverse temperature data sources and correction methods.....	34
<b>Figure 12.</b> Location of the southern North Sea with the corresponding 25 selected wells. Red spots indicate gas occurrences.....	35
<b>Figure 13.</b> Plots Porosity vs depth at wells A15-03; B13-02 and F05-02. ....	38
<b>Figure 14.</b> Plots of Thermal Conductivity and Temperature vs depth at wells A15-03; B12-03; F05-02. ....	40
<b>Figure 15.</b> Detailed temperature data for the Cenozoic showing the fluctuation of temperatures (°C) during time (Ma) at well A15-03.....	42

<b>Figure 16.</b> Detailed temperature data for the Cenozoic showing the fluctuation of temperatures (°C) during time (Ma) at well B13-02.....	43
<b>Figure 17.</b> Detailed temperature data for the Cenozoic showing the fluctuation of temperatures (°C) during time (Ma) at well F05-02. ....	43
<b>Figure 18.</b> Location of the wells showing the seismic units confined within the optimal temperature window. ....	46
<b>Figure 19.</b> Measurements of TOC percentage vs depth at the wells A15-03; A16-01; F04-01 and B14-01 (TNO internal report).....	47
<b>Figure 20.</b> Scheme that shows the portion of reactive TOC and the subsequent generation of substrate that will be used by the methanogens to convert CH <sub>4</sub> (After Clayton C., 2009).....	54
<b>Figure 21.</b> Gas Volumes (m <sup>3</sup> STP/ m <sup>3</sup> rock) at well A15-03 of Thermal Model and Hybrid Model Legend; blue line: adsorbed gas; green line: dissolved gas; red line: total free gas; green dashed line: maximum soluble and black line: expelled gas. ....	57
<b>Figure 22.</b> Generation rate of Thermal Model and Hybrid model at well A15-03. ....	58
<b>Figure 23.</b> Gas volume (m <sup>3</sup> STP/ m <sup>3</sup> rock) at well A15-03 with 1, 2 and 3% total organic content.....	59
<b>Figure 24.</b> Generation rate (m <sup>3</sup> STP/ m <sup>3</sup> /My) of Hybrid Model at well A15-03 with 1, 2 and 3% total organic content. ....	60
<b>Figure 25.</b> Gas volume (m <sup>3</sup> STP/ m <sup>3</sup> rock) at well B03-02 with 1, 2 and 3% total organic content.....	63
<b>Figure 26.</b> Generation rate (m <sup>3</sup> STP/ m <sup>3</sup> /My) of Hybrid Model at well B03-02 with 1, 2 and 3% total organic content. ....	64
<b>Figure 27.</b> Gas volume (m <sup>3</sup> STP/ m <sup>3</sup> rock) at well F05-02 with 1, 2 and 3% total organic content. ....	67
<b>Figure 28.</b> Generation rate (m <sup>3</sup> STP/ m <sup>3</sup> /My) of Hybrid Model at well F05-02 with 1, 2 and 3% total organic content. ....	67

## CHAPTER 1 INTRODUCTION

---

This study is part of the Shallow Gas Project that is being developed by TNO's department of Oil & Gas with the support of another five operators, to enhance the prediction of prospective areas in Dutch offshore and evaluate whether shallow gas occurrences are either economic profitable or hazardous for production. This joint industry sponsored project consisted in building a 3D basin reservoir model of the Cenozoic Eridanos Delta, focused on the characterization of shallow gas systems.

The high demand on the gas market in the last decades, have aroused renewed interest to explore the potential of the North Sea's shallow gas, considering the evidence of gas occurrences in the Netherlands North Sea sector at depths below 1000 meters and the availability of advanced production technology.

In fact, recent geophysical interpretations of 2D and 3D seismic data in the northern Dutch offshore revealed information about hydrocarbon indications in Pliocene-Pleistocene unconsolidated sediments. Several subsurface expressions have been identified at shallow depths in the blocks A, B and F; amongst these anomalies were acoustic blanking, acoustic turbidity, enhanced reflections and bright spots. Undoubtedly, the latter features suggest highly dynamics systems with on-going and/or migration of shallow gas.

In this context, in order to establish a relationship between these features found at shallow depths and the origin of the gas system, a model of Eridanos Delta has been created, allowing to evaluate whether the area provides the favourable conditions required for Biogenic gas generation.

The presence of shallow gas accumulations in the Eridanos Delta deposits can be an indicator for deeper hydrocarbon reserves (Schroot & Schüttenhelm, 2003) and it may represent a valuable additional source.

On the other hand, Biogenic gas is an important target because of its relevance to global warming (Clayton, 2009) and since it occurs in geologically predictable settings, it is expected to be widespread in large quantities at shallow depths and also, to be large enough to be considered as commercial gas-field (Rice & Claypool, 1981).

## 1.1 Objectives

The main purpose of the present study is to model the biogenic gas generation in southern North Sea Basin, specifically in blocks A, B and F, estimating the produced gas volumes per seismic stratigraphic unit that were defined for the Eridanos Delta deposits.

### 1.1.1 Specific Objectives

- PetroMod® 1D Modelling of unconventional shallow biogenic gas in Tertiary sediments, particular focus upon the Eridanos Delta deposits.
- To explain the origin of biogenic gas and mention some representative world analogues of their occurrence.
- To describe the conditions required for the generation of methane and correlated them with the Eridanos Delta sediments.
- To establish where and when gas generation occurred, and combine the modelling results with the seismic stratigraphic units of the Eridanos Delta deposits.
- To examine the effects of surface temperature oscillation in the Cenozoic on the biogenic gas generation.
- To review the aspects that are favourable for the accumulation of biogenic gas in the Tertiary deposits of the Dutch Central Graben and Step Graben.
- To select one representative well for each block as case study based on several criteria and evaluate three possible scenarios for the volume of gas generation.
- To estimate the volume of shallow microbial gas generated using Biogenix® modelling.
- To assess of potential unconventional biogenic gas resources in northern Netherland offshore.
- To illustrate the distribution of gas generation among 25 wells in A, B and F offshore blocks, which correspond respectively to the area the Eridanos Delta sediments.

## 1.2 Case Study Area

The study area covers the three offshore quadrants A, B and F in northern Netherlands including the Dutch Central Graben and the Step Graben, indicated in Figure 1. Main focus of the project is the clastic sequences deposited after the Mid Miocene Unconformity within the southern North Sea Basin, which belong to the Eridanos Delta. Geophysical data reported shallow gas accumulation trapped in a silty-sandy reservoir unit. This reservoir unit is apparently overlain by a seal, although evidence of gas seepage features to the seabed were found (Schroot, Klaver, & Schüttenhelm, 2005).

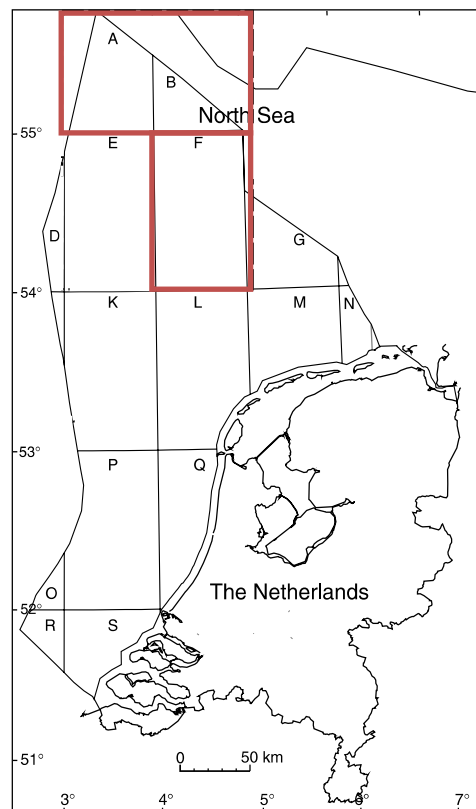


*Figure 1.* Dutch North Sea Sector showing the location of study area, Blocks A, B and F (Modified after Schroot, Klaver & Schüttenhelm, 2005).

### 1.2.1 Geological Setting: Eridanos Delta

The Eridanos fluvio-deltaic system developed during the Late Cenozoic as a result of simultaneous uplift of the Fennoscandian Shield and accelerated subsidence in the North Sea Basin (Overeem, Weltje, Bishop-kay, & Kroonenberg, 2001). The interplay of the tectonic factors mentioned above have been recognised as the main controlled mechanisms for long-term processes whilst for short-term control, variable climate conditions have been proposed to play an important role (Kuhlmann & Wong, 2008).

The proto-delta in Poland has been named as Eridanos a mythical amber-bearing river in the north of Europe (Kosmowska-Ceranowicz, 1988). This denomination was proposed by Overeem, Weltje, Bishop-kay, & Kroonenberg (2001), as a reference to the entire ancient fluvio-deltaic system.

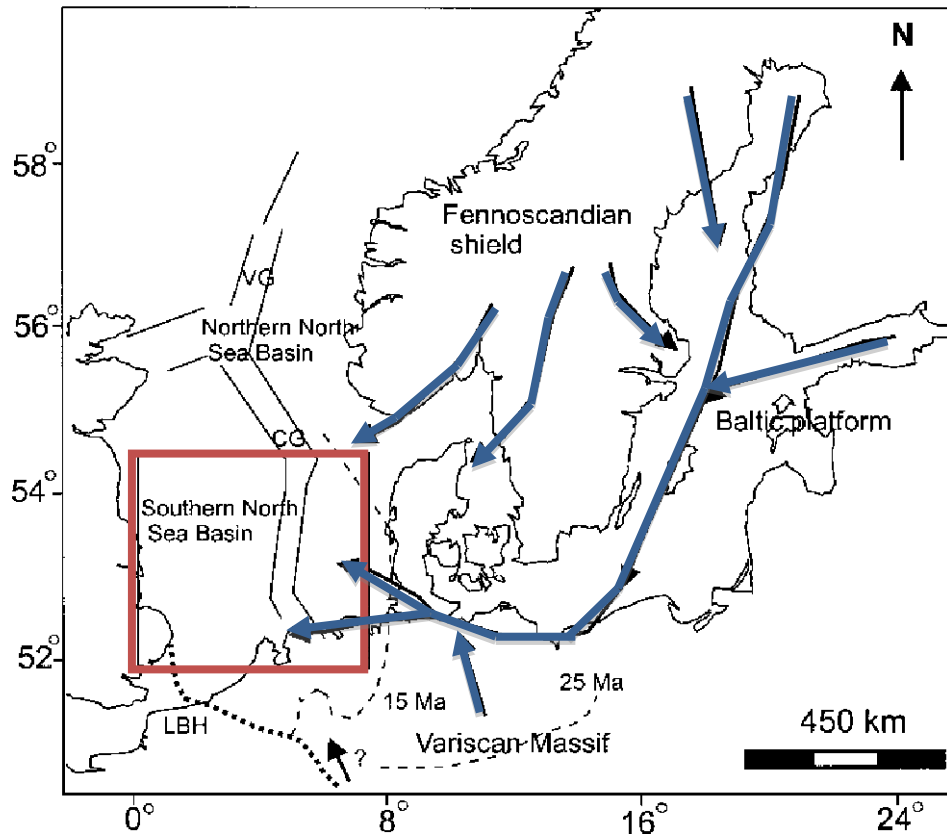


**Figure 2.** Eridanos fluvio-deltaic System. The inset shows the Southern North Sea Basin. Legend: LBH: London-Brabant High, CG: Central Graben and VG: Viking Graben (Modified after Overeem, Weltje, Bishop-kay, & Kroonenberg, 2001).

As seen in figure 2, the sediments were delivered by river draining the Fennoscandian Shield through the Baltic river system (Bijlsma, 1981; Zagwin, 1989; Gibbard, et al., 1991 in Kuhlmann, De Boer, Pedersen, & Wong, 2004). The transport direction of the sediments is given by the delta progradation. From the Paleocene to Lower Miocene, the prograding system advanced to the south and southwest, then it rotated clockwise and infill occurred towards the west and northwest during the Late Miocene to Pleistocene (Sørensen et al., 1997; Michelsen et al., 1998; Clausen, Gregersen, Michelsen, & Sørensen, 1999; Huuse & Clausen, 2001 in Kuhlmann, De Boer, Pedersen, & Wong, 2004).

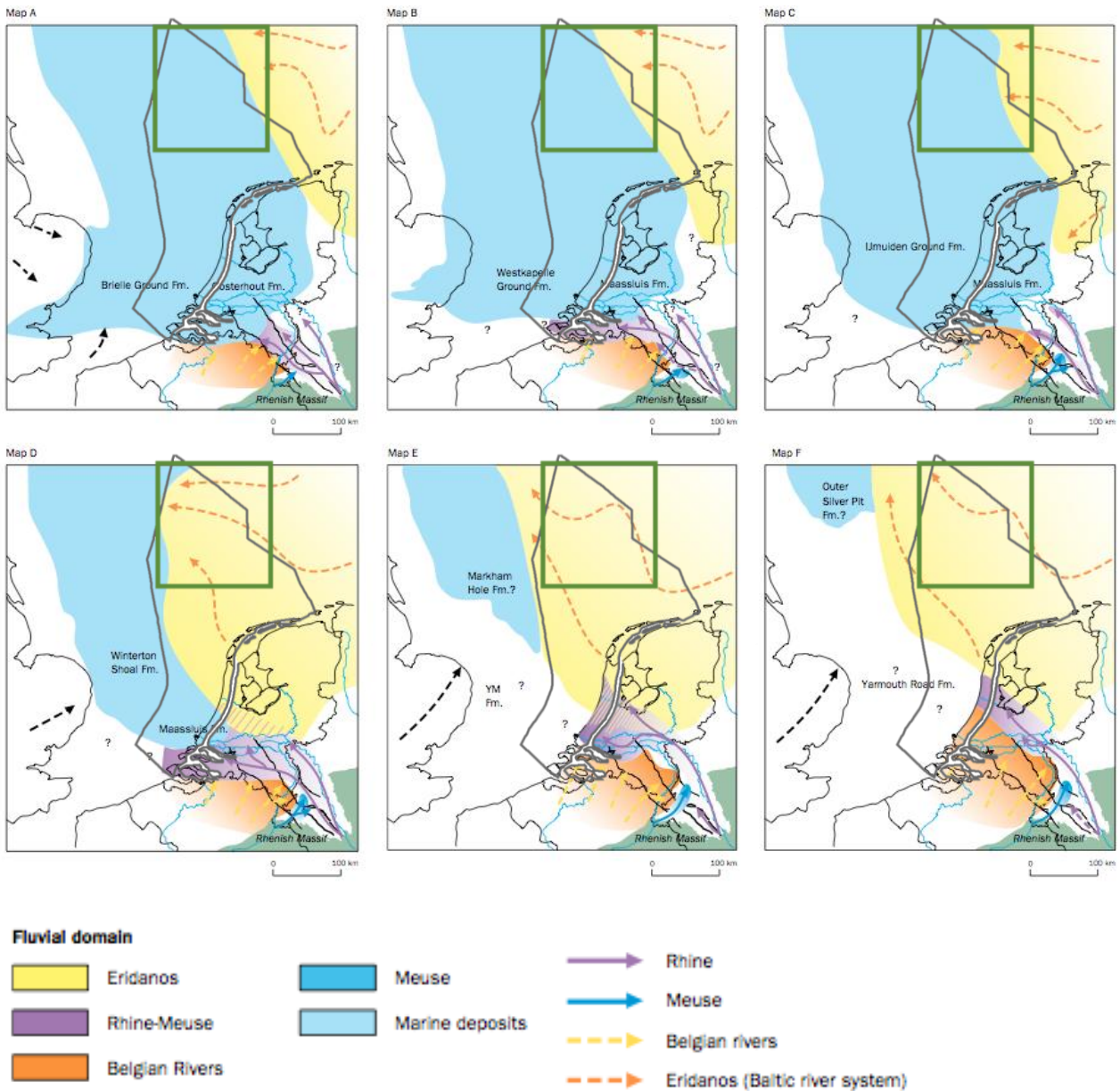


**Figure 3.** Paleogeographical maps showing the development of the Eridanos fluvio-deltaic systems and Rhine Meuse River during the Early Pleistocene. The inset shows the study area, corresponding to blocks A, B and F. (Modified after Westerhoff, Geluk, & De Mulder, 2003).

An overview of the fluvial history in the southern North Sea Basin was compiled based on previously published palaeogeographical reconstructions. As illustrated in Figure 3, the Palaeogeographical maps are presented at six steps in the lithostratigraphical record and show the development of the Eridanos Delta in the Early Pleistocene (Westerhoff W., 2009). During the Late Pliocene, the Rhine-Meuse river system draining from the south became gradually important for the supply towards the North Sea (Gibbard et al., 1991). Coleman & Roberts (1989) pointed out the deltaic deposits in the present North Sea are comparable to those of the present Orinoco Delta System in Venezuela.

Progradation of the delta resulted in several major sequences within the Upper Cenozoic section in the North Sea Basin (Michelsen, Thomsen, Danielsen, Heilmann-Clausen, Jordt, & Lauser, 1998).

### 1.2.2 Seismic Stratigraphic Units

The sedimentary section in which shallow gas and the migration to the seabed are observed postdates the Mid-Miocene unconformity, a transgressional surface which is buried at 1000 to 1500 m depth in the north of the Netherlands North Sea. From the end of the Miocene onwards, a complex fan delta system, with associated pro-delta deposits, gradually evolving into a fluvial delta and alluvial plain, prograded from the east over the Mid-Miocene unconformity (Sha, 1991; Overeem, Weltje, Bishop-kay, & Kroonenberg, 2001 in Schroot & Schüttenhelm, 2003).

The system's Upper Miocene and Lower Pliocene sediments consist of thick, laterally confined sequences, which have been deposited in deep-marine water.

Marginal gas reservoirs were found in Miocene and Plio-Pleistocene deltaic units, displaying their hydrocarbon potential (Sørensen, Gregersen, Breiner, & Michelsen, 1997; Tigrek, 1998 in Overeem, Weltje, Bishop-kay, & Kroonenberg, 2001).

Initial studies provided a regional seismostratigraphic framework describing the main depositional units for the Neogene North Sea. A first sequence stratigraphic framework for the entire Cenozoic succession was established by Michelsen, Danielsen, Heilmann-Clausen, Jordt, Laursen, & Thomsen, (1995), based on the integration of log, seismic and biostratigraphy. Then, this framework was further improved by (Sørensen & Michelsen, 1995);(Michelsen, Thomsen, Danielsen, Heilmann-Clausen, Jordt, & Lauser, 1998);(Overeem, Weltje, Bishop-kay, & Kroonenberg, 2001);(Kuhlmann, De Boer, Pedersen, & Wong, 2004); (Kuhlmann, et al., 2006) and(Kuhlmann & Wong, 2008).

Kuhlmann & Wong (2008) identified thirteen seismic units (S1-S13), based on 2D seismic interpretation in the northern part of the Dutch offshore sector (Figure 4) and distinguished five paleoenvironmental intervals for the Pliocene section of the study area.

A synthesis of the five-paleoenvironmental intervals with their corresponding seismic units is presented in table 1. Paleointerval 1 comprehends seismic units S1-S4; these units were deposited at low sedimentation rates during warm climate conditions. Towards the base of seismic unit S5 cold conditions appeared. Alternating warm and cold phases depicts Paleointerval 2. The following interval, Paleoenvironment 3, was dominated by cold climate conditions. This is explained by high erosion rates during frequent waxing and waning of initial glacier activity (Kuhlmann & Wong, 2008; Overeem et al., 2001).

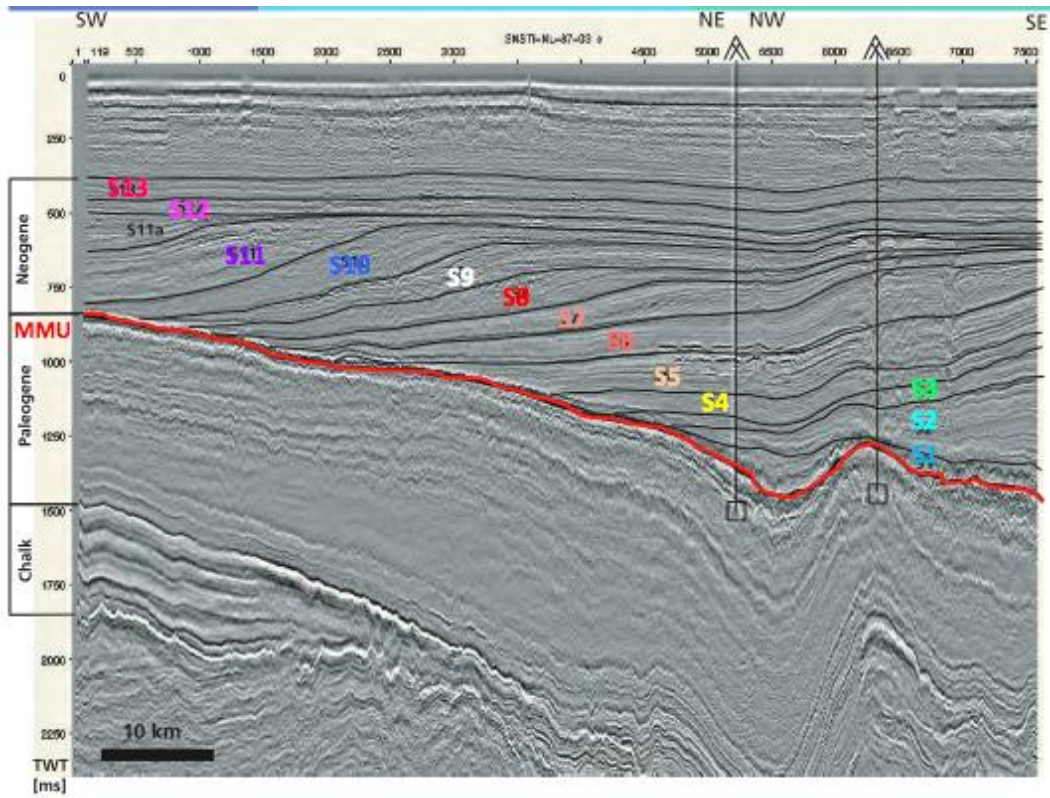


*Figure 4.* East west trending seismic section showing the prograding character of Upper Cenozoic Delta deposits and the main seismic stratigraphic units (Modified after Kuhlmann & Wong, 2008).

The preceding cold temperatures led the glaciers to grow and stay more stationary resulting in a lowering of sediment accumulation rates for seismic units. From seismic unit S8 onward arctic conditions prevailed. The uppermost seismic units, S12- S13, belong to a fluvial, paralic environment (paleoenvironment 5).

*Table 1.* Five paleoenvironments defined by Kuhlmann & Wong (2008).

Code	Paleoenvironmental Intervals
S13	Fluvial to Deltaic Paralic
S12	
S11	Shallow Marine
S10	
S9	
S8	Restricted Marine
S7	
S6	Transitional
S5	
S4	Open Marine temperate
S3	
S2	
S1	

- **Age Seismic Stratigraphic Units**

A comprehensive chronostratigraphy of the Neogene is difficult to establish within the North Sea Basin because of the progradational character of the deltaic deposits. Pliocene sediments are deposited towards the west and north while in the eastern part of the North Sea, Miocene sediments are more complete (Kuhlmann, et al., 2006).

For the Dutch North Sea sector, Kuhlmann et al. (2006) carried out a detailed study for the deltaic succession using dinoflagelates cyst, foraminifers, pollen and connected to a paleomagnetic record.

Below the unconformity, evidence indicates a Middle Serravallian age (approximately 12 Ma) or older and a Middle to Late Miocene age directly above it. The onset of sedimentation onto the unconformity is estimated at 12.4 Ma for the Danish sector (Michelsen, Thomsen, Danielsen, Heilmann-Clausen, Jordt, & Lauser, 1998) and at 10.7 Ma for the German sector (Streif, 1996). In the southern Norwegian sector the unconformity is dated at 11.2 Ma (Eidvin, Riis, & Rundberg, 1999). Hence, the MMU is younger than the Savian unconformity and therefore it does not separate the Middle North Sea Group from the Upper North Sea Group (Kuhlmann, et al., 2006).

Seismic unit S1 comprises condensed Middle to Late Miocene sediments. The Zanclean-Piacenzian boundary corresponds with the boundary of seismic units S2-S3 at 3.6 Ma. The Gauss-Matuyama boundary at around 2.6 Ma coincides with the boundary of seismic unit S4 and S5. The base of the Olduvai subchron at 1.9 Ma is linked to the top of seismic unit S11 (Kuhlmann, et al., 2006).

### **1.3 Pleistocene Glaciation in the Dutch area of the North Sea**

The two main factors determining the terrigenous sediment composition (i.e., the weathering conditions on the surrounding land areas and the sorting effects of various transport processes) are highly dependent on the prevailing climate conditions (Kuhlmann, De Boer, Pedersen, & Wong, 2004)

Within the Late Neogene this includes the shift from warm Miocene conditions towards the cold Pliocene climate related to the onset of Northern Hemisphere Glaciation with first glacier build up and retreat in the surrounding areas of the North Sea and Scandinavia. (Kuhlmann & Wong, 2008)

The first glacial event directly affecting the depositional conditions in the present Netherlands North Sea was the **Elsterian glaciation**. Scandinavian and British ice masses coalesced and spread over most of the Dutch sector, excluding south area, which remained ice-free (Long et al., 1988; Laban, 1995 in (Schroot & Schüttenhelm, 2003).

Sediments generally consist of planar deposits of glacial clays and sandy outwash, while within the channels a coarse basal fill is overlain by laminated, clayey, lacustrine deposits with sandy transgressive

deposits on top (Praeg, 1996). Ice-loading affected pre-existing faulting and salt tectonics, while the glacial channels disrupted sediment continuity and created pathways for fluids and gases (Schroot, Klaver, & Schüttenhelm, 2005).

The following **Holsteinian** and subsequent transgressions resulted in sheets of marine transgression sands with some clays near the transgression limits (Schroot & Schüttenhelm, 2003).

The subsequent **Saalian glaciation** brought Scandinavian ice to the eastern part of the Netherlands sector where tills, glacial clays and sandy and gravelly outwash were laid down. Glacial channels were fewer and much shallower, but ice-pushing and tongue basins more common (Joon, Laban, & van der Meer, 1990; Laban, 1995 in (Schroot, Klaver, & Schüttenhelm, 2005).

Falling sea-level at the end of the **Eemian** interglacial in combination with a glacial-conditioned seabed morphology resulted in sheet-like clays deposited in depressions (Cameron et al., 1989). British ice of the youngest glacial, the **Weichselian**, covered the NW of the Dutch North Sea sector resulting in glacial deposits and some glacial channels (Long, Streif, Cameron, & Schüttenhelm, 1988; Laban, 1995). Outside the ice limit, discontinuous eolian sands and fluvial channel-fills were deposited (Schroot & Schüttenhelm, 2003).

The present interglacial, the Holocene, has so far seen a drowning of the Netherlands sector, resulting in scattered, thin, muddy, lagoonal and tidal flat deposits overlain in most places by transgressive, reworked sand sheets (Cameron, Schüttenhelm, & Laban, 1989) in (Schroot, Klaver, & Schüttenhelm, 2005).

## CHAPTER 2: THEORETICAL FRAMEWORK

---

This chapter presents the conceptual framework of interest for this project regarding biogenic gas.

In this study, the methane-rich gas generated during the immature stage is discussed. However, a brief review about the different origins of shallow gas is presented. It is noteworthy to mention that the gas will be referred as “biogenic gas” or “microbial gas” to emphasize that microorganisms are responsible for its formation (Rice & Claypool, 1981).

Natural gases can be grouped into those that are generated directly by a sole source of organic matter, and those that no longer represent a single, original gas type but have been mixed or altered (Whiticar M., 1994).

Natural gases can be classified also according to its genetic characterization: thermogenic or biogenic gas.

### 2.1 Thermogenic Gas

Thermogenic gas is produced from organic precursors at high temperatures and pressure, and consequently normally at depths greater than 1000 m. However, it may migrate towards the surface to be trapped as shallow gas accumulations (Floodgate & Judd, 1992). Thermogenic gas can be subdivided in two different types depending on their conditions of formation:

- Primary Thermogenic Origin: Thermal decay of organic matter.
  - Gas from late primary cracking of kerogen and gas from secondary cracking of liquid hydrocarbons in source rocks.
  - Oil and gas are generated simultaneously; primary cracking of kerogen producing early gas.
- Secondary Thermogenic Origin: Cracking of Oil accumulation.

### 2.2 Biogenic Gas

Biogenic gas consists predominantly of methane (CH<sub>4</sub>), except in non-marine or brackish water (low pH) environments where biologically formed CO<sub>2</sub> also may be a major component (Rice & Claypool, 1981).

According to Liu & Whitman (2008), Methanogenesis is accomplished by more than 80 species of Archaea. The domain Archaea comprehends single-celled prokaryotic microorganisms that have distinct molecular characteristics, separating them from the domains bacteria and eukaryotes. The term ‘Archaeobacteria’ was a misnomer and shortened it to ‘Archaea’ (Cohen, 2011).

Much of what is known about methanogenesis has come from the study of rumen of cattle, and from

pure cultures. Comparatively not much is known about the process in marine deposits(Floodgate & Judd, 1992).

Molecular analysis has shown that domain Archaea comprises several phyla, according to the sequence of theirribosomal-RNA (Allers & Mevarech, 2005), the Crenarchaeota, Euryarchaeota, Korarchaeota and Nanoarchaeota (Figure 5).

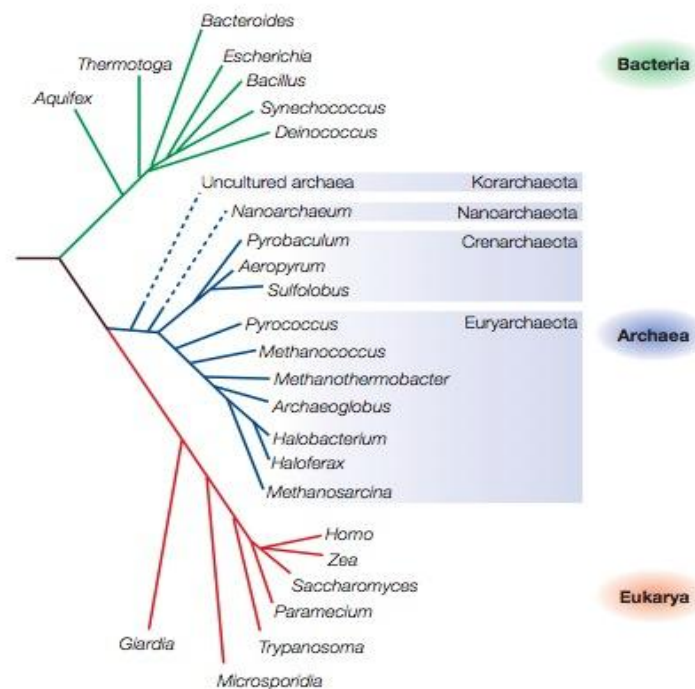


**Figure 5.** Tree r-RNA showing the main domains; Bacteria, Archaea and Eukarya. The Korarchaeota and Nanoarchaeota phyla are indicated with dashed branches(Allers & Mevarech, 2005).

**a)Euryarchaeota**

Cultured members of the Euryarchaeota are the most diverse group. Among this phylum, there are some subtypes, which include those organisms that can be conveniently divided, according to their extreme environmental niche, into three broad phenotypes: methanogens, halophiles and thermophiles(Allers & Mevarech, 2005).

- **Methanogens:** archaeans that produce methane gas as a waste product of their "digestion," or process of making energy.
- **Halophiles:** those archaeans that live in salty environments.
- **Thermophiles:** the archaeans that live at high temperatures.

### *b) Crenarchaeota*

Members of Crenarchaeota are renowned as hyperthermophiles (all temperature record-breaking species belong to this phylum), but include the psychrophile *Cenarchaeum symbiosum* (Allers & Mevarech, 2005). Crenarchaeota, which are characterized by their ability to tolerate extremes in temperature and acidity, are postulated to be the most abundant ammonia-oxidizing organisms in soils and to account for a large proportion (roughly 20%) of the microorganisms present in the picoplankton in the world's oceans (Britannica, 2011).

- **Psychrophiles:** those that live at unusually cold temperatures.
- **Hyperthermophiles:** those that live at extremely high temperatures.

### *c) Nanoarchaeota and Korarchaeota*

Of the remaining phyla, Nanoarchaeota has one known member (*Nanoarchaeum equitans*), and so far Korarchaeota are indicated only by environmental DNA sequences. Owing to the paucity of identified species, the positions of these phyla on the ribosomal RNA tree are uncertain (Allers & Mevarech, 2005). Organisms in the lineages Korarchaeota and Nanoarchaeota also inhabit high-temperature environments (Britannica, 2011).

## **2.2.1 How is formed Biogenic gas in Marine Sediments?**

A cross section through an open-marine, organic-rich sedimentary environment is shown in Figure 6 and it also illustrates the succession of microbial ecosystems. The interactions between sedimentologic and ecologic factors result in three distinct biochemical environments, each of which is characterized by a dominant form of respiratory metabolism (Rice & Claypool, 1981).

The three resulting zones are: the aerobic zone; the anaerobic sulphate-reducing zone; and the anaerobic carbonate-reducing zone. The presence of these zones, which are characterized by successively less efficient modes of respiratory processes, can be inferred in the sediments and interstitial waters by systematic changes in the concentration and isotopic composition of the respiratory metabolites. In each of the zones, the dominant microbial population exploits the environment and eventually creates a new environment that favours a different population. Therefore, the transitions between the various zones are a geochemical consequence of environmental changes induced by microorganisms (Rice & Claypool, 1981).

The aerobic zone in the marine environment is normally developed in the water column and uppermost part of the sediment column. In this zone, oxygen is rapidly used and the demand often exceeds the rate at which the dissolved gas can be introduced from the atmosphere or overlying water column, particularly in areas of high sedimentation rates. When the oxygen is depleted, obligatory aerobic organisms cannot grow (Rice & Claypool, 1981).

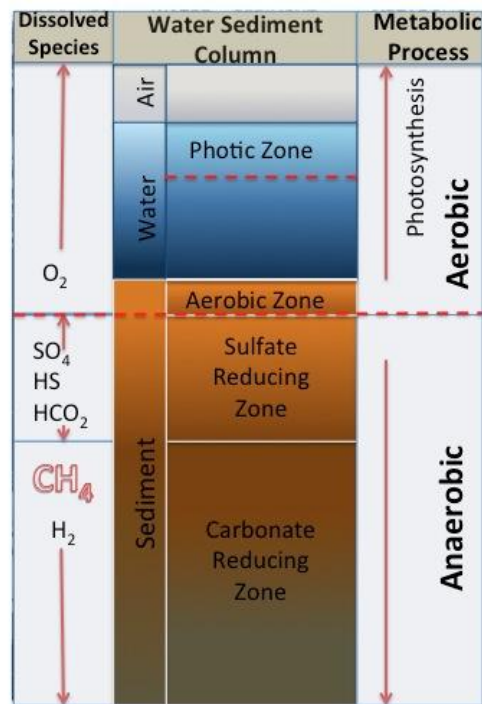


**Figure 6.** Cross section of open marine environment showing succession of ecosystem that leads to methane generation (Modified after Rice & Claypool, 1981).

In the marine environment, sulphate reduction becomes the dominant form of respiration after the onset of anaerobic conditions because of the relatively high concentration of sulphate in normal seawater. Sulphate-reducing bacteria are restricted in their range of oxidizable substrates and these compounds are probably present in limited amounts at a given time. Therefore, active sulphate-reducing bacteria require a symbiotic association with an anaerobic fermenting population to provide a source of oxidizable carbon substrate (Rice & Claypool, 1981).

In the carbonate-reducing zone, anaerobic respiration is present and different processes occur which leads to the formation of methane.

One feature of the methanogens is that they can only form hydrocarbons from a very limited number of substrates. The most important of these are hydrogen/carbon dioxide, acetate, methanol and methylamines. Not every strain is capable to use each substrate (Floodgate & Judd, 1992).

Methanogens are unable to directly utilize the larger molecules such as cellulose, polysaccharides, and proteins that may be incorporated into sediments. These large complex molecules need to be broken down to smaller compounds and eventually acetate, H<sub>2</sub> and CO<sub>2</sub>, through a sequence of microbial processes including denitrification, manganese, iron, and sulphate reduction (Katz, 2011).

Methanogenesis represents the terminal biochemical decomposition stage and can occur through several processes, but is generally represented as either CO<sub>2</sub> reduction or as acetate fermentation (Katz, 2011).

Substrates used for fermentation, such as acetate, result from a succession of many steps by distinct microbial populations that break down the complex organic substrates of the organic matter into smaller fragments until the level of acetate is reached (Mechal, 1974 in Rice D., 1992).



Carbon dioxide needed for reduction to generate methane is available from several sources. At the beginning, at low temperature, a shallow source of CO<sub>2</sub> is generated from oxidation of organic matter by microbiological processes (sulphate reduction and fermentation). At later, higher temperature, a deeper source of CO<sub>2</sub> results from thermal decarboxylation of organic matter (Tissot & Welthe, 1984 in Rice D., 1992). A third possible source of CO<sub>2</sub> for reduction is the alteration of deeply buried thermogenic hydrocarbons (Hovland & Irwin, 1992 in Rice D., 1992). Several sources of CO<sub>2</sub> are probably needed to carry on the volume of methane generation necessary to form significant accumulations.



### 2.2.2 Conditions for Methane gas generation

The generation of microbial methane is controlled by several physiologic, ecologic, and geologic factors. Among these requirements that influence the rate of methanogenesis in marine sediments are: anoxic environment, low temperatures, presence of organic matter, high sedimentation rate, sulphate deficient environment and sufficient pore space.

#### *a) Anoxic environment*

Methanogenic microorganisms are obligate anaerobes, which implies that these organisms are intolerant to the presence of oxygen. The anoxic conditions are usually set up by a wide range of bacteria that remove the oxygen while degrading organic matter (Floodgate & Judd, 1992).

#### *b) Low Temperature*

Methane generation by microorganisms can occur at depths that are equivalent to temperatures between 0 and 75 °C (Buswell & Mueller, 1952; Zeikus & Winfrey, 1972 in Rice & Claypool, 1981).

Although methanogens can function over a wide temperature range, the optimum for a specific population generally is confined to several degrees (Katz, 2011). The temperature range for the growth of methanogens is from mesophilic conditions (>25°C) to extremely thermophilic conditions (<97°C) (Rice D., 1992). As can be seen in figure 7, the peak microbial activity for the mesophiles occurs between 35 and 45°C. Neither the psychophiles nor thermophiles are considered important to the formation of commercial gas accumulations. Much of the gas produced by the psychophiles would form prior to seal development. Thermophilic methanogens would produce much of their hydrocarbons coincident with the onset of thermogenic hydrocarbon generation, which would be the dominant gas formation process (Katz, 2011).

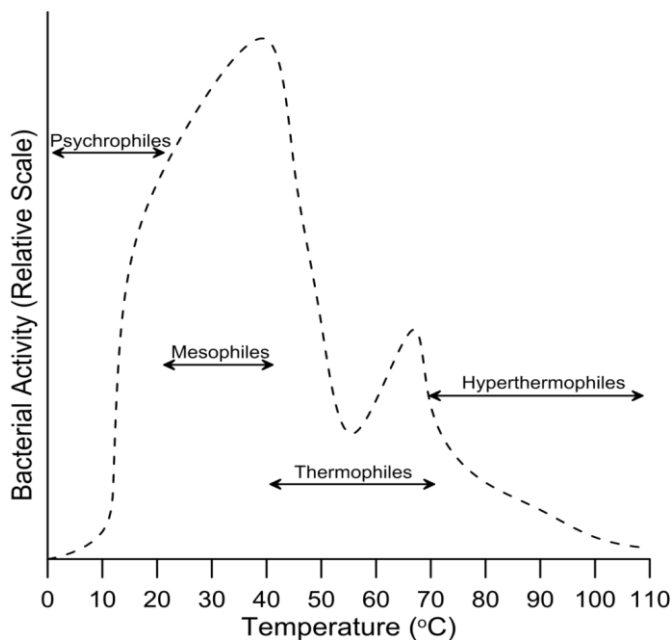


*Figure 7. Methanogen activity level as a function of temperature (Katz, 2011).*

*c) Presence of organic matter*

Organic matter is required for methanogenesis and the various metabolic processes that precede it (Rice & Claypool, 1981). It has been suggested that the substrates for methanogenesis may be produced within mudstones, where organic matter is relatively enriched (Katz, 2011).

Several authors proposed that a minimum of metabolizable organic matter equivalent to about 0.5% organic carbon is required to support methane production in marine sediments.

According to Clayton(1992) in *Source Volumetric for Biogenic gas generation*,“the potential yield of gas can be estimated from the mass fraction of carbon lost from the sediment in the methanogenic zone”.A cubic meter of sediment containing 1% total organic carbon will yield approximately 4.9m<sup>3</sup> of gas under optimum conditions. This is equivalent to the conversion of about 10% of the total organic matter. Based on the above, Clayton (1992) proposed that enough methane could be generated under hydrostatic conditions from sediments with at least 0,12% total organic content. In case of highly overpressure conditions, “the sediments containing greater than 0,2% of TOC can potentially generate a free gas phase, which can be trapped if there are sufficient isolated reservoir intervals present”.

**d) *Rate of sediment deposition***

It is a critical factor in controlling not only generation, but also the accumulation of microbial gas. If depositional rate is too slow, organic matter is destroyed by oxidation and any generated gas is lost to the atmosphere. In contrast, if the rate is too high, the organic matter is preserved, but diluted and the sediment passes too quickly through the temperature and depth zone of optimum gas generation(Rice D. , 1992). In general, the generation of microbial gas is favoured by rates of deposition in the range of 200 to 1000m/my; this rate is influenced by geothermal gradients (Clayton C. , 1992).

**e) *Sulphate-deficient environment***

Another key control is the availability of sulphate in the pore waters. At elevated salinities methanogenic activity may be inhibited (Katz, 2011). In environments where the sulphate concentration of the water is low, such as brackish or fresh water, methane production begins immediately after the oxygen is depleted. However, in the marine environment, sulphate must be reduced almost completely before significant amounts of methane can accumulate (Rice & Claypool, 1981).

Although there has been considerable discussion as to why the near absence of sulphate is required, it is now generally believed that the methanogens are less energy efficient relative to the sulphate reducers and are thus unable to effectively compete (Katz, 2011).

**f) *Pore Space***

Sufficient pore space needs to be present for the microbial population to grow. It has been suggested that the methanogenesis itself may occur within sands and silts, where greater pore space could accommodate larger methanogen populations(McMahon, Chapelle, Fells, & Bradley, 1992 in Katz, 2011).

### 2.2.3. Conditions for Biogenic Gas Accumulation

To reach biogenic gas accumulation, it should be necessary to meet certain conditions for concentration and entrapment:

*a) Physical state*

In marine settings, large amounts of gas are retained in solution in the interstitial waters because of the higher hydrostatic pressures caused by the overlying water column (Rice & Claypool, 1981). A free gas state results from generation in excess of the solubility or from exsolution following reduction of the hydrostatic pressure. Exsolution is usually a consequence of lowering of sea level or uplift and erosion (Rice D. , 1992).

*b) Early structures and stratigraphic traps*

A reservoir, seal and trap must be present *prior* to release of gas from solution to insure its retention (Rice D. , 1992).

*c) Seals and timing*

Effective seals are typically thick, laterally continuous, ductile rocks with high capillary entry pressures. Biogenic gas reservoirs are often interbedded with organic-rich shales, which serve not only as a source of gas, but also as a seal (Rice D. , 1992).

Another key trapping mechanism of biogenic methane may be the formation of early diagenetic carbonate cements as either layers or concretions. A first major mechanism of precipitation is when CO<sub>2</sub> is removed from the dissolved bicarbonate reservoir of interstitial waters by reduction and formation of methane, the pH increases, which can result in the precipitation of authigenic carbonates in anoxic sediments (Rice & Claypool, 1981). Also, the early diagenetic carbonate cement may form fairly continuous layers. The carbonate results from the precipitation of CO<sub>2</sub> by oxidation of methane under both aerobic and anaerobic conditions. (Rice D. , 1992).

Under certain conditions of high pressure and low temperature, such as those of deep-sea sediments or area of permafrost, biogenic methane will combine with water to form hydrates. The hydrates can serve both as trap for the methane enclosed in the clathrate structure, and also a seal for hydrocarbons, including biogenic methane generated below the hydrate, or liberated at the base of a gas hydrate zone subsiding into a region of temperature instability (Rice & Claypool, 1981).

*d) High Sedimentation rates*

When traps and seals are formed quickly by rapid deposition, less bacterial gas is lost to the atmosphere. In addition, rapid deposition results in thicker sequences of sediments, which slow down the diffusion of the gas (Rice D. , 1992).

*e) Low Pressure*

Most recognizable biogenic gas accumulations have low reservoir pressures because of their shallow depth of burial. However, they are also underpressured in relation to normal hydrostatic pressure gradients. This underpressuring, which is probably related to the removal of overburden and thus may coincide with exsolution of the gas, helps to trap the gas. The subnormal pressures have probably resulted from dilation of pore volume and from a decrease of reservoir temperature associated with uplift and erosion (Barker, 1972; Dickey & Cox, 1977 in Rice & Claypool, 1981).

#### **2.2.4. Biogenic Gas Characterization and Properties**

The biogenic gas is subdivided in two types that can be differentiated by their geochemical attributes and conditions of formation:

- Primary Biogenic Gas: Microbiological decay of organic matter
- Secondary Biogenic Gas: Biodegradation of Oil accumulation

The primary microbial gas is formed as part of the initial diagenetic sequence of sedimentary organic matter whilst secondary microbial gas is formed during the biodegradation of oil within conventional reservoirs or through the microbial attack of disseminated bitumen and/or possibly labile kerogen in coals or organic-rich shales (Katz, 2011).

The characteristics of primary biogenic gas are depicted in the table 2. The carbon isotope compositions are light. Gases produced by CO<sub>2</sub> reduction and through acetate fermentation are dry, where ethane content is typically less than 0.2% (Katz, 2011).

**Table 2.** Carbon Isotopic compositions of the primary biogenic gas.

	Primary Biogenic Gas	
<b>General characteristics</b>	$\delta^{13}\text{C}$	-110 to -50 ‰
	$\delta\text{D}$	-450 to -150 ‰
<b>Gas generated via CO<sub>2</sub> reduction</b>	$\delta^{13}\text{C}$	-110 to -50 ‰
	$\delta\text{D}$	-250 to -150 ‰
<b>Gas generated via Acetate fermentation</b>	$\delta^{13}\text{C}$	-70 to -50 ‰
	$\delta\text{D}$	-450 to -250 ‰

Source: Whiticar M (1999)

In contrast, secondary microbial gas displays a much more variable  $\delta^{13}\text{C}$  content, which often overlaps with what may typically be considered representative of thermal gas ( $\delta^{13}\text{C}$  -55 to -35‰). A key for identification of secondary microbial gas is its common association with isotopically heavy CO<sub>2</sub>, with  $\delta^{13}\text{C}$  CO<sub>2</sub> values greater than -10‰ and often exceeding 2‰ (Milkov, 2011) in (Katz, 2011).

### 2.2.5. Discriminating between Thermogenic and Biogenic gas

Part of the difficulty to predict the occurrence of microbial gas in unconventional reservoirs may be related to the wide variations in gas compositions (Brown A., 2011). The most common gas produced by both the biogenic and the thermogenic processes described above is methane. In order to distinguish a microbial imprint versus a thermogenic one, the following parameters may be used: methane to higher hydrocarbons ratio, carbon stable isotope ratio and hydrogen stable isotope ratio (Schoell, 1980;Faber & Stahl, 1984 in Floodgate & Judd, 1992).

There is a set of classification schemes available to distinguish microbial gas from gas generated by thermal decay of organic matter. These schemes are based on the assumption that microbial genesis produce gas enriched in methane, isotopically light compared to a thermal generation. Gases with intermediate compositions are interpreted to be of mixed biogenic and thermogenic origins. The main characteristics of the Biogenic and Thermogenic gas are presented in table 3.

**Table 3.** Carbon and Hydrogen signatures of Biogenic Gas and Thermogenic Gas.

Origin	Carbon Stable Isotope ratio	Isotope Hydrogen ratio
Biogenic	$\delta^{13}\text{C}/\text{C}_1 < -50 \text{ ‰}$	-400‰ to -150‰
Thermogenic	$\delta^{13}\text{C}/\text{C}_1 -50\text{‰ to } -20\text{‰}$	-275‰ to -100‰

Source: Whiticar, M. (1999)

The isotopic abundances of heavy isotope of carbon of hydrocarbons play an important role in studying the sources of hydrocarbons in natural gas accumulation. The ratio difference ( $\delta$ ) between  $^{13}\text{C}$  and  $^{12}\text{C}$  in parts per thousand, relative to standard; belemnite from the Peedee Formation in South Carolina (PDB). The heavy isotope of hydrogen is deuterium (D or  $2\text{H}$ ). The standard for D is mean ocean water (SMOW). Hydrogen isotope ratios are given in ‰ SMOW (Whiticar M. , 1999).

### 2.2.6. Biogenic gas occurrences

More than 20% of the world's discovered gas reserves are from biogenic origin (Rice & Claypool, 1981). Several environments are considered to be suitable for the generation and accumulation of biogenic gas, including; deltas, deep water clastic, shelves (clastic and carbonate) and non-marine settings (coal swamps) (Rice D. , 1992). The review of microbial gas occurrences documented would be limited to delta environments.

Cenozoic deltas were a very favourable setting for the generation and accumulation of hydrocarbons, both biogenic and thermogenic (Rice D. , 1992). Most representative examples of gas accumulation associated with large deltaic system are indicated in table 4.

*Table 4. Synthesis of published gas occurrences in Tertiary delta deposits.*

Location	Country	References
<b>Carpathian Foredeep</b>	Poland	(Kotarba, Szafran, & Espitalie, 1987) (Kotarba M. , 1992, 1998) (Bessereau, Roure, Kotarba, Kusmieriek, & Strzetelski, 1996)
<b>Offshore Gulf of Mexico</b>	United States	(Whelan, Coleman, Suhayda, & Roberts, 1977a) (Whelan, Purvis, Hart, Albright, & Smith, 1977b) (Addy & Worzel, 1979) (Anderson & Bryant, 1987, 1990)
<b>Niger Delta</b>	Nigeria	(Bustin, 1988)
<b>Mahakam Delta</b>	Indonesia	(Hovland & Judd, 1988) (Combaz & De Matharel, 1978)
<b>Baram Delta</b>	Brunei	(Rijks, 1981)
<b>Orinoco Delta</b>	Venezuela Trinidad & Tobago	(Butenko & Barbot, 1979) (Roberson, 2011)
<b>Po Delta</b>	Italy	(Stefanon, 1980) (Curzi, 1990) (Orange, et al., 2005)
<b>Ganges Delta</b>	India	(Murthy & Rao, 1990)
<b>Nile Delta</b>	Egypt	(Vandré, Cramer, Gerling, & Winsemann, 2007)
<b>Amazon Delta</b>	Brazil	(Figueiredo, Nittrouer, & Costa, 1996)
<b>Mekong Delta</b>	Vietnam	(Stiles, Breslau, & Beeston, 1969)

Source: Fleischer, Orsi, Richardson, & Anderson, 2001 and Rice D., 1992

## CHAPTER 3 METHODOLOGY

---

In order to accomplish the objectives, three different computer programs were used. Petrel® (Schlumberger) was used to extract the depth of the interpreted seismic stratigraphic layers at the position of the studied wells and for the evaluation of microbial gas generation in the Late Cenozoic Eridanos Delta Deposits in the northern Dutch offshore, the 1D Petroleum System modelling tool of PetroMod® (Schlumberger) was used in conjunction with Biogenix® (Clayton C. , 2009).

The methodology carried out for this project encompasses then the softwares indicated below:

- Petrel® Simulation Software for building the basin model, that was used to extract the information concerning the burial history of the southern North Sea basin, using the results of Shallow Gas project. As indicated in Schlumberger website, the software provides the construction of geocellular models through dynamic forward modelling of geological processes in sedimentary basins over geological time spans.
- PetroMod® 1D Petroleum System Modelling Software for simulating the generation of hydrocarbons in the Dutch offshore, specifically in the blocks A, B and F.  
PetroMod package combines seismic, well, and geological information to model the evolution of a sedimentary basin. The software will predict if a reservoir has been charged with hydrocarbons, including the source and timing of hydrocarbon generation (Schlumberger, 2013).
- Biogenix® Excel program for the volumetric estimation of the potential biogenic gas generation in the interested area.  
Biogenix is an algorithm, which can be used to predict the presence and quantities of free microbial generated methane in buried sediments. The program uses as an input a defined buried TOC or the primary organic matter productivity in surface waters and “calculates on a volumetric basis the total gas present, the amount adsorbed and dissolved, the volume of free gas and gas saturation in the pore spaces” (Clayton C. , 2009).

### 3.1 Workflow Used

A General Workflow was proposed, including the following four phases:

#### *Phase 1. Preparation (gathering of the data)*

- Depth maps from North Sea Group until Carboniferous Limestone Group were used as input.
- Selection of several wells according to diverse criteria.
- Collection of well data (coordinates, azimuth, depth).

- Compilation of the boundary conditions (SWIT, Heat Flow, PWD) and source parameters (TOC) for the selected wells.

*Phase 2. Building of Basin Model.*

- Creation of the Mixed Lithologies for the corresponding Formation or group and seismic stratigraphy units.
- Extraction of the pick wells from the seismic stratigraphic units from a foregoing project.

*Phase 3. Run 1D Simulation Modelling with PetroMod®*

- Run simulation for the construction of the burial history.
- Calibration with Temperature measurements, and in some cases (when available) with Vitrinite data.

*Phase 4. Run Simulation 1D Biogenix® Modelling with the output generated by PetroMod®*

- Selection of a representative well for each block.
- The input data considered for the 1D Biogenix encoded algorithm, involved the results obtained from the previous 1D Petroleum System Modelling PetroMod.
- Input of age, depth and lithology and temperature information at different depths.
- Selection of model (Hybrid, Thermal and Force Decay model)
- Assessment of three TOC scenarios in the selected wells.
- Evaluation of the simulation results.

Each of the previously mentioned steps involved in the workflow process includes a detailed description of the data used and explanation of the procedure.

### **3.2 Database**

The information used in the present study has been compiled from several published sources: the Stratigraphic Nomenclature of the Netherlands (Van Adrichem Boogaert & Kouwe, 1997) and NLOG database.

NLOG database provides information about oil, gas, geothermal energy exploration and production in the Netherlands and also, in the Dutch sector of the North Sea continental shelf (NLOG). This site was produced at the request of the Dutch Ministry of Economic Affairs and is being managed by Dutch Organization for Applied Scientific Research (TNO), Geological Survey of the Netherlands, the central geoscience institute for information and research to promote the sustainable management, use of the subsurface and its natural resources (TNO).

The stratigraphy, lithology, TOC, calibration temperatures for the wells were largely derived from publicly available information (data and information on the Dutch subsurface is available at the website: [www.nlog.com](http://www.nlog.com)). Also some input comes from internal company studies and reports thereof: for example deposition maps, sediment-water interface temperature, water depth data and source rock properties.

In order to perform the modelling, a literature study (public papers, conferences) of the geology of the area (blocks A, B, F) was performed. Main references used in this project encompasses:

- The Late Cenozoic Eridanos Delta system in the southern North Sea Basin: a climate signal in sediment supply? (Overeem, Weltje, Bishop-kay, & Kroonenberg, 2001).
- Expressions of shallow gas in the Netherlands North Sea (Schroot & Schüttenhelm, 2003).
- Provenance of Pliocene sediments and paleoenvironmental changes in the southern North Sea region using Samarium-Neodymium (Sm/Nd) provenance ages and clay mineralogy (Kuhlmann, De Boer, Pedersen, & Wong, 2004)
- Surface and subsurface expressions of gas seepage to the seabed-examples from the Southern North Sea (Schroot, Klaver, & Schüttenhelm, 2005).
- Chronostratigraphy of Late Neogene sediments in the southern North Sea Basin and paleoenvironmental interpretations (Kuhlmann, et al., 2006).
- Pliocene paleoenvironment evolution as interpreted from 3D-seismic data in the southern North Sea, Dutch offshore sector (Kuhlmann & Wong, 2008).

### **3.3 Selection of the Wells**

The availability of the data was considered as the main criteria for the selection of the wells, that includes the TOC and temperature measurements for calibration.

To get a better picture of the distribution of gas occurrences, the location of the wells within the study zone with respect to the progradation of the Eridanos Delta was taken into account. A total of 25 wells were selected: A11-01, A12-03, A14-01, A15-02, A15-03, A18-01, A18-02, B10-02, B13-02, B14-01, B16-01, B17-05, B17-06, B18-03, F01-01, F04-01, F05-02, F09-02, F12-02, F17-03 and F17-07. They were evaluated along the progradation units (North- South oriented) and perpendicular to the mentioned progradation (northeast-southwest oriented).

The purpose of this selection is to assess the overall trend of biogenic gas generation and related it to the seismostratigraphic units of the Delta deposits situated in Central Graben and Step Graben respectively.

## CHAPTER 4 PETROMOD BASIN MODELLING

---

The creation and running of the 1D model to simulate the burial history and associated history of porosity, permeability, temperature, source rock maturity and hydrocarbon generation requires a wide variety of input data, boundary conditions and calibration data. The PetroMod default set-ups that were used in the simulations concern the lithology and mixed lithology and their associated default properties (thermal conductivity, radiogenic heat production, and heat capacity), default mechanical compaction equations and default porosity-permeability relations. It has been selected the Sekiguchi model to calculate the thermal conductivity (Sekiguchi, 1984). The heat capacity is calculated with the Waples model (Waples & Waples, 2004), and Athy's Law is used to derive the mechanical compaction.

There are a number of assumptions and conditions underlying the presented 1D modelling:

- Compaction is mechanical, according to vertical effective stress-based rock property model. Chemical compaction is not included.
- Density of pore water is held constant (no density changes with temperature and salinity).
- Pore water and solid rock are incompressible.
- Heat flow is conductive.
- No erosion.

Basic data requirements for the modelling include present-day stratigraphy, lithological properties, source rock properties (total organic carbon, hydrogen index), and quantified time-sequence of events during geological history, boundary conditions (sediment-water interface temperature; basal heat flow; paleo water depth) and calibration data (temperature).

### 4.1 Input data for Basin Modelling

In order to initiate with the creation of a new model in PetroMod<sup>®</sup> v12 version, Schlumberger, it has been extracted a 1D model from previous 3D project.

The following model input is described below:

- Present day stratigraphy and age assignment
- Lithological description of the layers
- Boundary Conditions
- Source rock properties (Geochemical data)

All the steps involved in the model building process are explained hereafter.

#### 4.1.1 Present- day Stratigraphy and Age Assignment

The age assignment associates each horizon with the corresponding age of their deposition and erosion; understanding horizon as the interface between two layers (Hantschel & Kaueauf, 2009). In the present model, the chronostratigraphic units from the Carboniferous until Quaternary were included (Table 5). The ages of deposition were assigned based on the International Geologic Time Scale (Gradstein, Ogg, & Smith, 2004) and adjusted for the Netherlands (Nelskamp & Verweij, 2012) (Appendix 1).

It has been introduced a continuous sequence of deposition. The ages of erosion and hiatus have not been incorporated in the stratigraphic table because it would have required additional maps for the amounts of erosion related to a respective event. The former data is not relevant for the assessment of biogenic gas generation, since the maximum depth of interest for this study includes just until the deposition of recent sediments (Pliocene-Pleistocene).

*Table 5.* Age assignment for each layer of the North Sea Basin from Carboniferous until Quaternary, expressed in Millions of years.

Code	Official Name Nomenclature	Base GS (Ma)	Top GS (Ma)
N	North Sea Supergroup	61,70	0,00
CK	Chalk Group	99,10	61,70
KN	Rijnland Group	140,20	99,10
SK	Niedersaksen Group	150,30	140,20
AT	Altena Group	203,60	163,40
RN	Upper Germanic Trias Group	246,20	203,60
RB	Lower Germanic Trias Group	251,00	246,20
ZE	Zechstein Group	258,00	251,00
RO	Upper Rotliegend Group	267,50	258,00
DC	Limburg Group	326,40	299,00
DCH	Hunze Subgroup	308,70	299,00
DCD	Dinkel Subgroup	311,00	308,70
DCC	Caumer Subgroup	315,30	311,00
DCCU	Maurits Formation	312,30	311,00
DCCB	Baarlo Formation	313,60	313,10
DCCR	Ruurlo Formation	313,10	312,30
DCKK	Klaverbank Formation	315,30	312,30
DCG	Geul Subgroup	326,40	315,40
DCGE	Epen Formation	326,40	317,00
DCGEG	Geverik Member	326,40	316,40
CL	Carboniferous Limestone Group	355,90	326,40

Source: Nelskamp & Verweij, 2012

- **Age Assignment for the Seismic Units**

For the assignment of ages in the stratigraphic seismic units, the information obtained by the interpretation of previous palynology studies in the Late Cenozoic Eridanos Delta System were gathered (Table 6).

According to Kuhlmann *et al* (2006), a solid chronology is essential for the understanding of the basin development and the geological processes that control the stratigraphic sequences. Thus, the latter authors carried out a detailed study at the well A15-03, which was used as a reference for age control. They pointed out that most part of the succession comprises Piacenzian and Gelasian stages where:

- Seismic Unit S1 covers Middle to Late Miocene Sediments corresponding to the distal parts of the sedimentary system that started deposition onto MMU.
- Seismic Units S2 and S3 were assigned to the Zanclean- Piacenzian boundary at 3.6 Ma (Early Pliocene).
- The Gauss-Matuyama boundary dated at 2.58 Ma coincides with the polarity boundary of seismic units S4 and S5.
- The base of the Olduvai subchron (1.94 Ma) matches the top of the seismic unit S11.

In the present study were also included uncertain ages; these events have not been corroborated by a certain chronostratigraphy due to the paucity of absolute age data for the Neogene deposits.

- Short paleomagnetic events within the Matuyama Chron, the Reunion subchron (2.16 Ma) and the X-event (2.44 Ma).
- The Mid Miocene Unconformity (12.4 Ma), a major unconformity discernible on all seismic profiles, which age is difficult to establish within the North Sea Basin because of the progradational character of the Miocene and Pliocene sediments.

Since a complete chronostratigraphic analysis for all the seismic units does not exist, it has been implemented a distribution (interpolation) for those units, whose ages were not available. The reasons could be that the biostratigraphy study was performed in low quality samples, the scarcity of data in the area and/or lacks of resolution for detailed studies.

**Table 6.** Age assignment per each seismic unit of the southern North Sea Basin, expressed in Millions of years. The highlighted numbers (in red) indicate absolute ages obtained by previous chronology studies.

Seismic Unit	Deposition from (Ma)	Deposition to (Ma)	Stages	Series
Seabed	1,78	0	Calabrian / Ionian	Pleistocene
S13	1,86	1,78	Gelasian	Pliocene
S12	1,94	1,86		
S11	2	1,94		
S10	2,05	2		
S9	2,1	2,05		
S8	2,16	2,1		
S7	2,32	2,16		
S6	2,44	2,32		
S5	2,58	2,44		
S4	3,2	2,58		
S3	3,6	3,2		
S2	5,1	3,6	Zanclean	
S1	12,4	5,1		

Source: Kuhlmann et al, 2006

#### 4.1.2 Lithological Description

The model contains the lithological description of 35 layers. As seen in Table 7, the lithologies of 22 layers were assigned to depict the facies of each Group, Formation or Member of the study area from Carboniferous to present day.

There were created 34 mixed lithologies for each interval, based on the stratigraphic nomenclature of the Netherlands (Van Adrichem Boogaert & Kouwe, 1997), using PetroMod® Lithology Editor. Once the lithology of each layer had been established, its properties such as thermal conductivity, heat capacity, permeability, compressibility, porosity and density were automatically assigned by default. The Lithology's nomenclature embodies an approximation to the quantity of material contained for each layer, expressed in percentage (e.g. 50% Sand; 50% Shale).

*Table 7. Lithology of the stratigraphic horizons from Carboniferous Limestone Group to North Sea Supergroup.*

Code	Official name Nomenclature	Lithology
N	North Sea Supergroup	50_Sand_50_Shale
CK	Chalk Group	100_Chalk
KN	Rijnland Group	50_Shale_25_Marl_25_Sand
SK	Niedersaksen Group	50_Sand_50_Shale
AT	Altena Group	50_Shale_25_Marl_25_Sand
RN	Upper Germanic Trias Group	50_Shale_25_Marl_25_Sand
RB	Lower Germanic Trias Group	75_Sand_25_Shale
ZE	Zechstein Group	40_Shale_30_Anhy_30_Lime
RO	Upper Rotliegend Group	70_Sand_15_Silt_15_Shale
DC	Limburg Group	60_Shale_40_Sand
DCH	Hunze Subgroup	75_Shale_25_Sand
DCD	Dinkel Subgroup	60_Sand_20_Silt_18_Shale_2_Coal
DCC	Caumer Subgroup	48_Shale_25_Sand_25_Silt_2_Coal
DCCU	Maurits Formation	80_Shale_15_Sand_5_Coal
DCCB	Baarlo Formation	78_Shale_20_Sand_2_Coal
DCCR	Ruurlo Formation	48_Shale_25_Sand_25_Silt_2_Coal
DCCK	Klaverbank Formation	48_Shale_25_Sand_25_Silt_2_Coal
DCG	Geul Subgroup	75_Shale_25_Sand
DCGE	Epen Formation	75_Shale_25_Sand
DCGEG	Geverik Member	80_Shale_10_Sand_10_Silt
CL	Carboniferous Limestone Group	Limestone (Chalk, 95% calcite)

Source: Nelskamp & Verweij, 2012

- **Lithological description of the Seismic Units**

According to several reports published, a total of 13 depositional units were identified in the sequence seismostratigraphic framework for the Neogene in the North Sea.

For the establishment of the lithology, the information concerning the percentage of each component included in every unit has been extracted from a 3D model. Subsequently, 14 representative mixed lithologies for each stratigraphic seismic unit were generated (table 8).

*Table 8. Mixed Lithologies of the seabed and the 13 seismic stratigraphic units.*

Code	Mixed Lithology
Seabed	40_Sand_21_Shale_39_Silt
S13	36_Sand_35_Shale_29_Silt
S12	32_Sand_44_Shale_24_Silt
S11	31_Sand_48_Shale_21_Silt
S10	31_Sand_48_Shale_21_Silt
S9	33_Sand_41_Shale_26_Silt
S8	29_Sand_55_Shale_16_Silt
S7	29_Sand_55_Shale_16_Silt
S6	30_Sand_50_Shale_20_Silt
S5	34_Sand_45_Shale_21_Silt
S4	30_Sand_50_Shale_20_Silt
S3	33_Sand_51_Shale_16_Silt
S2	30_Sand_50_Shale_20_Silt
S1	28_Sand_58_Shale_14_Silt

#### 4.1.3. Boundary conditions

Boundary conditions comprise the sediment-water interface temperature, the water depth and the basal heat flow.

- **Sediment-water interface temperature**

TNO's Geo-biology team provided the data of the sediment-water interface temperature boundary conditions used in the model (Appendix 3). The sediment-water interface temperature influences subsurface temperature and as a consequence, the levels of thermal maturation of petroleum source rocks. As shown in the figure 8, the mean surface temperature was estimated by a default function of the PetroMod, which include the calculation of the evolution of ocean surface temperatures through time depending on the latitude of the area. Additionally, a more detailed temperature evolution was assigned for the Cenozoic (Nelskamp & Verweij, 2012). The later was determined using high-resolution pollen records and several organic geochemical proxies, that provided detailed insights in the climate evolution around the Pleistocene and Pliocene transition (Donders, et al., 2009).

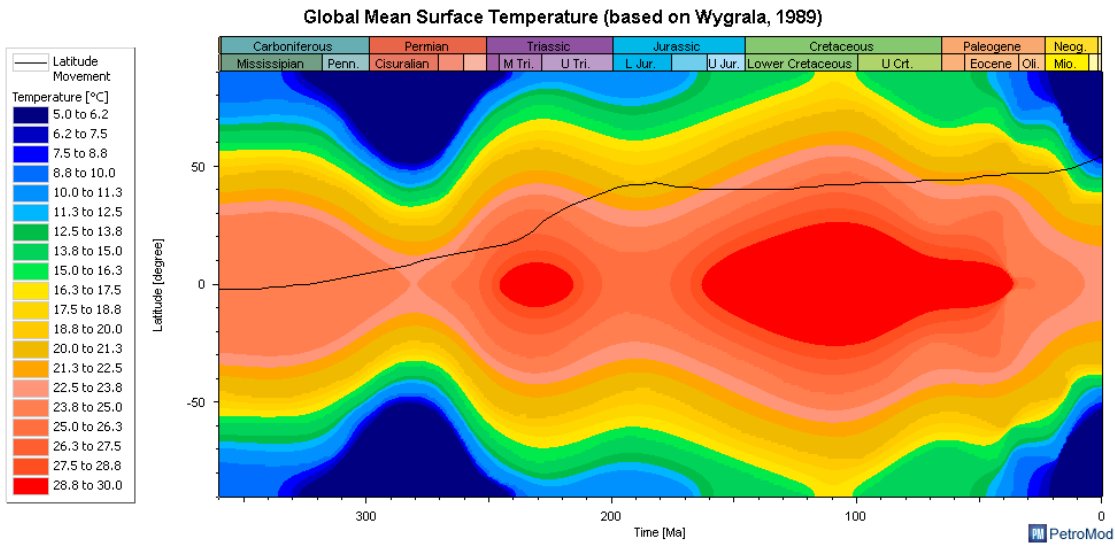


**Figure 8.** Global Mean Surface Temperature based on Wygrala study; history of surface temperature for a certain location on earth (indicated with the black line).

In the figure 9, it can be appreciated a strong variation in temperatures during the Neogene, from global warming in the Miocene to a cold climate presented in the Pliocene; this shift is related to the onset of the Northern Hemisphere Glaciation with the first glacier build up and retreat in the surrounding area of North Sea and Scandinavia (Mangerud, Jansen, & Landvik, 1995 in Kuhlmann & Wong, 2008)

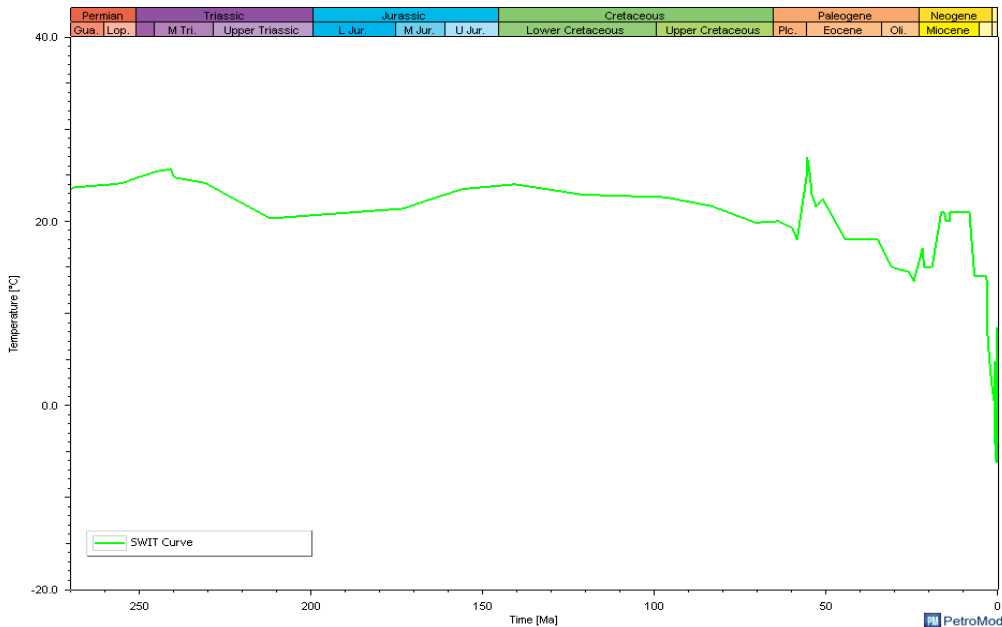


**Figure 9.** Sediment-water interface temperature boundary condition used in the model (Nelskamp & Verweij, 2012).

- **Water depth**

Fluctuations in water depth influence the burial history of the sediments and affect the sediment-water-interface temperatures. The water depth boundary condition is a requirement for the determination of the evolution of depth below sea floor through time.

In general, water depth history can be derived from isostasy considerations of crustal stretching models with assumptions on global sea level changes or from known distributions of sediment facies(Hantschel & Kaueauf, 2009).

The Water depth describes the burial and uplift of the basin. It is necessary to determine the evolution of depth below sea floor through time.

The water depth input data were based on sedimentological descriptions of the stratigraphic units given in Van Adrichem Boogaert & Kouwe (1997) (Appendix 2). Also diverse micropaleontological studies carried out by the TNO's Geobiology team, provided additional information about the evolution of the water depth during deposition of the North Sea Group in the Cenozoic (Figure 10).

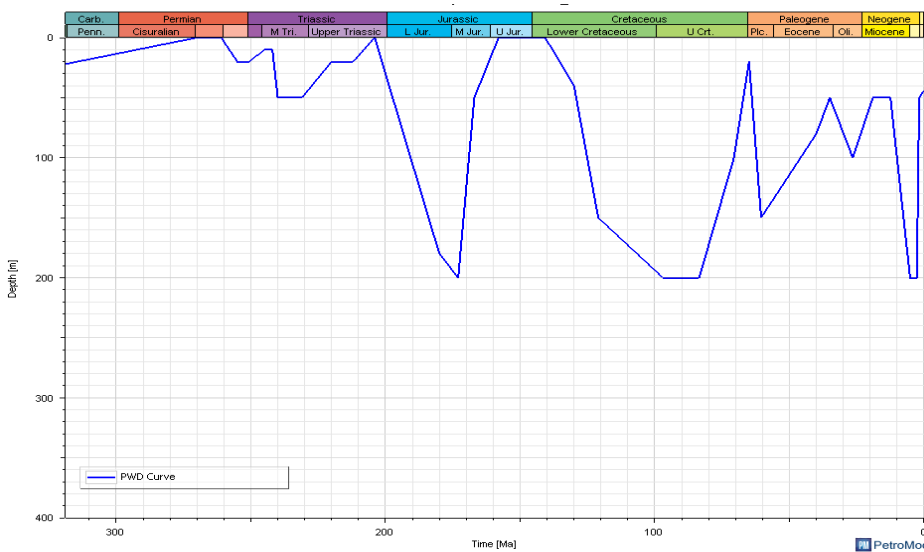


*Figure 10. Water depth through time used in the model (Nelskamp & Verweij, 2012).*

- **Basal Heat flow**

The basal heat flow through time describes the lower thermal boundary of the model. Basal heat flow history directly influences the temperature history of the sediments and hence the source rock maturity and hydrocarbon generation history.

The range of surface heat flow values for the Dutch offshore is between 55-70 mW/m<sup>2</sup> and is based

on analysis mantle P wave velocities (Goes, Govers, & Vacher, 2000). Subsequent, The output has been calibrated with measured temperatures in order to get the best fit.

Initially two suppositions were made for the basal heat flow values. It has been assumed a constant value of  $60 \text{ mW/m}^2$ , expressed in milliwatts per square meter ( $\text{mW/m}^2$ ), as an input for the modelling area.

However, for a specific number of wells, the heat flow value had been modified in order to have a better match with the measure data. For some wells, it have been introduced a high value of  $70 \text{ mW/m}^2$ . The latter is related to the salt structures near the area of the measurement.

#### **4.1.4 Geochemical Data (Source Rock Properties)**

Source Rock Properties encompass Total Organic Carbon (TOC), Hydrogen Index (HI) and kinetics parameters.

These essential properties are the total organic carbon (TOC) measured by combustion of rock samples and the hydrogen index (HI) obtained through pyrolysis of rock samples for petroleum-generation potential. Also required are kinetic parameters for the thermal conversion of the source-rock kerogen to petroleum.

Reaction kinetics is used to predict the phases and properties of hydrocarbons generated from source rocks of various types.

## **4.2 Calibration of the Model**

The model was calibrated principally with temperature data. Although there were vitrinite reflectance and pressure data available for few wells, they were not considered as main parameters for the calibration due to the high uncertainty of the measurement.

Drill-Stem Test Temperature (DST) measurements, corrected Bottom-Hole Temperature (BHT), Bottom-Hole Temperature extrapolated (BHTX), Formation test (FITP), Along hole temperature (AHT) and Formation interval test data (FITP) were also considered to be appropriate for the model calibration. A color code was implemented for a better identification of the quality of the measurement, that later would be taken into account to select the best-fit model.

It has been performed the calibration of the petroleum system model in order to check whether the simulation results are in accordance with measured temperature data available in the area of study.

### 4.2.1. Temperature

The main given data, which contained information about the subsurface temperature in the blocks A, B and F, were from bottom hole temperature (BHT). Unfortunately, the evaluation of subsurface temperatures using BHTs remains fraught with uncertainty (Luijendijk, Ter Voorde, Van Balen, Andriessen, Verweij, & Simmelink, 2009)

In view of the fact that drilling fluids may disturb the measurements of downhole temperatures, it would require to the well logger to carry out sequences of three logging runs (that record time and temperature) and then, apply certain mathematical correction methods. These methods should contain a rectification according to a ratio of cooling time divided by warming time (Cornford, 2009). Thus, the temperature *prior* drilling interfering would be determined by extrapolation.

Also, missing or false corrections for *in situ* conditions of temperature can cause systematic deviations from the correct thermal parameters. The uncertainties resulting from these errors are not considered in this project due to it could lead to a proportional error in the heat flow.

Whereas, the drill stem test (DST) temperatures, based on high flow volumes of oil from the producing formation, are generally most reliable for calibration of petroleum system models (Peters & Nelson, 2009). Therefore, it will be considered as good quality data. Figure 11 shows the temperature plot of one well in the block A, it can be noticed the different source data used for calibration. In general, the temperature data are lower than the true formation temperature.

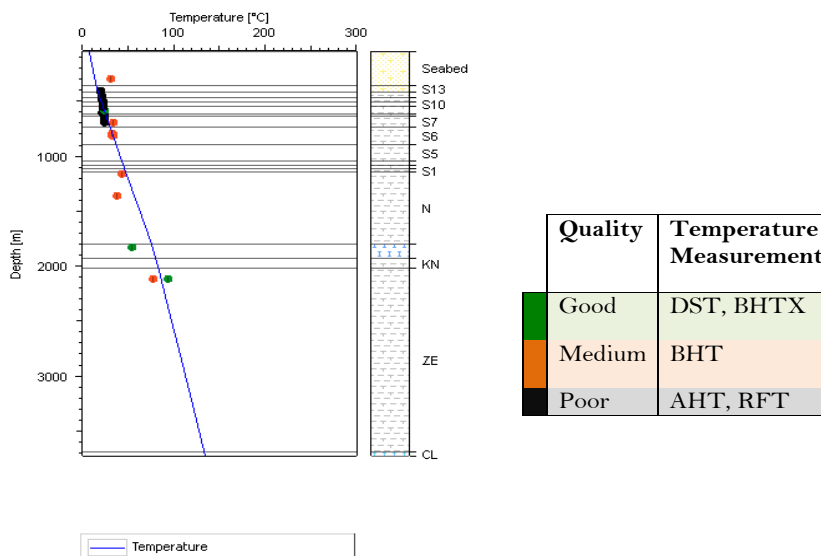


**Figure 11.** Temperature reconstruction plot validated by calibration against diverse temperature data sources and correction methods.

## 4.2.2 Heat Flow

Initially, It has been assumed two constant values of heat-flow as an input for the modelling area, but once the calibration with the temperature measurements was achieved for the different wells, it was obtained values in the range 55-70 mW/m<sup>2</sup>, that correspond with the values obtained by Goes, Govers, & Vacher (2000).

As mentioned before, in order to get the best match with the simulated curve, it has been modified the heat flow of several wells. Modelling results indicate that present day basal heat flow at the selected wells reach minimum values 56 – 60 mW/m<sup>2</sup> with a maximum values of 69-70 mW/m<sup>2</sup>

The wells with higher heat flow values were founded mainly in the north-western part of the area of study, particularly in the blocks A and B.

The Wells A12-03, A18-01, B13-02, F01-01 shows an abnormally heat flow outcome (70mW/m<sup>2</sup>). These wells are located above salt structures. Therefore, these higher values could be due to proximity of the measure to Zechstein Group salt domes(higher thermal conductivity).

In the figure 12, it can be observed the distribution of salt domes in the northern Netherland offshore and the location of the selected wells. These image a better visualization of those wells with high heat flow and their vicinity with the salt structures.

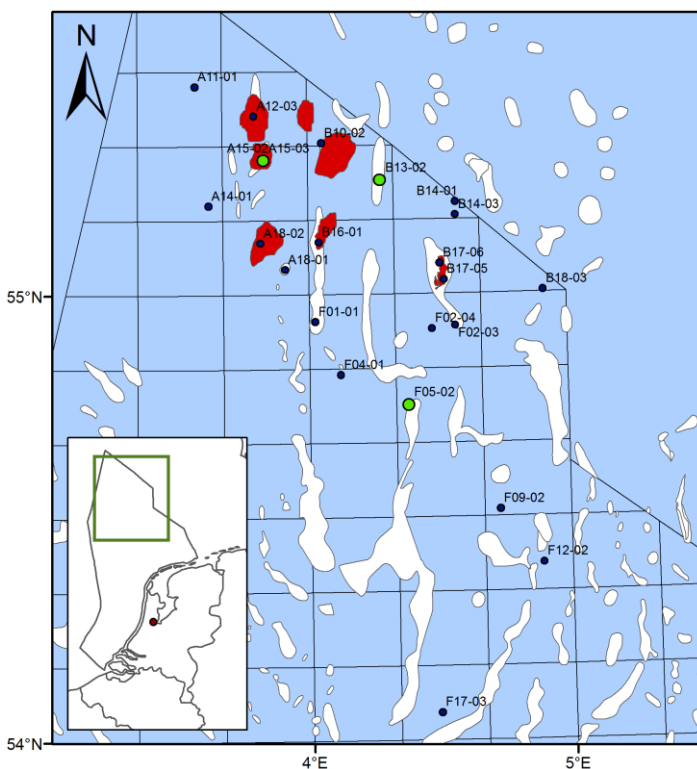


**Figure 12.** Location of the southern North Sea with the corresponding 25 selected wells. Red spots indicate gas occurrences.

## 4.3 PetroMod Modelling Results and Discussions

The aim of this section is to evaluate how the fluctuation of surface temperature in the Pleistocene and Pliocene sediments affects in the generation of methanogenic gas. This segment attempts to provide an overview of the results obtained with the software PetroMod. It was presented a *grosso modo* a discussion about porosity of the area, however, the main emphasis was given to the impact assessment of the temperature oscillation in the tertiary sediments for each of the selected wells.

Model output was compared with calibration parameters in order to adjust the conceptual model and improve the match between the simulation and measure data.

25 wells were selected for the completion of this study to evaluate whether the southern North Sea basin, specifically block A, B and F, gathers the requirements for the biogenic gas generation. However, as case of study, the simulation of three representative well (A15-03, B13-02 and F05-02) was performed and fully described. The results for the rest of the wells were included in the annexes.

### 4.3.1 Porosity

A comparison of the percentage porosity for each seismic stratigraphic unit per the selected wells is presented in table 9.

Since S1-S13 layers are unconsolidated sediments, present extremely high porosities. The porosity would decrease to the deeper depths due to an increase of the effective stress (compaction). As showed in table 9, porosity percentages presented at shallower depths are in a range of 26-47%.

However, It should be consider that there are uncertainties related to the mixed lithologies created for each formation, group, member and seismic stratigraphic unit in the southern North Sea basin. As it has been performed an average of the lithological content, a slightest modification in the content percentages will change their associated default properties and therefore, can produce a different output.

As seen in figure 13, a similar trend of high porosity values is showed in wells A15-03, B13-02 and F05-02, in the North Sea group whilst the deepest layers (Chalk, Zechstein and Limburg group) showed values less than 15%. Some porosity data values are presented for well A15-03, nonetheless it has not been taken into account for the calibration due to uncertainty of the quality data (Figure 13).

*Table 9. Porosity percentage per seismic stratigraphic layer for the 25 selected wells.*

Well	S13	S12	S11	S10	S9	S8	S7	S6	S5	S4	S3	S2	S1
A11-01	42,86	41,64	40,17	39,15	37,84	35,55	34,19	32,98	31,26	29,57	28,94	28,72	27,9
A12-03	43,19	42,15	41,24	40,36	39,25	38,43	37,24	35,16	33,53				
A14-01	44,14	43,09	41,89	40,65	38,66	36,15	34,73	33,32	31,49	30,30	29,77		
A15-02	44,52	43,68	42,7	41,64	40,43	39,11	37,64	35,65	32,87	30,68	29,87	29,19	28,25
A15-03	43,01	42,10	41,12	40,07	38,96	37,64	36,27	34,3	31,61	29,41	28,61	27,94	26,98
A18-01	44,03	43,09	42,01	41,06	39,83	38,59	37,46	35,05	31,95	29,54	28,93	28,31	
A18-02	44,03	43,28	42,51	41,59	40,21	38,97	37,57	34,79	31,93	30,09	29,48	28,65	
B10-02	43,73	42,93	42,25	41,5	40,52	39,82	39,22	36,81	33,53	31,56	30,67	28,94	27,18
B13-02	43,87	42,95	42,16	41,51	40,71	40,02	39,65	38,06	35,02	32,91	31,9	29,93	27,66
B14-01						41,35	41,36	39,66	37,62	34,50	29,46	25,64	
B16-01	44,59	44,08	43,5	42,89	41,95	41,4	40,66	37,98	34,62	32,27	31,25	30,45	29,12
B17-06	38,07	36,67	36,21	44,64	44,26	43,57		36,02	40,31	38,13	32		
B18-03	45,59	45,46	44,78	44,04	43,51		42,97	40,62	38,85	38,24	35,02	30,16	26,7
F01-01	45,56	44,86	43,83	43,06	42,13	41,14	40,37	37,6	33,64	31,48	31,14	30,38	
F02-03	46,04	45,78	45,39	44,72	43,94			42,56	38,79	35,7	33,58	31,28	29,27
F03-07	46,58	46,53	45,72	44,69				43,55	40,95	38,75	35,01	29,69	26,53
F03-08	45,54	45,47	44,85	44,08	43,57			43,08	40,78	39,08	38,21	34,96	27,24
F03-01	45,91	45,74	44,95	44,08	43,53			42,97	40,45	38,57	37,69	34,41	26,74
F04-01	43,76	42,59	41,54	40,84	39,73	38,62	38,16	35,93	32,05	29,72			29,29
F05-02	44,61	43,88	42,86	41,86	40,98	40,32	40,02	38,59	35,27	31,38	29,26	29,04	28,61
F09-02	45,96	45,57	44,63	43,71	42,7			41,21	37,73	33,16	30,46	29,93	29,61
F12-02	47,09	47,05	46,30	45,26	44,42			43,26	39,62				32,48
F17-03	47,62	46,6	45,4	44,4	43,51			41,71	38,29				31,8
F17-07	45,46	44,52	43,48	42,5	41,66	40,96		39,7	34,55				30,46

### 4.3.2 Thermal conductivity

In the figure 14 are depicted the variations in vertical thermal conductivity for the three wells selected. The blue line indicates temperature evolution and the black line represents the vertical thermal conductivity.

In general, higher values were found for the Zechstein Formation and Carboniferous Limestone group. Lower vertical thermal conductivity values were obtained in the North Sea Group and Caumer Subgroup.

The presence of salt domes produces an increment of the thermal conductivity within Zechstein Group and a decline of the values in Lower Germanic Triassic Group.

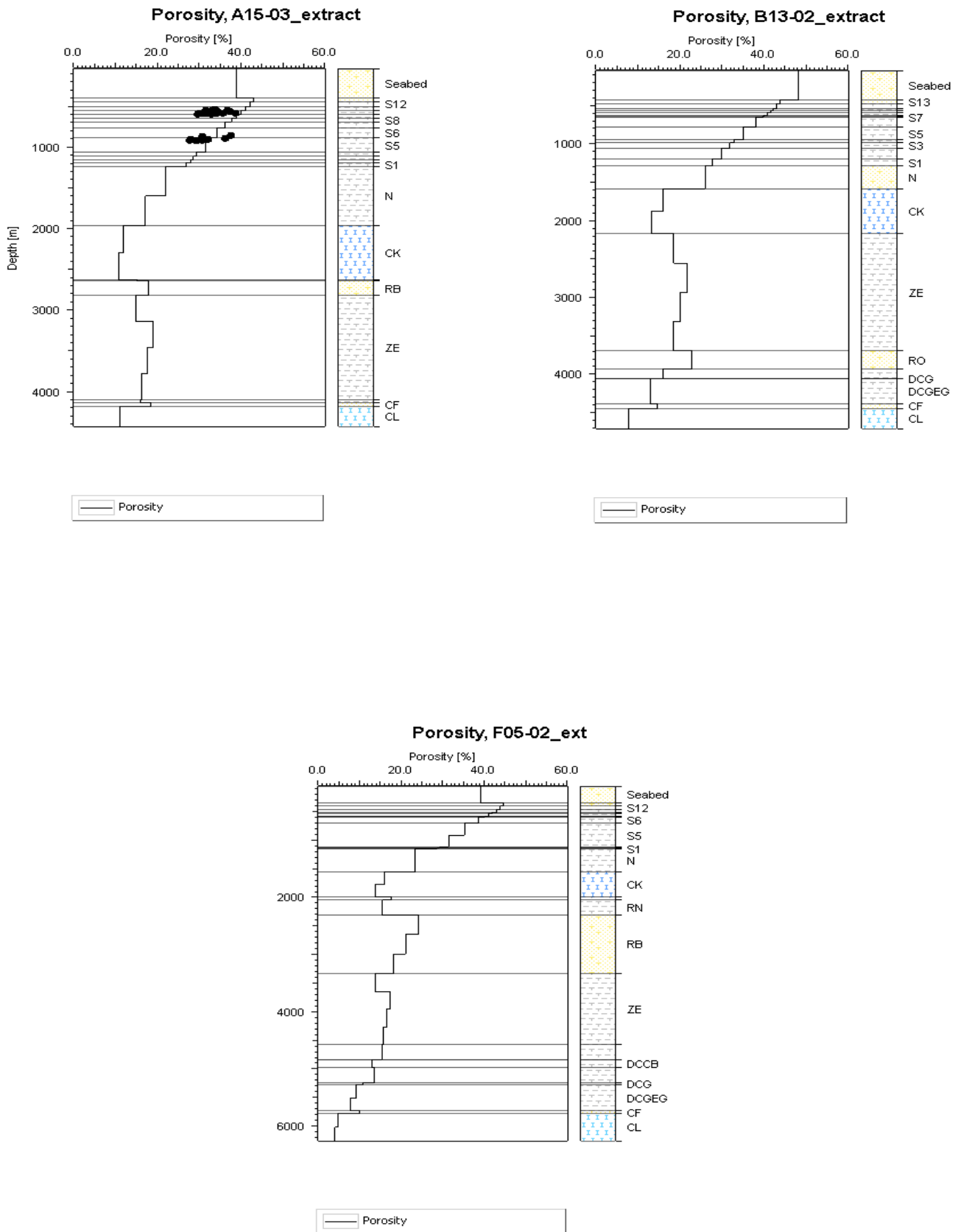


Figure 13. Plots Porosity vs depth at wells A15-03; B13-02 and F05-02.

As discussed earlier, high thermal conductivity of salt can cause abnormally high heat flow values, since the measurements were taken in the adjacency of salt structure.

### 4.3.3 Temperature

Methane in the marine environment is due to anaerobic microorganisms that use organic carbon or acetate in the sediment column as an energy source. Methanogens subsist with tolerance at certain temperatures and depend on the species. However, recent studies demonstrate that all species are less efficient at low and high temperatures.

As it can be observed in tables 10, 11 and 12, detailed information of temperature is emphasized, evidencing the depths of the layers (S1-S3) that fall into 30-50°C. This range has been defined making reference to the favourable temperature for the living conditions of the archaea. Optimum temperature varies with species. The range does not take into account those species that live in extreme environments (i.e. thermophile or psychrophile).

In the northern part of the study area (wells A15-03 and B13-02), more horizons are contained in the temperature optimal window.

Reconstructed burial results reveal that the optimal range of temperatures involve:

- At well A15-03, the seismic units between S1-S6 which are reached at depths 880 -1200 m approx.
- At well B12-03, there are more stratigraphic units included than in the other wells: S1-S9 and at shallower depths 600 to 1200 m.
- At well F05-02 the optimal condition comprise S1-S5 at depths 900 to 1100 m approx.

As can be seen in figure 14, the well A15-03 does not present a perfect match, however it should be highlighted that poor quality data for the calibration was used. The well B13-02 presents a good fit considering that the calibration was done with good quality temperature data. In general, well F05-02 shows good correspondence between the temperature curve and the temperature data used.

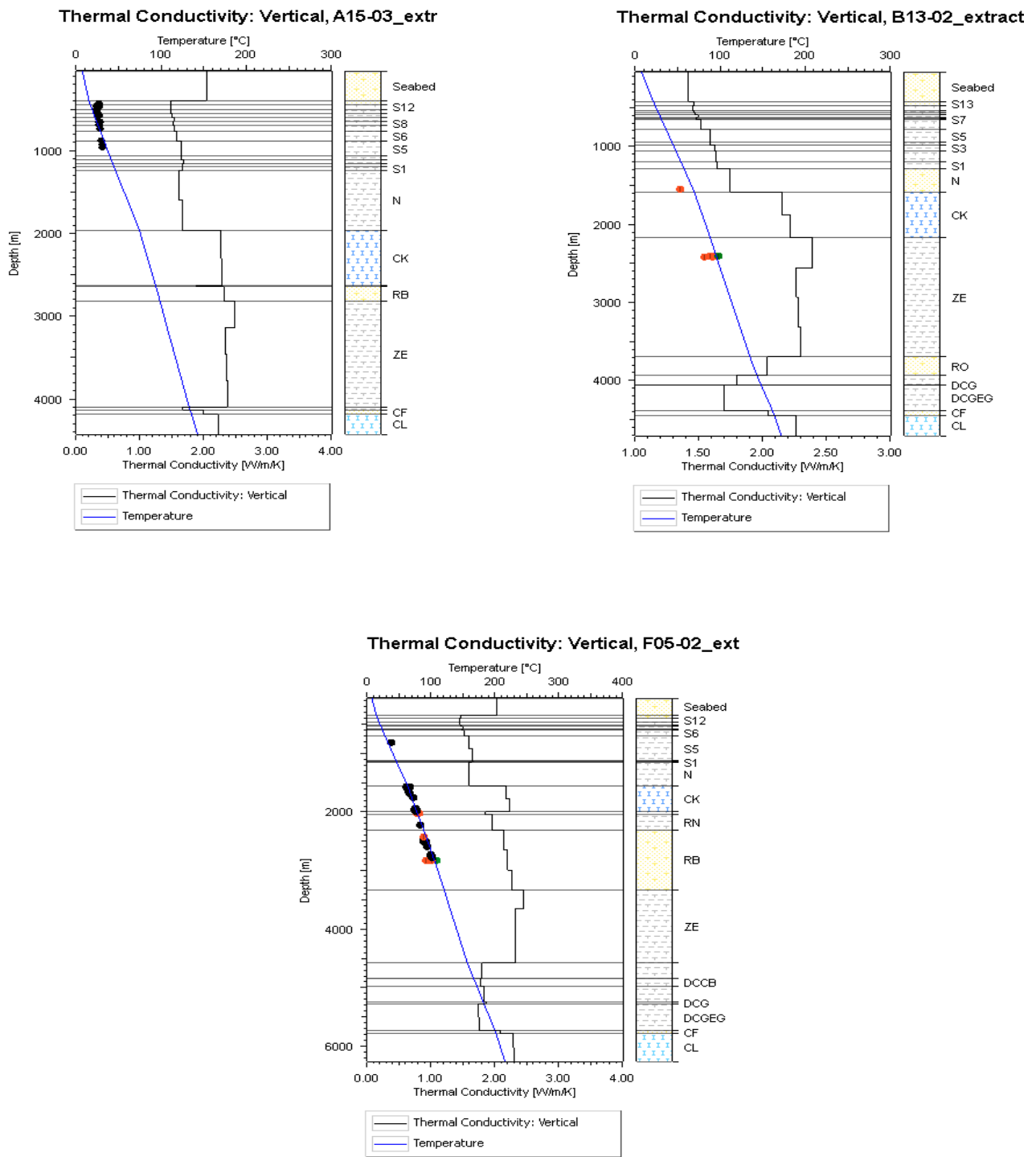


Figure 14. Plots of Thermal Conductivity and Temperature vs depth at wells A15-03; B12-03; F05-02.

*Table 10.* Temperature per each seismic unit at well A15-03. The values in red represent the units that belong to the optimal temperature window.

WELL A15-03		
Layer	Depth meter[m]	Temperature Celsius[°C]
Base of S13	443	16,5
Base of S12	508	18,8
Base of S11	551	20,35
Base of S10	596	21,99
Base of S9	646	23,81
Base of S8	691	25,49
Base of S7	767	28,34
Base of S6	886	32,81
Base of S5	1063	39,36
Base of S4	1112	41,2
Base of S3	1157	42,87
Base of S2	1192	44,19
Base of S1	1236	45,85

*Table 11.* Temperature per each seismic unit at well B12-03. The values in red represent the units that belong to the optimal temperature window.

WELL B13-02		
Layer	Depth meter[m]	Temperature Celsius[°C]
Base of S13	475	23,8
Base of S12	545	26,8
Base of S11	568	27,81
Base of S10	598	29,1
Base of S9	628	30,41
Base of S8	648	31,28
Base of S7	659	31,76
Base of S6	782	37,15
Base of S5	948	44,33
Base of S4	984	45,86
Base of S3	1054	48,88
Base of S2	1199	55,15
Base of S1	1286	58,91

*Table 12.* Temperature per each seismic unit at well F05-02. The values in red represent the units that belong to the optimal temperature window.

WELL F05-02		
Layer	Depth meter[m]	Temperature Celsius[°C]
Base of S13	403	16,09
Base of S12	460	18,27
Base of S11	514	20,43
Base of S10	540	21,44
Base of S9	580	23,02
Base of S8	590	23,43
Base of S7	604	23,98
Base of S6	708	28,22
Base of S5(Part 2/2)	913	36,43
Base of S5(Part 1/2)	1117	44,65
Base of S4	1131	45,23
Base of S3	1142	45,69
Base of S1	1151	46,04

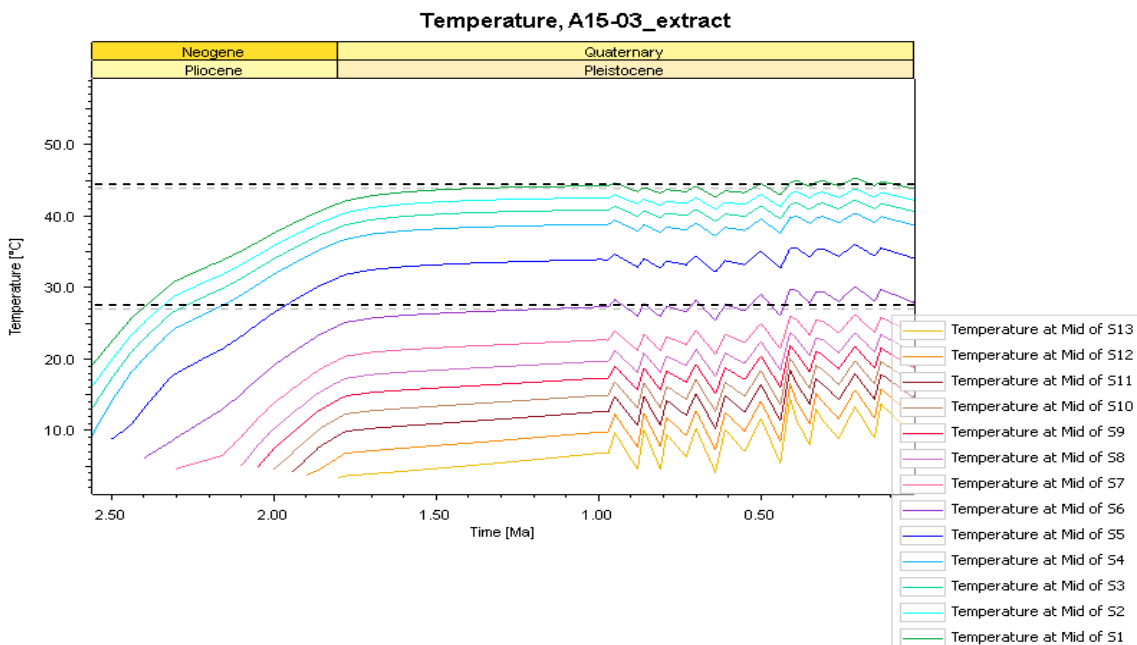


*Figure 15.* Detailed temperature data for the Cenozoic showing the fluctuation of temperatures (°C) during time (Ma) at well A15-03.

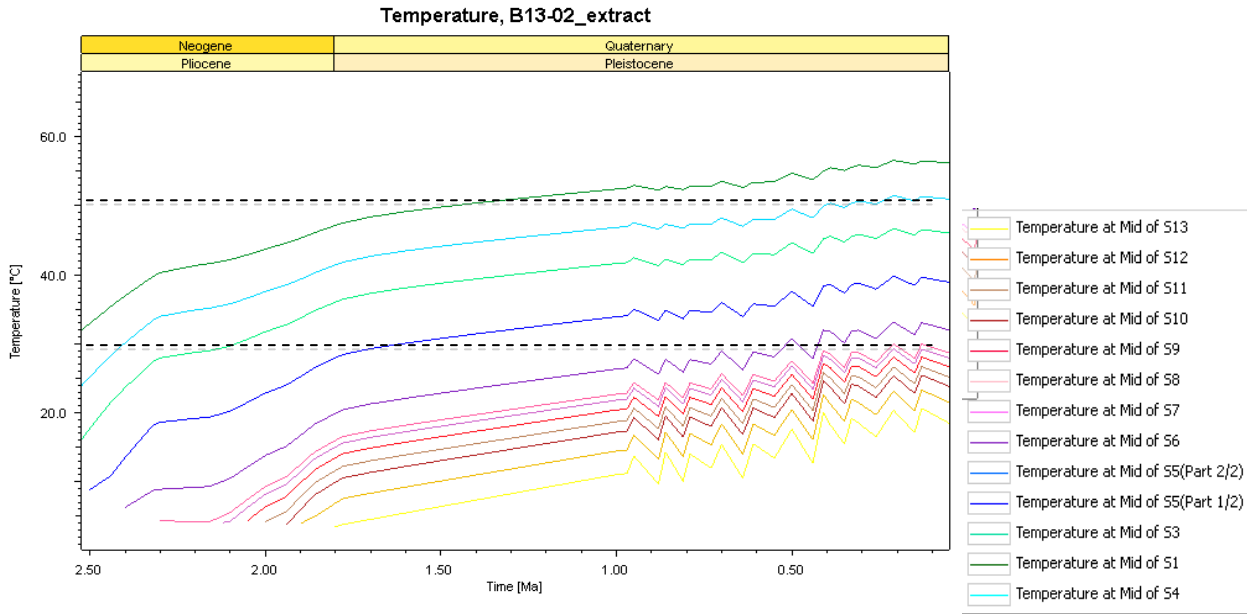


**Figure 16.** Detailed temperature data for the Cenozoic showing the fluctuation of temperatures (°C) during time (Ma) at well B13-02.

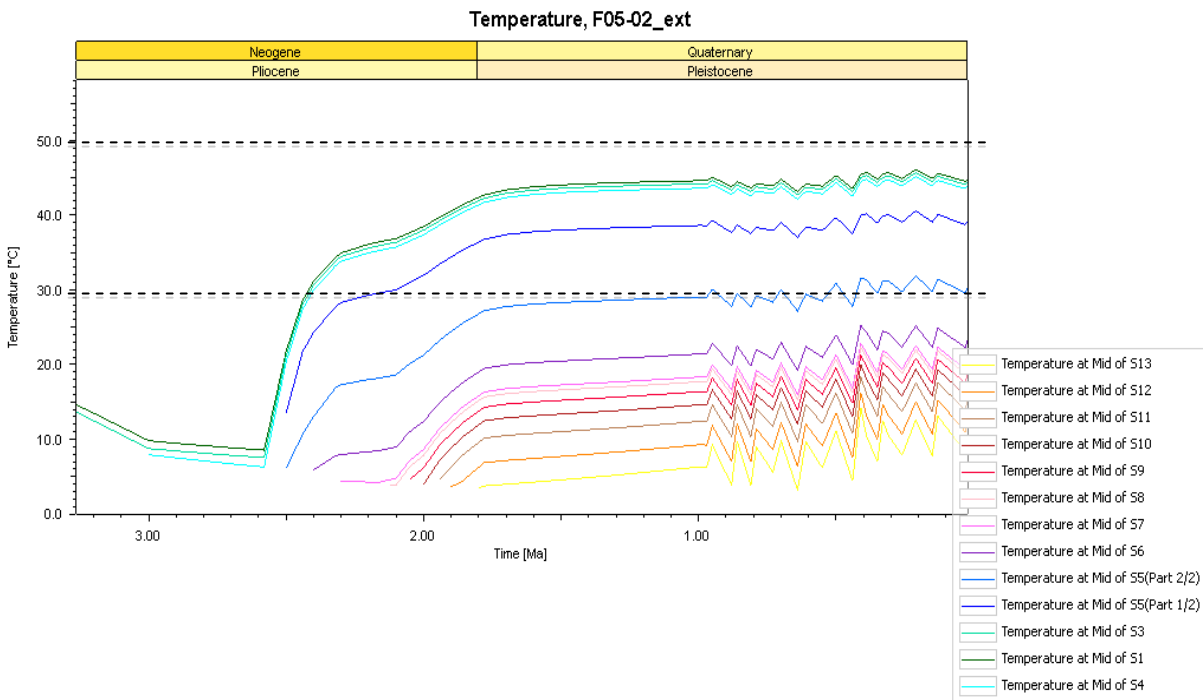


**Figure 17.** Detailed temperature data for the Cenozoic showing the fluctuation of temperatures (°C) during time (Ma) at well F05-02.

#### 4.3.4. Does the subsurface temperature fluctuation affect the Biogenic Gas generation?

It has been introduced a detailed input data to depict the variations of surface temperatures taking into account the effects of warming and cooling fluctuations during the late Cenozoic (Appendix 3). In figure 15, 16 and 17 a reconstructed temperature history of the basin for the wells A15-03, B13-02 and F05-02 provided by PetroMod is presented.

The temperature (expressed in Celsius) is represented by the ordinate axis and the time (expressed in Million years) is showed in abscise axis. The dash linedenotesthedomain, where theoptimal temperature window for biogenic gas generationappears. The temperate evolution of each seismostratigraphicunit is represent by diverse colours. The sharp peaks represent thedrastic climate variation in the Pleistocene.

The incorporation of a detailed glacial-interglacial temperature data does not have a relevant effect on the overall behaviour due to the oscillations of temperatures for each horizon diminished with increasing depth.

#### 4.3.5. Relation between the Seismic Stratigraphy Units and Biogenic Gas generation

According to Rice & Claypool (1981), the conditions for generation of biogenic gas are the following

- Temperature
- Presence of organic matter
- High sedimentation rates
- Anoxic environment
- Pore Space

In addition to the above listed general limiting assumptions and conditions, the results obtained with PetroMod were compared with the five Paleo-environments interpreted by Kuhlmann, et al., (2006) in previous studies.

- Temperature:

In order to study the wells that meet the conditions for the potential creation of biogenic gas, it has been evaluated which of the seismic stratigraphic units are constrained within the optimal range of temperature. Although the temperature varies with species, it can be observed that all species are less efficient at low temperature and high temperature, a notable optimum around 30-50°C can be defined (Clayton C. , 2009).

In all blocks there are seismic units that accomplish temperature conditions: the seismic units that gather the first requirement for methanogenesis in block Fare from S1 to S5 andin the case of blocks A and B correspond to S1-S6 and S1-S7, respectively.

As can be seen in table 13, some exceptions are foundat the well B13-02,where it can be observed that window range is extended until unit S9 whilst for some wells from block F (F03-07, F03-08) and few

wells belonging to block B (B14-01, B18-03) located in the southeastern part of area of study, the optimal temperature is found in intervals S1 until S3.

*Table 13. Seismic Units within the optimal range of temperature (30-50°C) for all blocks considered.*

Blocks	Well	Seismic Units
A	A11-01	S1-S6
	A12-03	S5-S7
	A14-01	S1-S7
	A15-02	S1-S7
	A15-03	S1-S6
	A18-01	S1-S6
	A18-02	S1-S7
B	B10-02	S1-S6
	B13-02	S1-S9
	B14-01	S2-S3
	B16-01	S1-S6
	B17-05	S1-S5
	B17-06	S3
	B18-03	S2-S3
F	F01-01	S1-S6
	F02-03	S1-S5
	F03-01	S1-S2
	F03-07	S1-S2
	F03-08	S1-S3
	F04-01	S1-S5
	F05-02	S1-S5
	F09-02	S1-S5
	F12-02	S1-S5
	F17-03	S1-S5
	F17-07	S1-S5

The location of the wells is depicted at figure 18 showing the distribution of optimal range temperature domain in the northern Dutch offshore.

It has been suggested that an increase of the temperature follows the delta progradation. In the blocks A and B, which correspond to thicker deposition sequence, the favourable temperature window encompasses the largest range of seismic units.

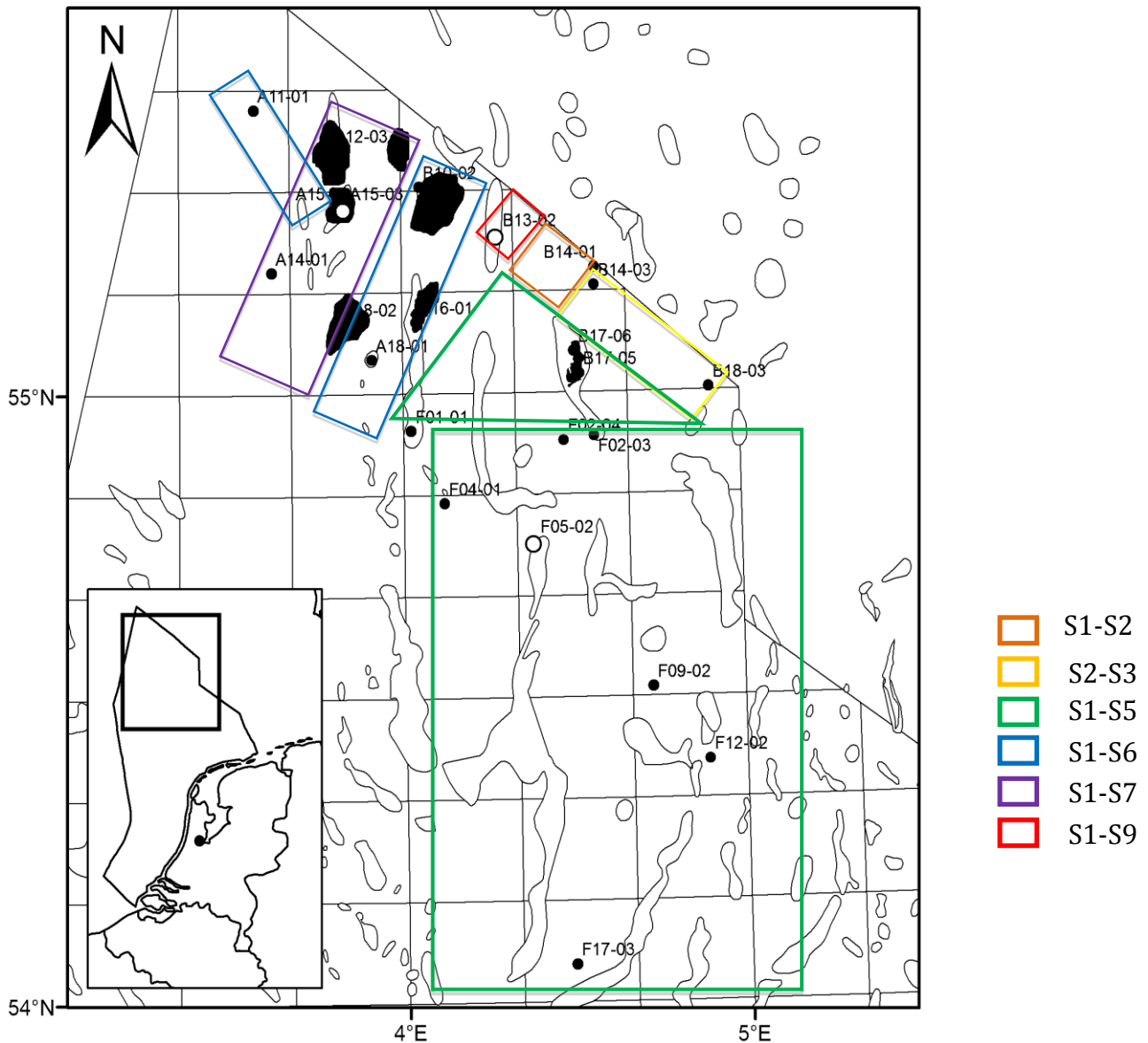


*Figure 18.* Location of the wells showing these seismic units confined within the optimal temperature window.

- *Presence Organic Matter (Total Organic Content)*

The potential gas available is dependent on the amount of organic matter present in the fetch area and the heating history. The conditions favouring source-rock accumulation are anoxia and high sedimentation rate, which promote the survival of organic matter, while burial of the source rock to an adequate surface temperature is the basis for maturation and generation (Cornford, 2009)

The present model includes the TOC of the shallower layers because particular attention is paid to processes and conditions affecting gas potential from Pleistocene to Present day. As an example, it has been included some total organic content measurements at certain depth for the wells A15-03; A16-01; F04-01 and B14-01. As can be seen in figure 19, the ranges of depth are in between 500-1500m.

In general, the ranges of TOC percentages comprehend values from 0,55 up to 3,5. For that reason and due to the scarcity of the complete data in most of the wells, three scenarios are presented in the next chapter for the evaluation of the shallow biogenic gas accumulation in the northern of Netherlands offshore.

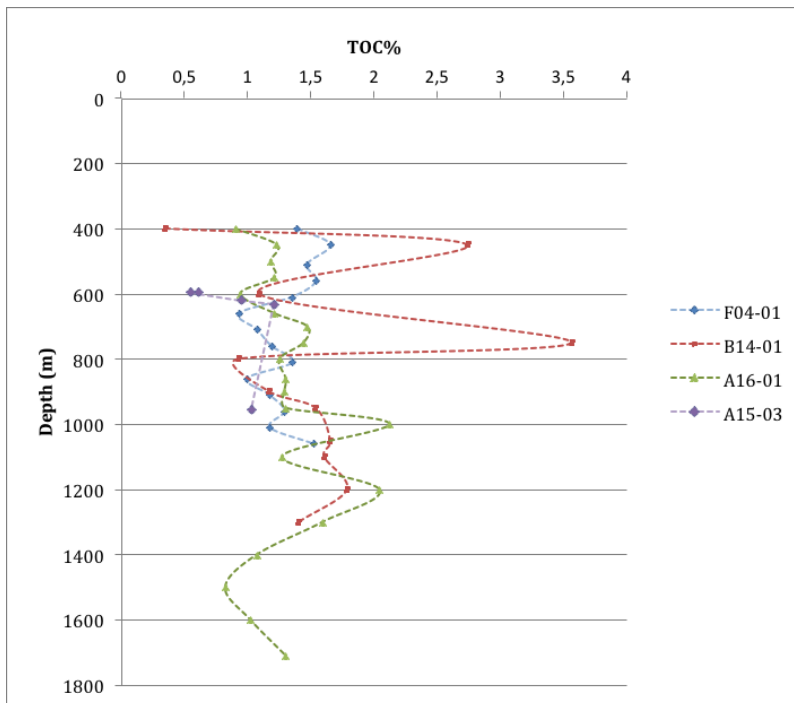


**Figure 19.** Measurements of TOC percentage vs depth at the wells A15-03; A16-01; F04-01 and B14-01 (TNO internal report).

- **Sedimentation Rate**

As mentioned before, the biogenic gas forms soon after sediment deposition and their accumulations are associated with rapid sedimentation and lower geothermal gradients.

A key control is the burial rate of the source rock: if it is too slow, little metabolizable organic carbon survives into the methagenic zone and any methane generated is lost to the surface; but if it is too fast, the temperature rapidly becomes too high for the bacteria to cope. The optimum burial rate for a basin depend on the geothermal gradient, and varies from 200 to 1000 m/Ma (Clayton C. , 1992).

Kuhlmann & Wong (2008) calculated the accumulation rates in the intra delta deposits dividing the volume of each seismic unit by their corresponding duration. The latter was inferred from the gradient of the line between age points. Results of these calculations indicate that seismic units S2-S4 show relatively low accumulation rates (less than 6km<sup>3</sup>/Ma) and during deposition of seismic units S5-S7 sediment accumulation increased substantially (up to 30km<sup>3</sup>/Ma). They found that the Paleo environment-2, which encompasses the seismic units S4 and S5, is generally favourable for Biogenic gas generation since in this interval the rates of sedimentation are higher, assuming an increment rate in the cooler periods because of the enhanced erosion and precipitation under glacial conditions. The

S4 and S5 interval units were deposited in a transitional paleoenvironment of alternating cold and warm periods. This lowermost interval of the Pleistocene prograding succession is early Gelasian in age. During this time, coarser silty sandstones were deposited. The authors refer that one conspicuous feature of the alternation is, that during cold period grain size was very fine (clayey to clayey silt) while during warm periods grain size is coarse (silty). Kuhlmann (2004) has explained this behaviour by the interplay of glacial activity during cold periods and enhanced precipitation during warm periods.

A comparison of the sedimentation rates per seismic units in Block A (specifically wells A11-01, A12-03, A14-01, A15-02, A15-03, A18-01, A18-02); Block B (B10-02, B13-02, B14-01, B16-01, B18-03, B17-06, B17-05); and Block F (F01-01, F0203, F03-07, F04-01, F05-02, F09-02, F12-02, F17-07, F03-01, F03-08) is presented (tables 14, 15 and 17).

**Table 14.** Sedimentation rate (m/Ma) per seismic stratigraphic layer for the selected wells located in Block A.

Block A							
Layer	A11-01	A12-03	A14-01	A15-02	A15-03	A18-01	A18-02
S13	875,19	893,68	787,28	722,71	733,42	743,75	776,24
S12	1354,29	1094,4	1209,53	1076,8	1076,2	1160,88	839,95
S11	1604,69	823,5	1111,81	932,38	1004,71	1035,33	844,1
S10	597,67	1100,49	1452,82	1235,35	1284,12	922,77	1003,3
S9	2804,4	1511,57	3269,06	1387,06	1419,6	1864,16	1956,49
S8	2154,13	36,29	2124,57	1278,81	1140,67	652,54	532,88
S7	455,47	909,15	2124,57	672,75	711,17	642,53	862,57
S6	1163,93	1241,23	1309,22	1399,69	1513,29	1958,2	2014,11
S5	1250,78	831,9	1309,22	1872,05	1899,38	1879,56	1560,24
S4	141,29			111,31	130,02	192,44	90,49
S3	78,42			202	186,89		142,23
S2	8,28			33,23	40,03		
S1	13,38		7,85	11,76	10,65	9,45	

It is worth to highlight that PetroMod® Model results in the three blocks suggest that the units up to

S5 present higher sedimentation rate values.

It should be taken into account that the mixed lithologies created for each formation, group, member and seismic stratigraphic unit in the study area could incorporate certain level of uncertainties in the model results, since a change in the lithological content average will change their associated default properties.

In tables 14, 15 and 16 can be seen that the layers that meet the condition of high sedimentation for microbial gas generation and after the evaluation of the sedimentation rates per seismic units at the selected wells in the delta system are:

- Block A: S5-13
- Block B: S5-S13
- Block F: S5-S13

**Table 15.** Sedimentation rate (m/Ma) per seismic stratigraphic layer for the selected wells located in Block B.

Block B							
Layer	B10-02	B13-02	B14-01	B16-01	B18-03	B17-06	B17-05
S13	700,62	720,09		604	300,39	315,75	211,52
S12	1011,17	1138,51		784,93	705,74	818,82	750,55
S11	496,36	534,25		612,67	876,43	339,25	
S10	1092,2	820,92		570,22	452,97	143,4	860,31
S9	993,1	836,58		1173,19	236,47	698,16	624,09
S8	376,67	481,67	194,66	85,25		629,53	701,41
S7	308,36	99,18	506,89	482,37			
S6	2128,55	1474,32		1991,25	382,3	543,4	
S5	1624,89	1710,92	982,58	1623,25	1372,12	1381,43	2352,96
S4	96,25	88,51	190,31	176,79	32,61	160,77	143,5
S3	235,53	275,1	625,05	152,52	140,9	862,05	432,66
S2	155,57	161,48	392,78	55,16	521,88		118,28
S1	8,96	20,12	35,66	16,89	28,13		11,26

**Table 16.** Sedimentation rate (m/Ma) per seismic stratigraphic layer for the selected wells located in Block F.

Block F											
Layer	F01-01	F02-03	F03-07	F04-01	F05-02	F09-02	F12-02	F17-07	F03-01	F03-08	F17-03
S13	709,2	781,72	479,86	886,47	744,94	527,66	591,52	983,34	380,81	331,1	1046,15
S12	967,18	395,27	511,02	1298,0	910,24	813,38	433,68	967,07	706,66	600,73	1072,83
S11	1132,36	820,38	1344,1	785,44	1244,94	1157,66	1338,33	1155,46	1054,4	932,73	1183,06
S10	265,64	355,12	418,71	692,73	697,34	499,62	392,59	715,85	497,4	438,29	572,47
S9	1432,98	750,88		1820,6	1101,43	1279,05	764,36	878,13	216,93	194,74	815,44
S8	687,99			410,69	239,89			573,7			366,02
S7	287,64			206,42	125,42						
S6	2364,42	914,92	633,32	2202,4	1248,72	790,28	711,18	881,85	408,4	359,61	914,26
S5	1999,01	2130,9	1311,3	2375,6	4322,62	4581,71	4386,25	3815,76	1482,6	1338,4	4099,12
S4	52,97	147,12		35,45	38,46	133,24			30,53	26,43	
S3		533,01	201,03			35,54				227,6	
S2	17,91	105,85	575,68						496,92	479,23	
S1		22,57	15,67						23,55	25,96	

Reconstructed burial output of the 25 wells indicates that the highest sedimentation rates are found at the youngest units.

- *Pore Space*

Is noteworthy to mention that the TOC measurements at S5 horizon showed a particular tendency, lowest TOC values are reached in the clay intervals (<0,5%) whilst highest values are found in the coarser sand-siltstone intervals (2-3%). It has been suggested that the latter may contribute for microbial gas generation because it would provide an adequate pore space for methanogenesis to occur.

- *Discussion of conjunct behaviour for all conditions*

Overall, constraining the PetroMod® output with the limiting assumptions previously discussed (temperature, sedimentation rate, presence of organic matter and pore space), the potential intervals that gather all the conditions in the unconsolidated sediments are:

- In block A: Units S5-S7
- In block B: Units S5-S6
- In Block F: Units S5

These seismic units correspond to paleoenvironments 2 and 3 (transitional and Restricted Marine, respectively)

## CHAPTER 5 MODELLING BIOGENIC GAS GENERATION

---

This chapter comprises a detailed description of the different phases involved in the Biogenix® modelling workflow, for a better comprehension of microbial gas calculation. It was used Biogenix®, an algorithm created by Clayton (2009), which main objective is to predict the occurrence and amounts of “free microbial generated methane in buried sediments”.

As case of study, It has been performed the simulation of three representative wells in the area (Wells A15-03, B13-02 and F05-02) for the assessment of the potential gas generation in the unconsolidated sediments of the southern North Sea basin.

The Biogenix® program is based on three diverse models that reproduce the natural process: Hybrid model, Thermal substrate generation and Temperature controlled bacterial activity, which are supported by microbiological studies.

It is important to emphasize that the program is a 1D model, therefore the migration of the fluids are not included.

### 5.1. Input Biogenix Modelling

The key point of the project is implementing an interactive approach: with the output from previous simulations (1D PetroMod® model) the proper data is delivered to Biogenix® in order to model the biogenic gas generation.

This section encompasses the selection of the main constrains for the evaluation of the microbial gas generation. All gathered data regarding water depth, bottom water temperature and sedimentation rate of the selected wells were included.

#### 5.1.1. Depth Profile Options

The options offered by the program in this segment include burial history, thermal, pressure and salinity profile.

The shallow gas in the Netherland North Sea Sector occurs between seabed and depths 1000 m below mean sea level, therefore the target biogenic gas reservoirs are in the unconsolidated clastic sediments above the Mid Miocene Unconformity (Schroot & Schüttenhelm, 2003).

The Mid Miocene Unconformity, which belongs to the deeper part of the basin, reaches max 1500 m, displaying the location in the depocenter during the late Neogene (Kuhlmann & Wong, 2008).

Thus, for the **Burial History**, the maximum depth selected was 1500 m. It was not consider deeper layers because does not belong to the scope of this study.

According to Clayton (2009), the **water depth and sedimentation rate** are used for the computation of quantity of primary productivity reached to the sediment surface. The bottom water temperature would influence in the thermal profile and solubility calculations and hence, the kinetic scheme of bacterial gas generation.

The **pressure profile** is based in lithology and sedimentation rate. In this study, a hydrostatic regime was adopted.

The **salinity profile** was not employed in this study due to the paucity of the data. The default value proposed by the program was 35 ppt (parts per thousand).

### 5.1.2 Custom Input

It has been consider only the gas bearing layers, therefore, unconsolidated clastic sediments of Miocene until Holocene age. The lithology, temperature and ages obtained by previous 1D PetroMod® modelling simulation were incorporated in the 1D Biogenix model.

The simulation model was constrained by three Total Organic Content scenarios. It was consider 1%, 2% and 3%, being this last value the maximum TOC found in core samples at shallow depths (in Tertiary sediments).

In the present model, it has been introduced TOC data values directly. However, the program offers a default function to calculate the buried TOC based on “primary productivity in the water column photic zone” (Clayton, 2009). Thus, Biogenix calculates how much becomes buried into the methanogenic zone in sediment from the introduced primary organic productivity in per year and it is based on the investigations presented by Suess, (1980) and Sarnthein, Winn, Duplessy, & Fontugne (1988).

### 5.1.3. Biogenic Model Used

A comparison between the diverse models and their main characteristic are presented. The program can model methane generation in three distinct ways. Among the approaches that can be used for modelling are Hybrid Model, Thermal Model and Force decay Model.

### a) Hybrid Model

- First Order Reaction Kinetics: Converted TOC in Methane at rate related to Microbial activity.
- Model Substrate Generation: According to microbiologist Parkes, et al. (2007) the substrate is generated by slow thermal breakdown of proto-kerogen and the microbes feed of this at a temperature-controlled rate.
- The standard kinetics for kerogen breakdown is based on CO<sub>2</sub> generation from the Boom Clay supported by Lorant, Largeau, Behar, & De Cannière (2008) Although, the default kinetics relate only to CO<sub>2</sub> generation, it can be used as a proxy for all relevant metabolizable species (Clayton, 2009).

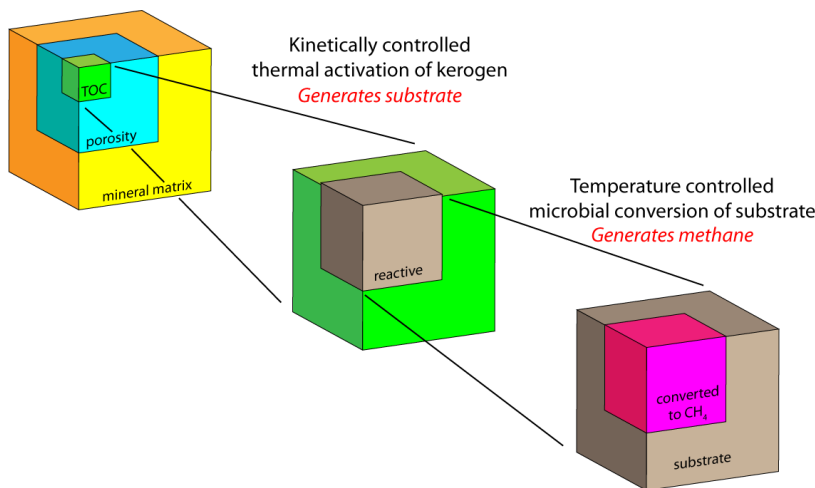


**Figure 20.** Scheme that shows the portion of reactive TOC and the subsequent generation of substrate that will be used by the methanogens to convert CH<sub>4</sub> (After Clayton C., 2009).

The kinetics of substrate generation is based on the **Arrhenius equation** which relates the reaction rate,  $k$  To temperature:  $k = Ae^{-E/RT}$  in which  $R$  is the universal gas constant,  $T$  is the absolute temperature and the pre-exponential factor,  $A$  is the  $k$  frequency factor and  $E$  is the activation energy (Clayton, 2009).

In the figure 20 is illustrated the portion of total organic matter that is reactive to create substrate, and lastly, to generate methane. Initially, TOC buried into the methanogenic zone, is highly reactive. Although, most of this methane is probably lost to overlying waters and deoxidized at the base of the sulphate reduction zone. Under optimum conditions, about 10% of TOC in a source rock can be converted in methane (Clayton C., 1992).

In on-going studies, it is believed that deeper in the sediments, bacteria are capable to slowly break down protokerogen or thermal breakdown of kerogen at low temperatures supplying a feedstock which subsequently is used by methanogens to generate CH<sub>4</sub> (Clayton C. , 2009).

#### *b) Thermal Model*

This model is a zero order reaction in which the gas generation is based only on methanogen temperature sensitivity. Consequently, the rate of biogenic gas generation is not substrate limited and it is controlled only by the temperature dependence of bacterial activity (Clayton, 2009).

#### *c) Decay Only Model*

This approach is a variant of the Hybrid Model, which assumes that the methanogens work at a maximum efficacy up to a temperature threshold (40°C by default). Once the optimum temperature is reached, the bacterial conversion efficiency decreases progressively up to 80°C (Clayton, 2009).

### 5.1.4 Expulsion Model

In the context of the study, it refers to the volume of gas expelled when reaches a certain percentage of gas saturation in pore space.

A saturation of 10% (that correspond to the program default value) is beyond the threshold required to cause a seismic response. On seismic surveys, the free gas can be recognized at 3% saturation. According to Schroot & Schüttenhelm (2003), Acoustic blanking may occur at gas concentrations of 0,5%, while Acoustic turbidity may happen up to 1% of gas present. These features represent the most commonly observed gas-related shallow expressions in the Netherlands North Sea Sector.

For this model, it has been assumed that 6% of the gas is contained in the fraction of pore space; the latter would be the minimum percentage needed in order to ensure the migration of the fluid.

### 5.1.5 Calculation of Gas Volumes

According to Clayton (2009), the gas volumes are estimated at standard temperature and pressure employing TOC inputs, the Gas Generation Index (GGI), and a scaling factor.

The scaling factors accounts for the maximum likely conversion of kerogen to methane and were derived from C/O mass balance calculations based on the carbon dioxide reduction pathway, the dominant methanogenic process in marine sediments (Clayton, 1992).

The **potential yield of gas** can be estimated from the mass fraction of carbon lost from the sediment in the methanogenic zone.

The **free gas** formed below the sulphate reduction zone is presumed that it become adsorbed onto the matrix, by bacterial reoxidation. The **adsorbed gas** calculation is based on the equation of Pepper & Corvi(1995) in their research “*Simple kinetic models of petroleum formation*”:

$$\alpha_{CH_4} = 6.7e^{-3} + 9.4e^{-3} \cdot \log(P) - 6.2e^{-5} \cdot \log(T)$$

Where:

$\alpha_{CH_4}$ : the adsorption coefficient (g.g-1C)

P: pressure(MPa)

T: temperature (°C)

For the calculation of **methane solubility** at a given temperature and specific salinity, Clayton (2009) suggested the equation used by Yamamoto, Alcauskas, & Crozier (1976) in their project “*Solubility of methane in distilled water and seawater*”:

$$\ln \beta = A_1 + A_2(100/T) + A_3 \ln(T/100) + S(B_1 + B_2(T/100) + B_3(T/100)^2)$$

Where:

$\beta$ : Bunsen solubility coefficient

A and B: constants

T: temperature (in Kelvin)

S: salinity (in parts per thousand)

For the calculation of **total dissolved gas**, is assumed that methane is the only free gas phase present.

**Total dissolved Gas= solubility\*pore volume**

## 5.2 Output Biogenix Modelling

Three possible scenarios have been proposed with different percentage values of TOC, in order to address the gas volumetric generated by the software in the southern North Sea basin.

In this section, the most relevant results from the sensitivities performed are presented, using temperature and sedimentation rates derived from the previous model (PetroMod). The rest of the data was included as annexes at the end of this work.

It has been selected three representative wells, one per each block, for a comparison of the results obtained by the Biogenix program.

The final output generated was linked with the previous projects done by Kuhlmann & Wong(2008), Schroot & Schüttenhelm(2003)and Schroot, Klaver, & Schüttenhelm (2005). The first authors made a study in order to resolve climate-controlled changes in sedimentary facies of the depositional sequences in a 3D data set. The latter carried out a detailed study about the expression of the shallow gas in the Netherlands North Sea based on geophysical data. Lastly, the authors added a geochemical analysis for a better description of the surface and subsurface expression of shallow gas and its migration in blocks A,B and F and compared the geochemical analysis with the geophysical anomalies.

### 5.2.1 Model Comparison

A brief comparison between the two different models offered by Biogenix at the well A15-03 is presented, considering 6% free gas saturation and a constant value of 3% total organic content (TOC) along 300m until 1000m.

In figure 21 is represented the Gas volumes generated, where the ordinate axis denotes depths (meters) and the abscise axis represents by the gas volumes; expressed in cubic meters at standard conditions per cubic meter of the rock. The results are expressed in STP conditions; pressure 1 atm (101325 Pa) and temperature as 0°C.

In figure 22 the generation rate of Thermal and Hybrid models at the well A15-03, expressed in m<sup>3</sup> at STP per m<sup>3</sup> rock volume per million of year, is showed.

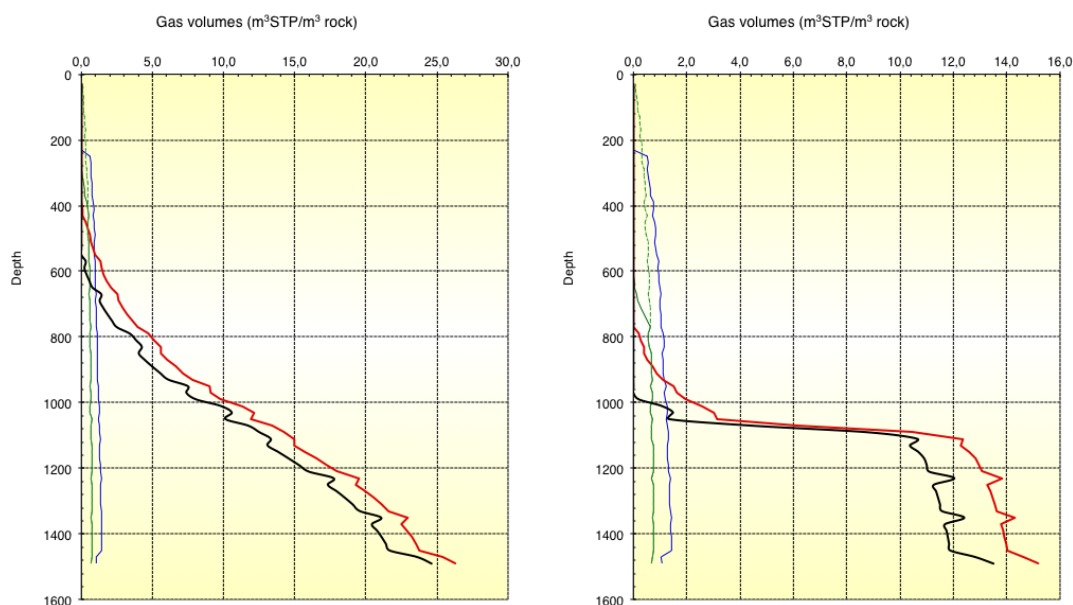


**Figure 21.** Gas Volumes (m<sup>3</sup>STP/ m<sup>3</sup>rock) at well A15-03 of Thermal Model and Hybrid Model Legend; blue line: adsorbed gas; green line: dissolved gas; red line: total free gas; green dashed line: maximum soluble and black line: expelled gas.

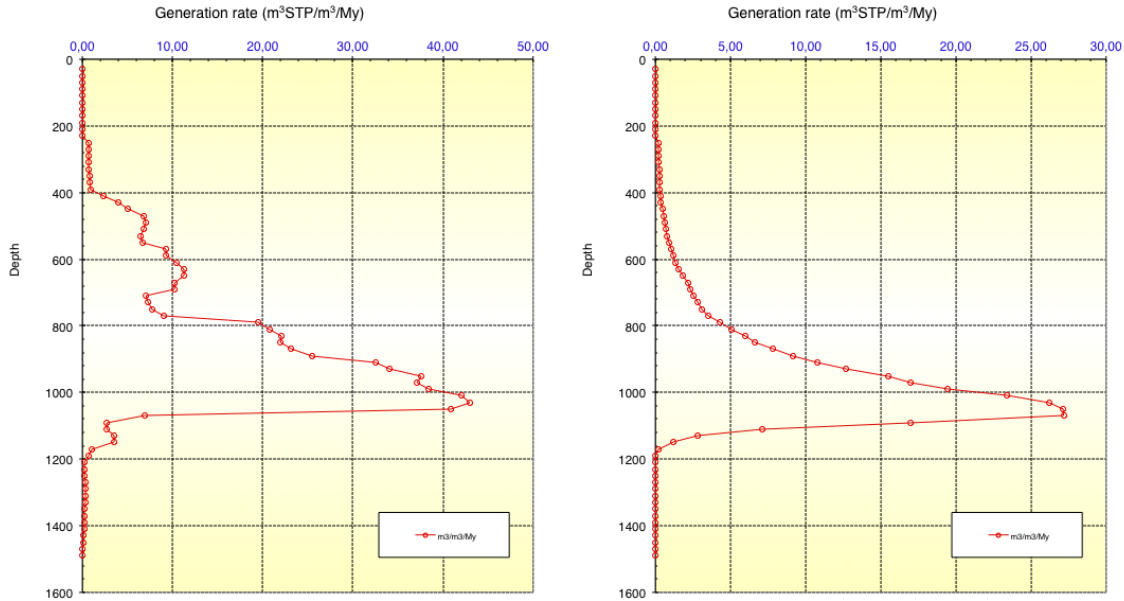


**Figure 22.** Generation rate of Thermal Model and Hybrid model at well A15-03.

The results obtained depict drastic differences. Although the maximum quantity of gas volume is reached at 1500m in both models, the gas volumes achieved with the thermal model almost duplicate those values obtained with the hybrid model (Figure 21).

In figure 21, the total free gas and expelled gas volume in the thermal model increased progressively from shallower to greater depths. Whereas in the hybrid model, it is raised abruptly at a determined depth, in this case 1070m (approx.), which normally coincide with the peak of gas generation. The dissolved and the adsorbed gas volumes are maintained at a constant value in both models.

As can be seen in figure 22, in both models the generation rate raise gradually until reach a top. In the hybrid model the generation peak occurs approximately 50 meters slightly below than in the thermal model. In the latter model the rate increment is more irregular since it only depends on methanogen temperature sensitivity.

Contemplating the evaluation of the different options, the author propose to use Hybrid model for the subsequent modelling and interpretation of results.

## 5.2.2 TOC Scenarios Assessment

Figures 23, 25 and 27 show the gas volumetric obtained at the wells A15-03, B03-02 and F05-02 respectively, considering the three TOC scenarios defined. The blue line indicates the adsorbed gas; while the green line is the dissolved gas. The total free gas is highlighted with red line. Dashed lines were used to show maximum soluble (green dashed line), expelled gas (black dashed line) and the depths of each seismic stratigraphic unit (blue dashed lines).

Figures 24,26 and 28 depict the generation rate for the corresponding wells (A15-03, B03-02 and F05-02) and for the three TOC cases. Also, an estimation of microbial gas volumes for each scenario is showed on tables 17 to 25.

a) Block A: Well A15-03

In general, there is a substantial rise of total free volumetric gas generated and the quantity of gas expelled with an increment of total organic content. Also, it is noteworthy to mention that as TOC increases, the microbial gas is found at lower depths.

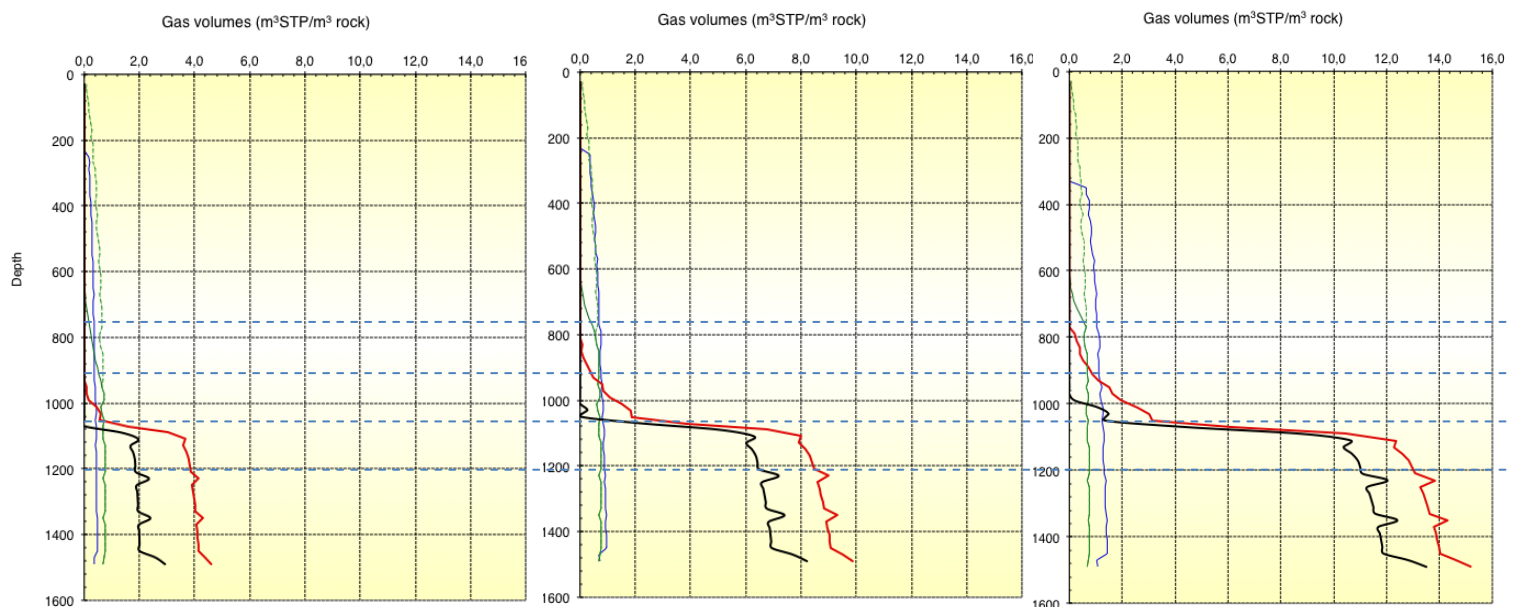


**Figure 23.** Gas volume ( $m^3STP/ m^3rock$ ) at well A15-03 with 1, 2 and 3% total organic content.

As it can be observed in figure 23 and tables 17, 18 and 19, expelled gas behaves with marginal quantities at depths 1000m and then it raises abruptly at a 1070m. Posteriorly, it continues with a gradual increment to deepest layers. Also, some peaks can be noticed that correspond to shaly layers.

In figure 23 is depicted the first horizons and it can be easily seen that gas is generated at S1 to S4 units. The dissolved gas quantities are kept constant with no significant changes along the entire sequence and for adsorbed gas there is only a small increment.

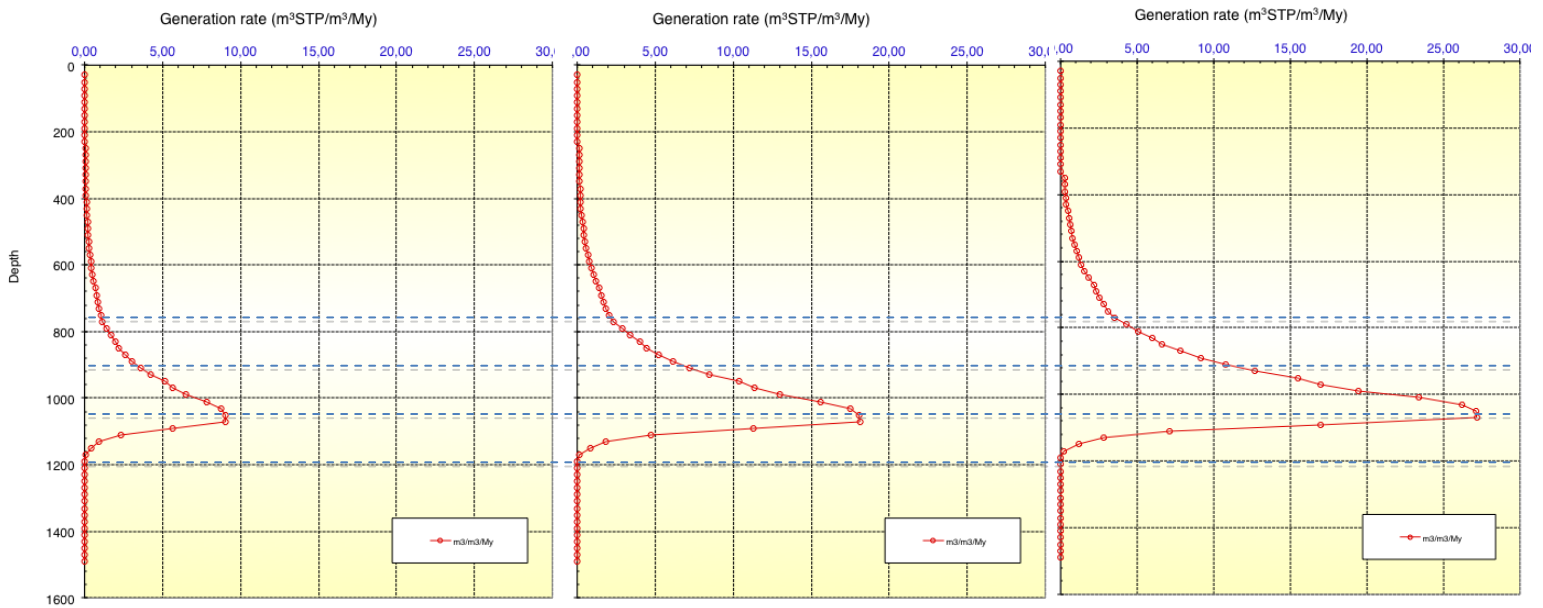


**Figure 24.** Generation rate ( $m^3STP/m^3/My$ ) of Hybrid Model at well A15-03 with 1, 2 and 3% total organic content.

In Figure 24, the generation rate starts at oldest layers S3, reaching a peak at depth 893mand then decreases to younger units; with the maximum rate atthe interval S5.

Regarding the Biogenix results, tables 17,18 and 19 show the behaviour for well A15-03 after the assessment of the three scenarios with 1,2 and 3 total organic content percentages considered, where:

- Seismic Units are displayed indicating their corresponding depth range,
- GGI corresponds to the fraction of the total substrate-potential which has been converted to methane(generally below 1),
- Generation rate is an important factor, as a potential chargeof the resource within the reservoir during well lifetime,
- Adsorbed gas is the gas accumulated on the surface of a solid material, such a grain of reservoir rock(Schlumberger, 2013),
- Total gas includes adsorbed, dissolved and total free gas,
- Total free gas refers to the gaseous phase present in a reservoir. It tends to form as a gas cap beneath the top seal on the reservoir trap (Schlumberger, 2013). A free gas state results when biogenic gas generation exceeds the gas solubility in the pore fluid or when gas exsolution from pore water is caused by reduction of the hydrostatic pressure. Exsolution of gas can be a consequence of falling sea level or uplift and erosion(Rice D. , 1992).

The behaviour applying the Hybrid model for well A15-03 evidences:

- The expulsion of the gas will occur at 6% of gas saturation that is reached at the oldest units (S1-S4) that correspond to deeper layers (1073-1193 m),
- The fraction of the total microbial gas potential is obtained at horizons S1-S4.
- Peak of generation rates is achieved in all the cases, at 893m approx. (Unit S5) but there is a significant difference in the volume of gas generated associated to the TOC percentage: 4,22; 8,44 and 12,65 m<sup>3</sup>/m<sup>3</sup>/My for 1%; 2% 3% TOC respectively.
- Adsorbed gas volumes slightly increase along the sequence in all cases: from 0,24 until 0,45 m<sup>3</sup>/m<sup>3</sup> of rock with 1%, from 0,48 until 0,92 m<sup>3</sup>/m<sup>3</sup> of rock with 2% and from 0,73 until 1,39 m<sup>3</sup>/m<sup>3</sup> of rock with 3%; The highest value in all the cases is found at S1.
- Total gas per volume of rock is achieved at units S1 until S4, where an increase of percentage of total organic content yielded considerable gas volumes.
- Total free gas volume is found at the oldest units.

**Table 17.** Biogenix results at well A15-03 considering 1 % total organic content.

Seismic Unit	Depth m	GGI	Gen Rate m <sup>3</sup> /m <sup>3</sup> /My	Total gas v/v of rock	Adsorbed gas v/v of rock	Dissolved gas v/v of rock	Total free gas v/v of rock	Expelled gas v/v of rock
s13	393	0,04	0,12	0,24	0,24	0,00	0,00	0,00
s12	453	0,04	0,21	0,28	0,28	0,00	0,00	0,00
s11	513	0,04	0,30	0,29	0,29	0,00	0,00	0,00
s10	553	0,04	0,40	0,31	0,31	0,00	0,00	0,00
s9	593	0,05	0,52	0,33	0,32	0,01	0,00	0,00
s8	653	0,05	0,77	0,39	0,34	0,06	0,00	0,00
s7	693	0,06	0,93	0,47	0,34	0,13	0,00	0,00
s6	753	0,08	1,43	0,63	0,38	0,26	0,00	0,00
s5	893	0,12	4,22	0,98	0,38	0,60	0,00	0,00
s4	1073	0,54	2,36	4,77	0,44	0,67	3,67	1,96
s3	1113	0,57	0,41	4,88	0,43	0,75	3,70	1,77
s2	1153	0,57	0,00	5,00	0,43	0,75	3,82	1,85
s1	1193	0,57	0,00	5,30	0,46	0,69	4,15	2,34

**Table 18.**Biogenix results at well A15-03 considering 2% total organic content.

Seismic Unit	Depth m	GGI	Gen Rate m3/m3/My	Total gas v/v of rock	Adsorbed gas v/v of rock	Dissolved gas v/v of rock	Total free gas v/v of rock	Expelled gas v/v of rock
s13	393	0,04	0,24	0,48	0,48	0,00	0,00	0,00
s12	453	0,04	0,41	0,56	0,56	0,00	0,00	0,00
s11	513	0,04	0,59	0,58	0,58	0,00	0,00	0,00
s10	553	0,04	0,79	0,62	0,62	0,00	0,00	0,00
s9	593	0,05	1,04	0,66	0,64	0,02	0,00	0,00
s8	653	0,05	1,55	0,78	0,67	0,11	0,00	0,00
s7	693	0,06	1,86	0,94	0,68	0,25	0,00	0,00
s6	753	0,08	2,86	1,27	0,75	0,51	0,00	0,00
s5	893	0,12	8,44	1,95	0,76	0,70	0,50	0,00
s4	1073	0,54	4,72	9,55	0,88	0,67	8,01	6,30
s3	1113	0,57	0,82	9,76	0,85	0,75	8,16	6,23
s2	1153	0,57	0,00	10,01	0,87	0,75	8,39	6,43
s1	1193	0,57	0,00	10,61	0,92	0,69	9,00	7,19

**Table 19.**Biogenix results at well A15-03 considering 3% total organic content.

Seismic Unit	Depth m	GGI	Gen Rate m3/m3/My	Total gas v/v of rock	Adsorbed gas v/v of rock	Dissolved gas v/v of rock	Total free gas v/v of rock	Expelled gas v/v of rock
s13	393	0,04	0,37	0,73	0,73	0,00	0,00	0,00
s12	453	0,04	0,62	0,84	0,84	0,00	0,00	0,00
s11	513	0,04	0,89	0,87	0,87	0,00	0,00	0,00
s10	553	0,04	1,19	0,93	0,93	0,00	0,00	0,00
s9	593	0,05	1,56	0,99	0,97	0,03	0,00	0,00
s8	653	0,05	2,32	1,17	1,01	0,17	0,00	0,00
s7	693	0,06	2,79	1,41	1,03	0,38	0,00	0,00
s6	753	0,08	4,30	1,90	1,13	0,57	0,20	0,00
s5	893	0,12	12,65	2,93	1,14	0,70	1,09	0,00
s4	1073	0,54	7,08	14,33	1,31	0,67	12,35	10,64
s3	1113	0,57	1,23	14,64	1,28	0,75	12,61	10,69
s2	1153	0,57	0,00	15,02	1,31	0,75	12,96	11,00
s1	1193	0,57	0,00	15,91	1,39	0,69	13,84	12,03

## Comparison of Biogenix Results with Literature

Shallow gas occurrences are related to gas escapement routes along salt structures and to subsequent accumulation in stratigraphic traps in the unconsolidated Pliocene sediments. Two levels of gas accumulation have been described from the 3D-seismic survey by Schroot, Klaver, & Schüttenhelm (2005). One level with high-amplitude reflectors is found approximately between 850 and 1100m depth and a second level is located between 450 and 750 m. The lower gas occurrence is confined to sediments deposited in the warm periods of paleoenvironmental interval 2 (Schroot, Klaver, & Schüttenhelm, 2005). The other level of gas occurrence is associated with the bright spot. This feature is more regional in its extent and is related to paleoenvironmental interval 4 comprising the seismic units with signs of ice-scratches (Schroot, Klaver, & Schüttenhelm, 2005).

Comparing these results of previous studies for the same block where well A15-03 is located with Biogenix results for estimated depths where microbial gas volumes would be found (1073-1193m approx.), it can be said that there is a good concordance with the lowest level of gas accumulation.

### *b) Block B: Well B13-02*

In this well, the potential gas volume that is produced by microorganisms is found at shallower depths. A considerable increase in the amount of gas expelled and total free gas volumes can be observed as total organic content percentage increases.

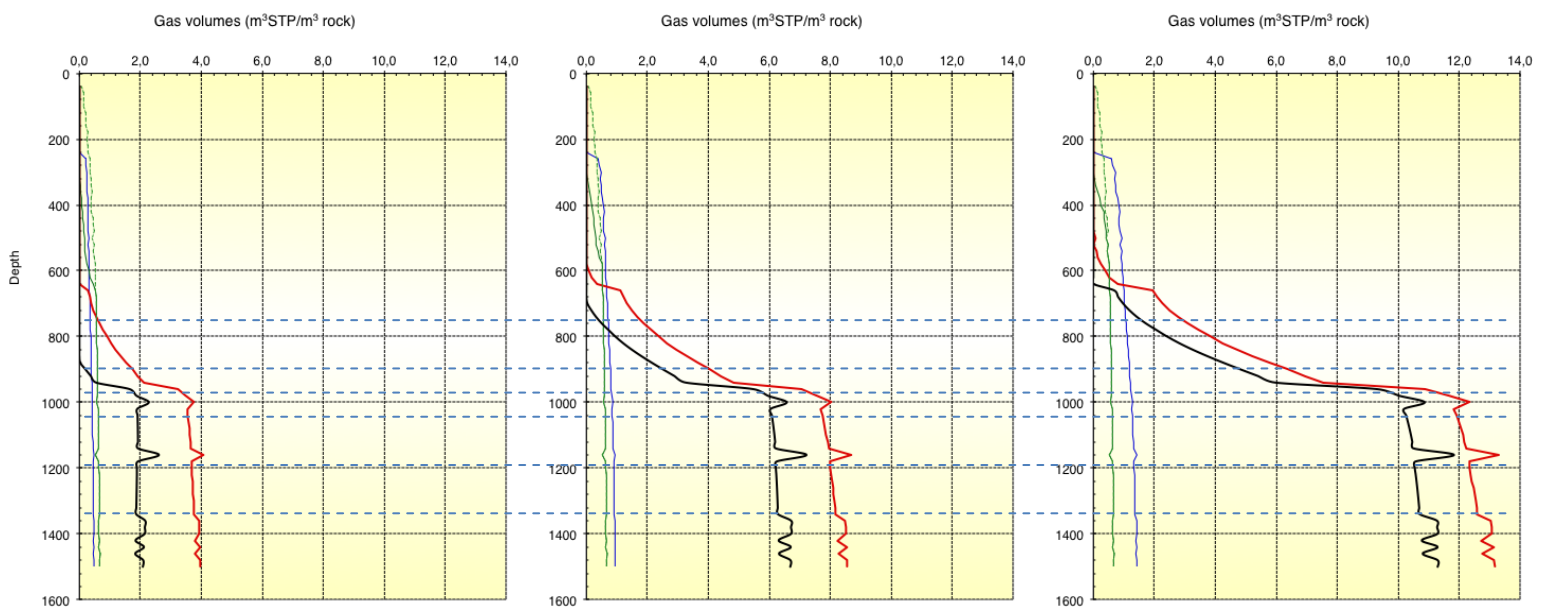


**Figure 25.** Gas volume ( $m^3STP/m^3rock$ ) at well B03-02 with 1, 2 and 3% total organic content.

As showed in figure 25, expelled gas generated rises gradually and leaps at a 1070m depth. Then, volumetric gas continues to increase steadily to deepest horizons. The sharp peaks are related to the clayed layers.

In figure 25 is depicted the first horizons and it can be noticed that gas is generated at S1 to S5 units. Concerning the adsorbed and dissolved gas the quantities are kept constant with no significant changes along the entire sequence.

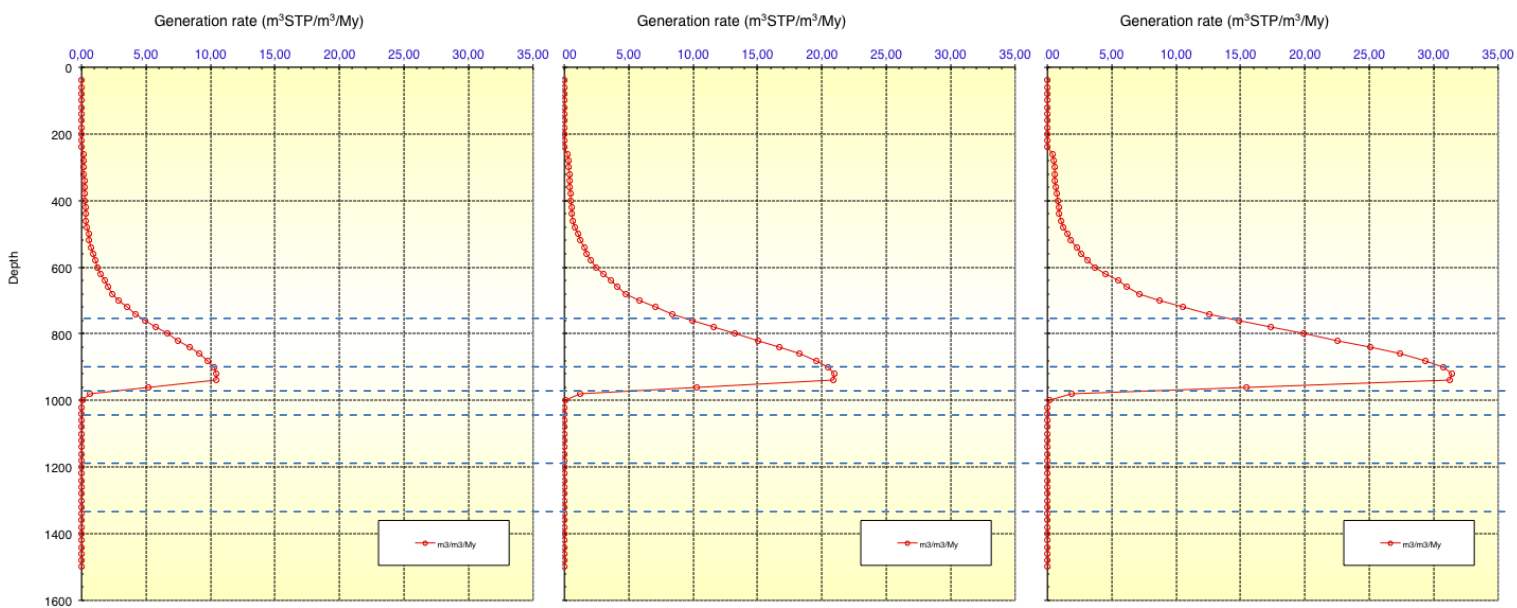


**Figure 26.** Generation rate ( $m^3STP/m^3/My$ ) of Hybrid Model at well B03-02 with 1, 2 and 3% total organic content.

In Figure 26, the generation rate reaches a peak at depth 796m and then decreases to younger units; with the maximum rate at the interval S6.

The behaviour when applying the Hybrid model for well B03-02 (tables 20, 21 and 22) suggest:

- The settings for gas saturation are met at intervals S1-S5 at 1073m with 1% TOC, while for 2% TOC is at layers S1-S7 and for 3% is expanded until layer S9. This behaviour can lead to major possibilities of finding microbial gas in this well.
- Maximum of gas generation rate in all the scenarios is achieved at 796m approx. (Unit S6).
- Adsorbed gas volumes increased marginally along the sequence from 0,30 until 0,46  $m^3/m^3$  of rock with 1%, from 0,59 until 0,92  $m^3/m^3$  of rock with 2% and from 0,89 until 1,37  $m^3/m^3$  of rock with 3%. The highest value is found at S1.
- Total gas per volume of rock is achieved at units S1 until S5, an increase total organic content percentages yielded considerable gas volumes.
- Total free gas range units expanded from S9 with 1% to S12 with 2% and 3%.

- The GGI, the fraction of the total gas potential which has been recognized as biogenic methane, shows the highest values at S1-S5.

**Table 20.** Biogenix results at well B2-03 considering 1 % total organic content.

Seismic Unit	Depth m	GGI	Gen Rate m <sup>3</sup> /m <sup>3</sup> /My	Total gas v/v of rock	Adsorbed gas v/v of rock	Dissolved gas v/v of rock	Total free gas v/v of rock	Expelled gas v/v of rock
s13	476	0,06	0,59	0,46	0,30	0,16	0,00	0,00
s12	556	0,08	1,24	0,61	0,32	0,30	0,00	0,00
s11	576	0,09	1,51	0,67	0,32	0,35	0,00	0,00
s10	596	0,10	1,82	0,77	0,33	0,44	0,00	0,00
s9	616	0,15	2,06	1,16	0,33	0,54	0,29	0,00
s8	636	0,16	2,37	1,21	0,34	0,54	0,34	0,00
s7	656	0,17	2,90	1,28	0,34	0,55	0,39	0,00
s6	796	0,26	8,36	2,14	0,38	0,58	1,19	0,00
s5	956	0,51	0,05	4,73	0,43	0,55	3,74	2,28
s4	996	0,51	0,00	4,60	0,42	0,62	3,56	1,91
s3	1056	0,51	0,00	4,68	0,43	0,63	3,62	1,92
s2	1196	0,51	0,00	4,81	0,45	0,65	3,71	1,88
s1	1296	0,51	0,00	4,88	0,46	0,67	3,76	1,86

**Table 21.** Biogenix results at well B2-03 considering 2% total organic content.

Seismic Unit	Depth m	GGI	Gen Rate m <sup>3</sup> /m <sup>3</sup> /My	Total gas v/v of rock	Adsorbed gas v/v of rock	Dissolved gas v/v of rock	Total free gas v/v of rock	Expelled gas v/v of rock
s13	476	0,06	1,19	0,91	0,59	0,32	0,00	0,00
s12	556	0,08	2,47	1,23	0,63	0,52	0,08	0,00
s11	576	0,09	3,01	1,34	0,64	0,52	0,17	0,00
s10	596	0,10	3,64	1,53	0,65	0,53	0,35	0,00
s9	616	0,15	4,13	2,31	0,66	0,54	1,11	0,00
s8	636	0,16	4,75	2,43	0,67	0,54	1,21	0,00
s7	656	0,17	5,81	2,57	0,68	0,55	1,34	0,04
s6	796	0,26	16,73	4,29	0,76	0,58	2,95	1,49
s5	956	0,51	0,09	9,46	0,87	0,55	8,04	6,57
s4	996	0,51	0,01	9,20	0,85	0,62	7,74	6,09
s3	1056	0,51	0,00	9,37	0,87	0,63	7,88	6,17
s2	1196	0,51	0,00	9,62	0,90	0,65	8,07	6,24
s1	1296	0,51	0,00	9,76	0,92	0,67	8,18	6,29

*Table 22. Biogenix results at well B2-03 considering 3% total organic content.*

Seismic Unit	Depth m	GGI	Gen Rate m <sup>3</sup> /m <sup>3</sup> /My	Total gas v/v of rock	Adsorbed gas v/v of rock	Dissolved gas v/v of rock	Total free gas v/v of rock	Expelled gas v/v of rock
s13	476	0,06	1,78	1,37	0,89	0,48	0,00	0,00
s12	556	0,08	3,71	1,84	0,95	0,52	0,37	0,00
s11	576	0,09	4,52	2,01	0,96	0,52	0,52	0,00
s10	596	0,10	5,47	2,30	0,98	0,53	0,79	0,00
s9	616	0,15	6,19	3,47	0,99	0,54	1,94	0,68
s8	636	0,16	7,12	3,64	1,01	0,54	2,09	0,81
s7	656	0,17	8,71	3,85	1,02	0,55	2,28	0,98
s6	796	0,26	25,09	6,43	1,14	0,58	4,72	3,26
s5	956	0,51	0,14	14,19	1,30	0,55	12,34	10,87
s4	996	0,51	0,01	13,80	1,27	0,62	11,92	10,26
s3	1056	0,51	0,00	14,05	1,30	0,63	12,13	10,42
s2	1196	0,51	0,00	14,43	1,35	0,65	12,43	10,60
s1	1296	0,51	0,00	14,64	1,37	0,67	12,60	10,71

### Comparison of Biogenix Results with Literature

The Biogenix model outputs are consistent when compared with the data found in literature on the block B. At the well B13-02 the model suggests that the layers of total free gas coincide with those level gas accumulation previously mentioned (first level 850-1100m and a second level 450-750 m) described by Schroot, Klaver, & Schüttenhelm (2005). For that reason this well would be suitable to support the hypothesis of gas occurrences in stratigraphical traps of shallower depths.

#### *c) Block F: Well F05-02*

In this well, also total free volumetric gas and the quantity of gas expelled starts at the deepest layers.

In figure 27 are represented the first horizons where the gas is generated. Referring to the adsorbed and dissolved gas, the values estimated does not present remarkable changes in the entire sequence.

In Figure 28, the generation rate initiates in all cases at 1154 m (S1) reaching a peak at depth 914 m and then decreases to younger units; with the maximum rate at the interval S5.

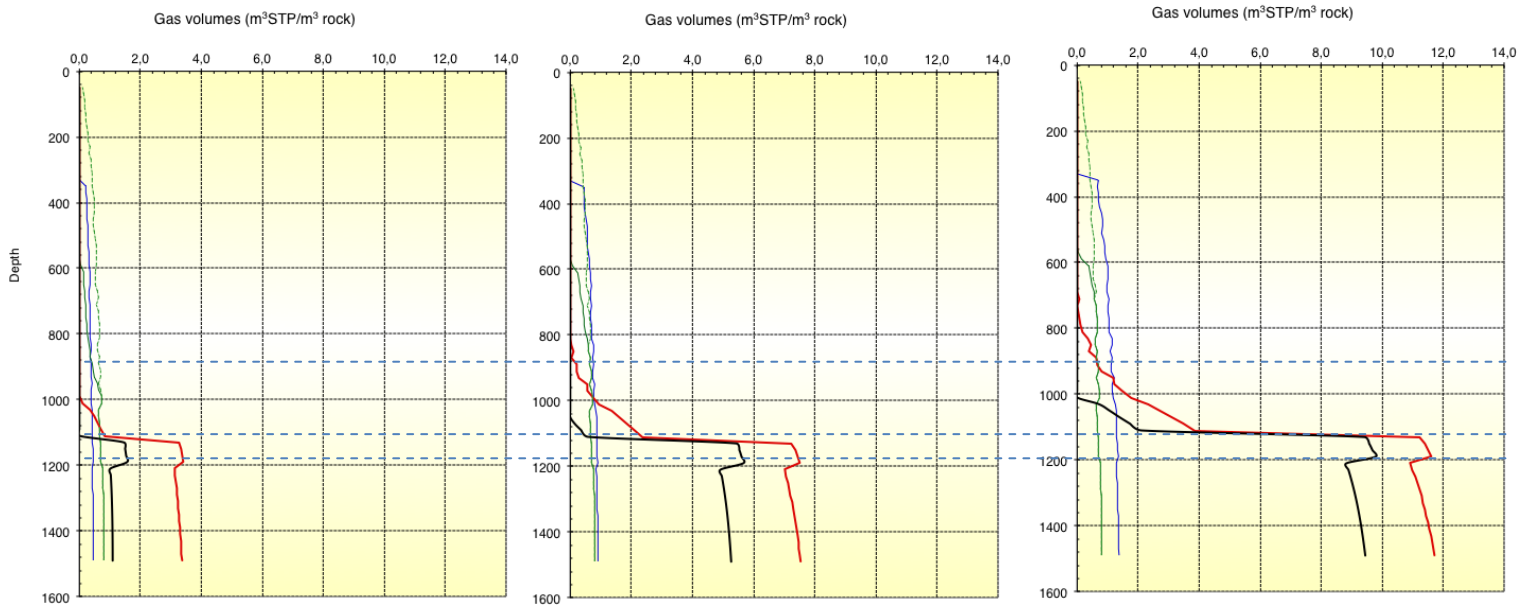


Figure 27. Gas volume ( $m^3STP/m^3 rock$ ) at well F05-02 with 1, 2 and 3% total organic content.

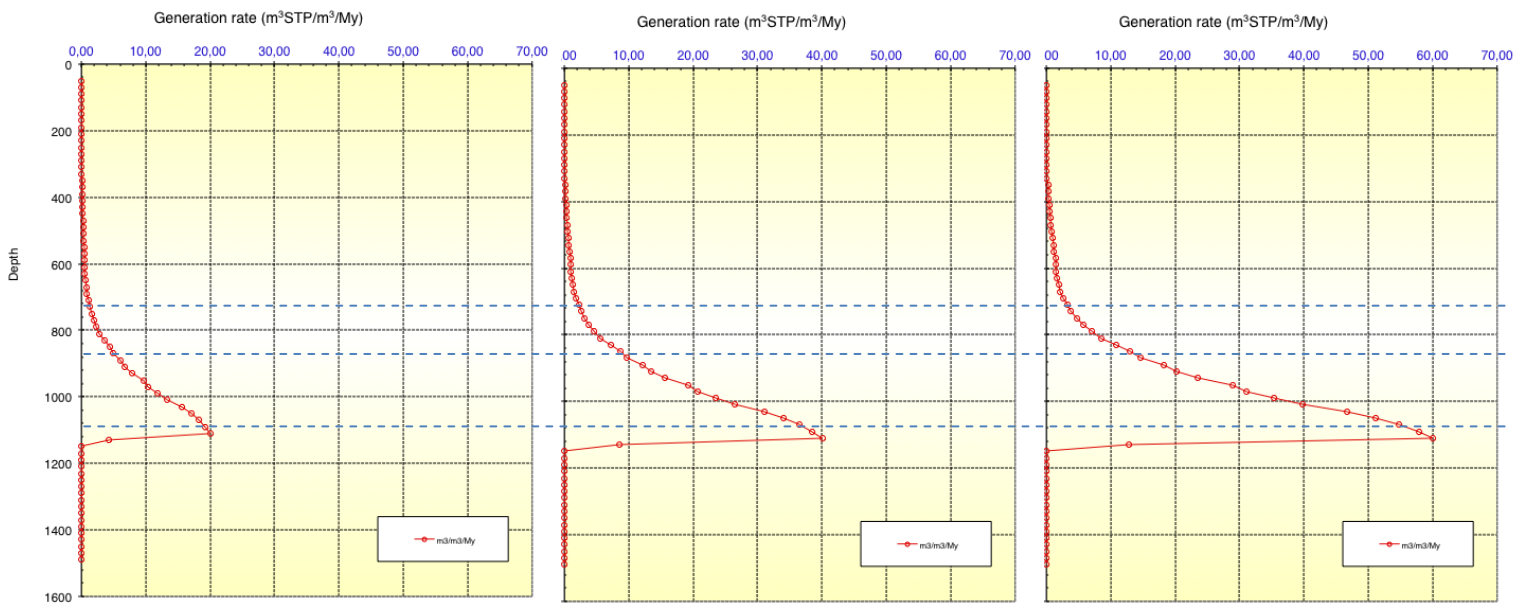


Figure 28. Generation rate ( $m^3STP/m^3/My$ ) of Hybrid Model at well F05-02 with 1, 2 and 3% total organic content.

The behaviour when applying the Hybrid model for well F05-02 (tables 23,24 and 25) indicates:

- 6% of gas saturation is gained at the oldest units (S1-S4) and the expulsion of the gas will occur at deeper layers (1154-1114m).
- GGI is obtained at horizons S1-S4.
- Peak of generation rate is achieved at 914m approx. (Unit S5).
- Adsorbed gas volumes slightly increase along the sequence from 0,28 until 0,43 m<sup>3</sup>/m<sup>3</sup> of rock with 1%, from 0,55 until 0,85 m<sup>3</sup>/m<sup>3</sup> of rock with 2% and from 0,83 until 1,28 m<sup>3</sup>/m<sup>3</sup> of rock with 3% of TOC.
- Total gas per volume of rock is achieved at units S1 until S4, increasing the percentage of total organic content that yield considerable gas volumes.

*Table 23. Biogenix results at well F05-02 considering 1% of total organic content.*

Seismic Unit	Depth m	GGI	Gen Rate m <sup>3</sup> /m <sup>3</sup> /My	Total gas v/v of rock	Adsorbed gas v/v of rock	Dissolved gas v/v of rock	Total free gas v/v of rock	Expelled gas v/v of rock
s13	414	0,04	0,24	0,28	0,28	0,00	0,00	0,00
s12	474	0,04	0,35	0,29	0,29	0,00	0,00	0,00
s11	514	0,05	0,46	0,31	0,31	0,01	0,00	0,00
s10	554	0,06	0,51	0,46	0,33	0,13	0,00	0,00
s9	574	0,06	0,54	0,48	0,34	0,14	0,00	0,00
s8	594	0,07	0,65	0,50	0,34	0,15	0,00	0,00
s7	614	0,07	0,73	0,49	0,33	0,16	0,00	0,00
s6	714	0,08	1,91	0,58	0,34	0,23	0,00	0,00
s5	914	0,13	10,38	1,03	0,38	0,64	0,00	0,00
s4	1114	0,50	0,00	4,50	0,44	0,69	3,37	1,53
s3	1134	0,50	0,00	4,54	0,45	0,69	3,41	1,56
s1	1154	0,50	0,00	4,32	0,43	0,78	3,11	1,02

*Table 24. Biogenix results at well F05-02 considering 2% of total organic content.*

Seismic Unit	Depth m	GGI	Gen Rate m3/m3/My	Total gas v/v of rock	Adsorbed gas v/v of rock	Dissolved gas v/v of rock	Total free gas v/v of rock	Expelled gas v/v of rock
s13	414	0,04	0,47	0,55	0,55	0,00	0,00	0,00
s12	474	0,04	0,70	0,57	0,57	0,00	0,00	0,00
s11	514	0,05	0,93	0,63	0,61	0,02	0,00	0,00
s10	554	0,06	1,03	0,93	0,67	0,26	0,00	0,00
s9	574	0,06	1,08	0,96	0,68	0,28	0,00	0,00
s8	594	0,07	1,29	0,99	0,68	0,31	0,00	0,00
s7	614	0,07	1,46	0,97	0,65	0,32	0,00	0,00
s6	714	0,08	3,81	1,16	0,69	0,47	0,00	0,00
s5	914	0,13	20,75	2,05	0,77	0,71	0,57	0,00
s4	1114	0,50	0,00	9,01	0,89	0,69	7,44	5,60
s3	1134	0,50	0,00	9,10	0,90	0,69	7,51	5,67
s1	1154	0,50	0,00	8,64	0,85	0,78	7,01	4,92

*Table 25. Biogenix results at well F05-02 considering 3% of total organic content.*

Seismic Unit	Depth m	GGI	Gen Rate m3/m3/My	Total gas v/v of rock	Adsorbed gas v/v of rock	Dissolved gas v/v of rock	Total free gas v/v of rock	Expelled gas v/v of rock
s13	414	0,04	0,71	0,83	0,83	0,00	0,00	0,00
s12	474	0,04	1,06	0,86	0,86	0,00	0,00	0,00
s11	514	0,05	1,39	0,94	0,92	0,03	0,00	0,00
s10	554	0,06	1,54	1,39	1,00	0,39	0,00	0,00
s9	574	0,06	1,62	1,44	1,02	0,42	0,00	0,00
s8	594	0,07	1,94	1,49	1,02	0,46	0,00	0,00
s7	614	0,07	2,19	1,46	0,98	0,48	0,00	0,00
s6	714	0,08	5,72	1,73	1,03	0,65	0,06	0,00
s5	914	0,13	31,14	3,08	1,15	0,71	1,21	0,00
s4	1114	0,50	0,00	13,53	1,33	0,69	11,51	9,68
s3	1134	0,50	0,00	13,66	1,34	0,69	11,62	9,79
s1	1154	0,50	0,00	12,97	1,28	0,78	10,92	8,83

## Comparison of Biogenix Results with Literature

When comparing the model results with the literature available for block F where well F05-03 is located, they are consistent with one level of gas accumulation (1114-1154m).

### *d) General conclusion*

In conclusion, the application of the model for the three wells reveals that the main possible source rock of biogenic gas in the Eridanos Delta sequence are the plio-pleistocene sediments, specifically those deeper layers of the stratigraphic sequences s1-s6.

## CONCLUSIONS

---

Literature suggests that 20% of methane gas worldwide reservoirs are from biogenic origin, a considerable percentage that could be available for exploitation. Therefore, studies looking for a better understanding of the processes involved in the biogenic gas generation are of high interest.

In this context, the aim of the present study was to model the biogenic gas generation in selected blocks that are part of the Eridanos delta system of the southern North Sea Basin.

For this purpose, in the first place, a theoretical review about microbial gas generation and the existent literature about the geological setting of the northern Dutch offshore were accomplished.

In a second stage, three different computer programs Petrel® (Schlumberger), the 1D Petroleum System modelling tool of PetroMod® (Schlumberger) and Biogenix® (Clayton C. , 2009) were used to model the biogenic gas generation for a group of selected wells in the study area, estimating the produced gas volumes per seismic stratigraphic units defined for the Eridanos Delta deposits.

Studies have identified that certain conditions are necessary to initiate the methanogenic process that generate the biogenic gas:

- Anoxic environment,
- Low temperature,
- Substrate rich in organic matter,
- High sedimentation rates,
- Low sulphate content and
- Sufficient pore space.

Also, for biogenic gas to accumulate, it should be necessary to meet certain conditions for concentration and entrapment:

- Early structures and stratigraphic traps,
- Physical state,
- High sedimentation rates,
- Low reservoir pressure.

Deltas, along with deep-water clastic and carbonate shelves and non-marine settings (e.g fluvial, lacustrine, coastal plain and coal swamp), are favourable areas that meet these conditions. Main Cenozoic Delta examples, analogous to the study area (the Eridanos Delta), are Niger, Nile, Baram, Mahakam, Mekong, Ganges, Orinoco and Po Deltas.

The modelling results corroborated that the Eridanos delta deposits constitute a perfect area for microbial gas generation attributable to the presence of the mentioned factors that foment methanogenesis.

In fact, the modelling process presented in earlier chapters, allowed to the following conclusions:

1. PetroMod® 1D Modelling for the selected wells demonstrated as an useful tool to overlook the geological settings, to identify which seismic units in the intradelta deposits meet the optimum temperature range and high sedimentation rates. Also, results offered the necessary data for the application of the Biogenix model. It is worth to mention that PetroMod results reveal the oscillation of temperatures data within the units (that portray the variation of climate conditions due to glacial-interglacial periods) not influence the outcome for the biogenic gas generation in the area of study.
2. PetroMod® results for the 25 wells selected indicate that the probability to find this unconventional source would increase at the northern part of the study area (blocks A and B).
3. Biogenix® output provided a better understanding of the minimum metabolizable organic matter needed for methanogenesis processes to occur in the study area. Also it was suitable for the evaluation of the three TOC scenarios (1%, 2%, 3%) at diverse wells in the three selected blocks (A,B,F) and the estimation of the possible depth range in the deltaic sequence for microbial gas generation. Although, the estimation gas volumes may differ significantly depending on the diverse evaluation methods provided by the program (Thermal-Hybrid Models), the model allowed to establish a general indication of the plausible units that biogenic gas could be found.
4. The Biogenix® model results also suggest that the potential biogenic gas would initiate at the oldest layers of the intra delta deposition, being the seismic stratigraphic horizon S5 the one that better depict the conditions for microbial gas generation in the Eridanos Delta deposits, where the presence of abundant organic matter was found, the optimal temperature window defined (30-50 °C) and high sedimentation rates were reached. Also, most of gas volume is generated at this unit when performing TOC scenarios.
5. A comparison between existing literature with model output regarding the depth where gas accumulations could be found indicates that while in wells A15-03 and F05-02 coincided with one zone of gas accumulation, the well B13-02 concord with the two levels of gas accumulation.
6. The model results indicate that the methanogenesis would initiate at a depth range 800-1200 m), contradicting the general expectation that microbial gas could be found at shallow depths (400-600m). It is important to indicate that this result would require further studies, as core samples analysis at different depth sequences in order to be considered definitive.

## RECOMMENDATIONS

---

In order to advance in a better knowledge of biogenic gas generation in the study area, the following recommendations are proposed

1. Since the model does not identified the gas origin in the marine sediments, it is recommended to perform a chemical-isotopic analysis of the gas samples at selected layers of the sequence for the selected wells.
2. To discuss whether the sealing capacity of the mud in the Tertiary sediments allows the migration of deeper fluids to shallower layers letting the mixture of thermogenic and biogenic fractions of gas in order to get a better understanding of the dynamics of the gas migration system.
3. To evaluate the possibility to add a salinity profile in Biogenix program to improve future modelling in the North Sea sector.
4. To estimate whether the formations contain economic quantities of gas or if they can produce at economic rates incorporating in the analysis factors that limit economical production, such as low permeability, insufficient thickness, gas storage, unfavourable mechanical properties and insufficient gas generation. This estimation could be assessed through 2D modelling of Biogenic system for better assessment of migration, generation and timing.

## REFERENCES

---

- Allers, T., & Mevarech, M. (2005). Archaeal Genetics-The third way. *Nature Review Genetics*( 5), 58-73.
- Addy, S., & Worzel, J. (1979). Gas seeps and sub-surface structure off Panama City. *AAPG* (63), 668-675.
- Anderson, A., & Bryant, W. (1987). Distribution of sea floor shallow gas in the northwestern Gulf of Mexico . *9th Offshore Technology Conference*, (pp. 295-299). Houston.
- Anderson, A., & Bryant, W. (1990). Gassy sediment occurrence and properties: Northern Gulf of Mexico. *Geo-Marine letters* (10), 209-220.
- Barker, C. (1972). Aquathermal pressuring-role temperature in development of abnormal-pressure zones. *AAPG* (56), 2068-2071.
- Bessereau, G., Roure, F., Kotarba, M., Kusmierek, J., & Strzetelski, W. (1996). Structure and hydrocarbon habitat of the Polish Carpathian. In P. Ziegler, & F. Horvath, *Structure and prospects of Alpine basins and forelands: Memoires du Museum National d'Histoire Naturelle* (Vol. 170, p. 547). Peri-Tethys Memoir 2.
- Bijlsma, S. (1981). Fluvial sedimentation from the Fennoscandian area into the northwest European Basin during the Late Cenozoic. *Geologie en Mijnbouw* (60), 337-345.
- Britannica, E. (2011). Types of Bacteria. In E. Britannica, *Bacteria and viruses* (p. 238). Kara Roger.
- Brown, A. (2011). Identification of source carbon for microbial methane in unconventional gas reservoirs. *AAPG Bulletin*, 95 (8), 1321-1338.
- Bustin, R. (1988). Sedimentology and characteristics of dispersed organic matter in Tertiary Niger delta:origin of source rocks in a deltaic environment. *AAPG*(72), 277-298.
- Buswell, A., & Mueller, H. (1952). Mechanism of Methane fermentation. *Ind.Eng.Chemistry* , 550-552.
- Butenko, J., & Barbot, J. (1979). Geological Hazards related to offshore drilling and construction in the Orinoco river delta of Venezuela. *11th Offshore technology conference*, (pp. 323-329). Houston.
- Clausen, O., Gregersen, U., Michelsen, O., & Sørensen, J. (1999). Factors controlling the Cenozoic sequence development in the eastern parts of the North Sea. *Journal Geological Society* (156), 809-816.
- Clayton, C. (2009, May 12). *A New Understanding of Biogenic Gas: an Explorer's Guide*. London, UK.
- Clayton, C. (2009). *Bacterial Gas Generation Models-Technical Manual*.

- Clayton, C. (1992). Source Volumetrics of Biogenic Gas Generation. In *Bacterial Gas* (pp. 191-204). Paris: Editions Technip.
- Cameron, T., Schüttenhelm, R., & Laban, C. (1989). Middle and Upper Pleistocene and Holocene stratigraphy in the Southern North Sea between 52° and 54° N, 2° to 4° E. In J. Henriët, & G. De Moor, *The Quaternary and Tertiary Geology of the Southern Bight, North Sea* (pp. 119-135). Brussels: Belgian Geological Survey .
- Coleman, J., & Roberts, H. (1989). Deltaic coastal wetlands. *Geologie en Mijnbouw* (68), 1-24.
- Cohen, G. (2011). The Archaea. In *Microbial Biochemistry* (pp. 133-137). Springer.
- Combaz, A., & De Matharel, M. (1978). Organic sedimentation and genesis of Petroleum in Mahakam delta, Borneo. *AAPG*, 62, 684-1695.
- Cornford, C. (2009). Source Rocks and Hydrocarbons of the North Sea. In K. W. Glennie, *Petroleum Geology of the North Sea: Basic Concept and Recent Advances* (p. 376). Oxford, UK: Blackwell science.
- Curzi, P. (1990). Some acoustic and sedimentological evidences of gas charged sediments in the Adriatic Sea. *Proc Int Worksh Marine Acoustics* (pp. 391-396). Beijing: China Ocean Press.
- Dickey, P., & Cox, W. (1977). Oil and in reservoirs with subnormal pressures. *AAPG* (61), 2134-2142.
- Donders, T., Weijers, J., Munsterman, D., Kloosterboer-van Hoeve, M. L., Buckles, L., Pancost, R., et al. (2009). Strong climate coupling of terrestrial and marine environments in the Miocene of northwest Europe. *Earth and Planetary Science Letters* (281), 215-225.
- Eidvin, T., Riis, F., & Rundberg, Y. (1999). Upper Cainozoic stratigraphy in the central North Sea (Ekofisk and Sleipner fields) . *Geologisk Tidsskrift* (79), 97-128.
- Fleischer, P., Orsi, T., Richardson, M., & Anderson, A. (2001). Distribution of free gas in marine sediments: a global overview. *Geo-Marine Letters* (21), 103 -122.
- Floodgate, G., & Judd, A. (1992). The origins of shallow gas. *Continental Shelf Research*, 12 (10), 1145-1156.
- Faber, E., & Stahl, W. (1984). Geochemical surface exploration for hydrocarbons in the North Sea. *AAPG* (68), 363-386.
- Figueiredo, A., Nittrouer, C., & Costa, E. (1996). Gas-charged sediments in the Amazon submarine delta. *Geo-Marine Letters*, 16, 31-35.
- Gibbard, P. L., West, R., Zagwijn, W., Balson, P., Burger, A., Funnel, B., et al. (1991). Early Middle Pleistocene correlations in the southern North Sea Basin. *Quaternary Science Reviews* (10), 23-52.
- Goes, S., Govers, R., & Vacher, P. (2000). Shallow mantle temperatures under Europa P and S wave tomography. *Journal of Geophysical Research* .

- Gradstein, F., Ogg, J., & Smith, A. (2004). *A Geologic Time Scale*. Cambridge University. Cambridge: Cambridge University Press.
- Hantschel, T., & Kaueauf, A. (2009). *Fundamental of Basin and Petroleum Systems Modeling*. Berlin, Germany: Springer.
- Hovland, & Irwin. (1992). Habitat of methanogenic carbonate cemented sediments in the North Sea. In R. Vially, *Bacterial Gas* (pp. 157-172). Paris: Editions Technip.
- Hovland, M., & Judd, A. (1988). *Seabed pockmarks and seepages. Impact on Geology, Biology and the Marine Environment*. London: Graham & Trotman.
- Huuse, M., & Clausen, O. (2001). Morphology and origin of major Cenozoic sequence boundaries in the eastern North Sea Basin: top Eocene, near-top Oligocene and the mid-Miocene unconformity. *Basin Research* (13), 13-41.
- Joon, B., Laban, C., & van der Meer, J. (1990). The Saalian glaciation in the Dutch part of the North Sea. *Geologie and Mijnbouw* (69), 151-158.
- Katz, B. J. (2011). Microbial Processes and Natural Gas Accumulations. *The Open Geology Journal* (5), 75-83.
- Kosmowska-Ceranowicz, B. (1988). Geheimnisse und Schönheit des Bernsteins. *Bernstein: Träger der Götter*, 585.
- Kotarba, M. (1998). Composition and origin of gaseous hydrocarbons in the Miocene strata of the Polish part of the Carpathian Foredeep. *Przegląd Geologiczny*, 46 (8/2), 751-758.
- Kotarba, M. (1992). Bacterial gases in Polish part of the Carpathian Foredeep and the flysch Carpathians—Isotopic and geological approach. *Bacterial Gas*, 133-146.
- Kotarba, M., Szafran, S., & Espitalie, J. (1987). A study of organic matter and natural gases of the Miocene sediments in the Polish part of the Carpathian Foredeep. *Chemical Geology*, 64, 197-207.
- Kuhlmann, G., Langereis, C., Munsterman, D., Van Leeuwen, R., Verreussel, R., Meulenkamp, J., et al. (2006). Chronostratigraphy of Late Neogene sediments in the southern North Sea Basin and paleoenvironmental interpretations. *Palaeogeography, Palaeoclimatology, Palaeocology* (239), 426-455.
- Kuhlmann, G., & Wong, T. (2008). Pliocene paleoenvironment evolution as interpreted from 3D-seismic data in the southern North Sea, Dutch offshore sector. *Marine and Petroleum Geology* (25), 173-189.
- Kuhlmann, G., De Boer, P., Pedersen, R., & Wong, T. (2004). Provenance of Pliocene sediments and paleoenvironmental changes in the southern North Sea region using Samarium-Neodymium (Sm/Nd) provenance ages and clay mineralogy. *Sedimentary Geology* (171), 205-226.

- Laban, C. (1995). The Pleistocene glaciations in the Dutch sector of the North Sea. *A synthesis of sedimentary and seismic data. PhD Thesis, University of Amsterdam* , (p. 200).
- Liu, Y., & Whitman, W. B. (2008). Metabolic, phylogenetic, and ecological diversity of methanogenic archaea. *Annals of the New York Academy of Sciences* (1125), 171-89.
- Long, D. L., Streif, H., Cameron, T., & Schüttenhelm, R. (1988). The sedimentary record of climatic variation in the southern North Sea. *Philosophical Transactions of the Royal Society London* , 523-537.
- Lorant, F., Largeau, C., Behar, F., & De Cannière, P. (2008). Improved kinetic modelling of the early generation of CO<sub>2</sub> from the Boom Clay kerogen. Implications for simulation of CO<sub>2</sub> production upon disposal of high activity nuclear waste. *Organic Geochemistry* (39), 1294-1301.
- Luijendijk, E., Ter Voorde, M., Van Balen, R., Andriessen, P., Verweij, J., & Simmelink, E. (2009). Estimation of deep subsurface temperatures in the Roer Valley Graben, using a new numerical model of borehole temperature recovery . *Geophysical Research Abstracts.11. EGU General Assembly* .
- McMahon, P. B., Chapelle, F. H., Fells, W. F., & Bradley, P. M. (1992). Role of microbial processes in linking sandstone diagenesis with organic rich clays . *Sediment Petrol* (62), 1-10.
- Mangerud, J., Jansen, E., & Landvik, J. (1995). Late Cenozoic history of the Scandinavian and Barents Sea ice sheets. . *Global Planetary Change* (299), 16.
- Mechalas, B. J. (1974). Pathways and environmental requirements for biogenic gas production in the ocean . *Natural Gases in Marine Sediments* , 11-25.
- Michelsen, O., Danielsen, M., Heilmann-Clausen, C., Jordt, H., Laursen, G., & Thomsen, E. (1995). Occurrence of major sequence stratigraphic boundaries in relation to basin development in Cenozoic deposits of the southeastern North Sea. In R. Steel, W. Felt, E. P. Johannessen, & C. Mathieu, *Sequence Stratigraphy: Advances and Applications for Exploration and Producing in North West Europe*. (pp. 415-427). Amsterdam: Norwegian Petroleum Society. Elsevier.
- Michelsen, O., Thomsen, e., Danielsen, M., Heilmann-Clausen, C., Jordt, H., & Lauser, G.-V. (1998). Cenozoic sequence stratigraphy in eastern North Sea. In C. Gracianky, T. Jaquin, P. Vail, & M. Farley, *Mesozoic and Cenozoic Sequence stratigraphy of European Basins* (pp. 91-118). SEPM.
- Milkov, A. (2011). Worldwide distribution and significance of secondary microbial methane formed during petroleum biodegradation in conventional reservoirs . *Organic geochemistry* (42), 184-207.
- Murthy, K., & Rao, T. (1990). Acoustic wipeouts over the continental margins off Krishna, Godavari and Mahanadi River Basins, East Coast of India . *Journal Geologic Society India* (35), 559-568.
- NLOG. (n.d.). *NL Olie en Gasportaal*. Retrieved 2 18, 2013 from nlog.nl: [http:// www.nlog.nl](http://www.nlog.nl)
- Nelskamp, S., & Verweij, J. (2012). *Using basin modeling for geothermal energy exploration in the Netherlands-an example from the West Netherlands Basin and Roer Valley Graben*. Utrecht: TNO report.

- Orange, D., Garcia-Garcia, A., Lorenson, T., Nittrouer, C., Milligan, T., Miserocchi, S., et al. (2005). Shallow gas and flood deposition on the Po Delta. *Marine Geology* (222-223), 159-177.
- Overeem, I., Weltje, G., Bishop-kay, C., & Kroonenberg, S. (2001). The Late Cenozoic Eridanos del system in the Southern North Sea Basin: a climate signal in sediment supply? *Basin research* (13), 293-312.
- Parkes, R., Wellsbury, P., Mather, I., Cobb, S., Cragg, B., Hornibrook, E., et al. (2007). Temperature activation of organic matter and minerals during burial has the potential to sustain the deep biosphere over geological timescales . *Organic Chemistry* (38), 845-852.
- Peters, K., & Nelson, P. (2009). Criteria to determine Borehole Formation Temperatures for Calibration of Basin and Petroleum System Models. *AAPG Annual Convention and Exhibition*. Denver.
- Praeg, D. (1996). *Morphology, stratigraphy and genesis of buried Elsterian tunnel valleys in the southern North Sea basin, PhD Thesis*. University of Edinburgh .
- Rice, D. (1992). Controls, habitat, and resource potential of ancient bacterial gas. *Bacterial Gas* , 91-118.
- Rice, D. D., & Claypool, G. E. (1981). Generation, Accumulation and Resource Potential of Biogenic Gas. *American Association of Petroleum Geologist* (65), 5-25.
- Rijks, E. (1981). Baram Delta geology and hydrocarbon occurrence. *Geological Society Malaysia Bulletin* (14), 1-18.
- Roberson, R. (2011). Brief Biography of a Biogenic Gas Play. *GeoExpro*, 8 (6).
- Schlumberger. (2013). *Schlumberger*. Retrieved 6 11, 2013 from PetroMod Petroleum System Models: [http://www.slb.com/services/software/geo/petromod\\_modeling\\_software/petroleum\\_sys\\_mod.aspx](http://www.slb.com/services/software/geo/petromod_modeling_software/petroleum_sys_mod.aspx)
- Schoell, M. (1980). The hydrocarbon and carbon isotope composition of methane from natural gases of various origins. *Geochimica et Cosmochimica* (44), 649-662.
- Schroot, B. M., Klaver, G. T., & Schüttenhelm, R. T. (2005). Surface and subsurface expressions of gas seepage to the seabed-examples from the Southern North Sea. *Marine and Petroleum Geology* (22), 499-515.
- Schroot, B., & Schüttenhelm, R. (2003). Expressions of shallow gas in the Netherlands North Sea. *Netherlands Journal of Geosciences/ Geologie en Mijnbouw* (82), 91-105.
- Sørensen, J., & Michelsen, O. (1995). Upper Cenozoic sequences in the south-eastern North Sea Basin . *Bulletin of the Geological Society of Denmark* (42), 74-95.
- Sørensen, J., Gregersen, U., Breiner, M., & Michelsen, O. (1997). High-frequency sequence stratigraphy of Upper Cenozoic deposits in the central and southeastern North Sea areas . *Marine and Petroleum Geology* (14), 99-123.

- Sekiguchi, K. (1984). A method for determining terrestrial heat flow in oil basinal areas. *Tectonophysics* (103), 67-79.
- Sha, L. P. (1991). *Quaternary Sedimentary Sequences in the southern North Sea basin*. The Modelling and Dynamics of the quaternary geology of the southern North Sea and their applications to environmental protection and industrial developments.
- Stefanon, A. (1980). The acoustic response of some gas-charged sediments in the northern Adriatic Sea. In W. A. Kuperman, & F. B. Jensen, *Bottom-interacting ocean acoustics* (pp. 73-84). New York: Plenum.
- Stiles, N., Breslau, L., & Beeston, M. (1969). The riverbed roughness and sub-bottom structure of the main shipping channel to Sai Gon, RVN (Nga Bay, Long Tau, Nha Be, and Sai Gon Rivers). *Naval Oceanography Off. Washington DC* (69-42).
- Streif, H. (1996). Deutsche Beiträge zur Quartarforschung in der südlichen Nordsee. In *Geologisches Jahrbuch* (p. 244). Hannover.
- Tigrek, S. (1998). *3D seismic interpretation and attribute analysis of the L08-block, Southern North Sea Basin*. Delft University of Technology, Faculty of Applied Earth Sciences, Delft.
- Tissot, B., & Welthe, D. (1984). *Petroleum formation and occurrence*. Berlin: Springer-Verlag.
- TNO. (n.d.). *TNO-innovation for life*. Retrieved 2 18, 2013 from tno.nl: [http://www.tno.nl/content.cfm?context=thema&content=innovatiegebied&laag1=895&laag2=917&item\\_id=917&Taal=2](http://www.tno.nl/content.cfm?context=thema&content=innovatiegebied&laag1=895&laag2=917&item_id=917&Taal=2)
- Van Adrichem Boogaert, H., & Kouwe, W. (1997). Stratigraphic nomenclature of the Netherlands. *Mededelingen Rijks Geologische Dienst* 50, I, 39.
- Vandré, C., Cramer, B., Gerling, P., & Winsemann, J. (2007). Natural gas formation in the western Nile delta (Eastern Mediterranean): Thermogenic versus microbial. *Organic Geochemistry*, 38 (4), 523-539.
- Waples, D. W., & Waples, J. (2004). A review and evaluation of specific heat capacities of rocks, minerals, and subsurface fluids. Part 1: Minerals and Nonporous rocks. *Natural resources* (13), 97-122.
- Westerhoff, W. (2009). *Stratigraphy and sedimentary evolution of the lower Rhine-Meuse system during the Early Pleistocene (southern North Sea Basin)*. Vrije Universiteit. Amsterdam: PhD Thesis.
- Westerhoff, W., Geluk, M., & De Mulder, E. (2003). *Opbouw van de ondergrond*. De Ondergrond van Nederland. Netherlands Institute of Applied Geoscience TNO – National Geological Survey.
- Whelan, T., Coleman, J., Suhayda, J., & Roberts, H. (1977a). Acoustical penetration and shear strength in gas-charged sediment. *Marine Geotechnology* (2), 147-159.

Whelan, T., Purvis, D., Hart, G., Albright, J., & Smith, H. (1977b). Seismic, fluorimetric and chromatographic studies of reservoir leakage. *9th Offshore Tecnology Conference*, (pp. 453-458). Houston.

Whiticar, M. (1999). Carbon and hydrogen isotope systematic of bacterial formation and oxidation of methane.. *Chem Geol* (161), 291-314.

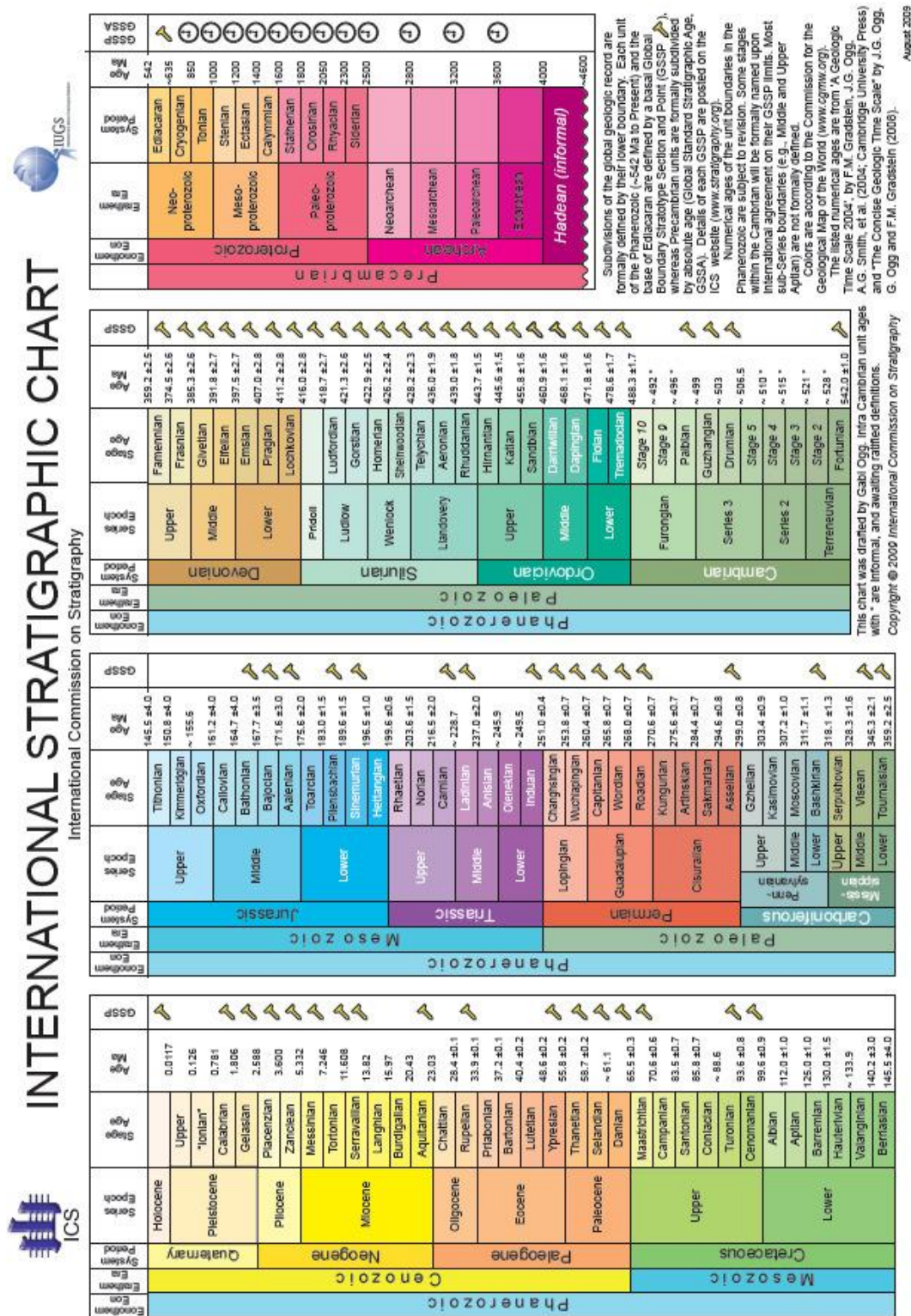
Whiticar, M. (1994). Correlation of natural gases with their sources. in L. B. Magoon, and W. G. Dow, eds., *The Petroleum System, From Source to Trap*. AAPG Memoir 60 , 261-283.

Yamamoto, S., Alcauskas, J., & Crozier, T. (1976). Solubility of methane in distilled water and seawater. *Journal of Chemical & Engineering Data*. (21), 78-80.

Zagwin, W. (1989). The Netherlands during the Terciary and the Quaternary: a case history of coastal lowland evolution. *Geologie en Mijnbouw* (68), 107-120.

Zeikus, J., & Winfrey, M. (1972). *Methanobacterium thermoautotrophicum*, an anaerobic, autotrophic, estreme thermophile. *Journal Bacteriology* , 707-713.

# APPENDIX 1 International Geologic Time Scale of Gradstein *et al*



## APPENDIX 2 Paleo-water depth (PWD) input

---

Age (Ma)	PWD(m)
0	45
1,8	50
2,12	100
2,16	150
2,44	150
2,58	200
5,2	200
12,5	50
19	50
26,5	100
35	50
40	80
60,5	150
65	20
70,6	100
83,5	200
97	200
121	150
130	40
140,7	0
154	0
158	0
167	50
173	200
180	180
204	0
212	20
220	20
231	50
240	50
241	30
242	10
245	10
250,5	20
255	20
258	10
261	0
270	0
318,8	22

### APPENDIX 3 Surface water interface temperature (SWIT) input

Age (Ma)	SWIT ( °C)
0	7,15
0,01	4,48
0,03	-4,06
0,13	5,33
0,15	-4,18
0,21	3,54
0,26	-3,14
0,31	0,19
0,33	5,42
0,35	-3,79
0,39	0,08
0,41	8,49
0,44	-6,23
0,5	3,45
0,55	-2,95
0,61	3,19
0,64	-6,09
0,7	3,24
0,73	-2,42
0,79	3,39
0,81	-4,22
0,86	4,72
0,88	-3,56
0,95	3,93
0,97	0,03
1	0,28
1,1	0,48
1,2	0,7
1,3	0,93
1,4	1,19
1,5	1,46
1,6	1,75

Age (Ma)	SWIT ( °C)
1,7	2,05
1,8	2,38
1,9	2,72
2	3,08
2,1	3,46
2,2	3,86
2,3	4,27
2,4	4,71
2,5	5,16
2,6	5,63
2,7	6,11
2,8	6,62
2,9	7,14
3	7,68
3,3	14
6,8	14
7,7	18
8,3	21
14	21
14,2	20
15,2	20
15,6	21
16,5	21
19,2	15
21,5	15
22	17
24,5	13,5
26	14,5
31	15
35	18
39	18
44,5	18
51	22,4

Age (Ma)	SWIT ( °C)
53	21,6
54,3	23
54,7	25
55,6	27
55,7	25
58,5	18
60	19,3
64	20
70,6	19,84
83,5	21,64
97	22,6
121	22,88
140,7	24
156	23,49
167	22,17
173	21,37
212	20,3
231	24,15
240	24,76
241	25,68
242	25,58
245	25,4
250,5	24,76
255	24,13
258	24
268,8	23,68
270	23,5
280	23
290	24
315,3	23
318,8	22
322,8	23

---